

Impact Assessment of Climate Change on Irrigation Water Requirements
for Agriculture in the Ma River Basin in Thanh Hoa Province in Viet Nam

TRINH DINH DUY

201826063

July 2020

A Master's Thesis Submitted to
The Graduate School of Life and Environmental Sciences,
the University of Tsukuba
in Partial Fulfillment of the Requirements
for the Degree of Master of Environmental Sciences

ABSTRACT

Vietnam has been identified as an agricultural country, with 68% of the population living in the countryside and approximately 47% share of employment in agriculture. Similar to other developing countries, Vietnam's agriculture depends mainly on the weather. In the meanwhile, it is one of the nations most likely to be adversely affected by climate change due to a long coastline and geographic location, which makes the country's agriculture more vulnerable to climate change's risks. The effects of climate change have been explored in the Ma river basin in Thanh Hoa, which is one of the major rivers in the north-central part of Viet Nam that provides water for 3.64 million people and irrigate around 369 thousand ha of agricultural area. The purpose of this research is to project local precipitation and temperature by Statistical Downscaling Model (SDSM) and explore the impacts of climate change on irrigation water requirements using Crop Water calculation software (CROPWAT).

This research utilized a database for Policy Decision making for future climate change (d4PDF) with horizontal resolutions of 60 km to downscale temperature and precipitation to climate station scale in the Ma river basin. Regression models between d4PDF's predictors and local climate variables were calibrated and validated before being used to simulate future temperature and precipitation. Next, the two future simulated precipitation and temperature using future d4PDF's simulations were used as input data to compute irrigation water requirements by CROPWAT. Finally, changes in irrigation water requirements were analyzed, quantified with corresponding solutions and recommendations to reduce any negative impacts of climate change in the region.

Two scenarios (the 2040s and 2090s) were used to project future precipitation and temperature in the Ma river basin for the period of 2040-2049 and 2090-2099. Based on the simulation results, a warmer and wetter climate is predicted for the region in general. However, the Ma river basin may experience a decrease in rainfall during the dry season, following by an increase in the rainy season. Irrigation water requirements are anticipated to rise, with the changing rate reaching approximately 14% by the end of the 21st century. This rise in irrigation water requirement poses a threat to water resources planning, and global warming is a potentially serious problem for agriculture in the region.

Keywords: Climate Change, Irrigation Water Requirements, Agriculture, Downscaling, Ma River Basin

CONTENTS

ABSTRACT	i
LIST OF TABLES	iv
LIST OF FIGURES	vi
LIST OF ABBREVIATIONS	viii
CHAPTER 1 INTRODUCTION	1
1.1 Background	1
1.2 Literature review.....	2
1.2.1 Approaches to climate change impact assessment on agriculture	3
1.2.2 Researches on global climate models	4
1.2.3 Researches on downscaling methods and bias correction.....	7
1.2.4 Researches on irrigation requirements	12
1.3 Objectives of this study.....	15
CHAPTER 2 METHODS AND MATERIALS	16
2.1 Introduction	16
2.2 Study area.....	17
2.2.1 Location.....	17
2.2.2 Climate	18
2.2.3 Water Resources	18
2.3 Methods.....	23
2.3.1 Global Climate Model.....	23
2.3.2 Statistical downscaling model	24
2.4 Data preparation	34
2.4.1 Global climate data	35
2.4.2 Observed data	35
2.4.3 Crop data	36
2.4.4 Soil characteristics	38
CHAPTER 3 RESULTS AND DISCUSSION	39
3.1 Introduction	39

3.2 Screening of predictors	39
3.3 Calibration of SDSM	43
3.4 Validation of SDSM without bias correction	46
3.5 Validation of SDSM with bias correction in downscaling precipitation	48
3.6 Climate projection	50
3.6.1 Precipitation.....	50
3.6.2 Temperature.....	53
3.7 Irrigation water requirement.....	56
3.7.1 Net irrigation water requirement (NIWR).....	56
3.7.2 Gross irrigation water requirement (GIWR)	66
3.8 Discussion	67
CHAPTER 4 CONCLUSIONS.....	73
4.1 Summary of the findings.....	73
4.2 Recommendations.....	74
4.3 Suggestions for future work.....	76
ACKNOWLEDGMENTS	78
REFERENCES	79
APPENDIX.....	84
Appendix A - Crop water requirements for each type of crop during 2040-2049 ...	84
Appendix B - Crop water requirements for each type of crop during 2090-2099 ...	99

LIST OF TABLES

Table 1.1 Comparison of statistical and dynamical downscaling	9
Table 2.1 Mean monthly discharge of main rivers in the Ma river basin for the period 1975-2004 (Hoang, 2009)	19
Table 2.2 Water consumption by sectors in the Ma river basin (Hoang, 2009).....	19
Table 2.3 Predictor description of d4PDF.....	35
Table 2.4 Observed mean monthly climate data for the period 1975-2004 at Thanh Hoa climate station.....	36
Table 2.5 Crop information in Thanh Hoa province.....	37
Table 2.6 Crop coefficients for wet crops (rice) with different growth stages.....	37
Table 2.7 Crop coefficients for dry crops	37
Table 2.8 Soil characteristic in the region.....	38
Table 3.1 Backward and forward selection for precipitation	40
Table 3.2 Backward and forward selection for temperature	40
Table 3.3 Parameters for monthly regression model of temperature.....	43
Table 3.4 Parameters for monthly regression model of precipitation.....	43
Table 3.5 Coefficient of determination (R^2) and standard error (SE) of the yearly model during calibration (1975-2004).....	44
Table 3.6 Comparison of observed and downscaled monthly mean precipitation and temperature by SDSM during the calibration period (1975-2004).....	44
Table 3.7 Comparison of observed and downscaled monthly mean precipitation and temperature by SDSM (without bias correction) during the validation period (2005-2011)...	46
Table 3.8 Downscaled monthly mean precipitation with bias correction for the validation period (2005-2011)	48
Table 3.9 Future changes in precipitation (with bias correction) in comparison with the baseline period (1975-2004)	50
Table 3.10 Statistical test for precipitation for the period 2040-2049 and 2090-2099 in comparison with the baseline	51
Table 3.11 Future changes in temperature in comparison with the baseline period (1975-2004)	53
Table 3.12 Statistical test for temperature for the period 2040-2049 and 2090-2099 in comparison with the baseline	54
Table 3.13 Reference Evapotranspiration of Thanh Hoa area in the periods 1975-2004, 2040-2049, and 2090-2099.....	56
Table 3.14 Rainfall and effective rainfall of Thanh Hoa area in the periods 1975-2004, 2040-2049, and 2090-2099.....	56

Table 3.15 Changes of monthly and annual NIWR between the 2040s and 2090s with respect to the baseline period (1975-2004)	57
Table 3.16 Changes of seasonal NIWR between the 2040s and 2090s with respect to the baseline period (1975-2004).....	59
Table 3.17 Annual IWR for each type of crop in the Ma river basin for the 2040s and 2090s	61
Table 3.18 Irrigation water requirements (mm) for each type of crop during the 2040s.....	63
Table 3.19 Irrigation water requirements (mm) for each type of crop during the 2090s.....	64
Table 3.20 Monthly GIWR in Ma river basin for the period of 1975-2004	66
Table 3.21 Monthly GIWR in Ma river basin for the period of 2040 to 2049.....	66
Table 3.22 Monthly GIWR in Ma river basin for the period of 2090 to 2099.....	66
Table 3.23 Water supply requirements for the baseline period (1975-2004) in the Ma river basin	67
Table 3.24 Water supply requirements for the 2090s in the Ma river basin.....	68
Table 3.25 Proposal of shifting planting time for rice in the Ma river basin	68
Table 3.26 GIWR of the Ma river basin under the shifting of rice’s planting date for the baseline period, the 2040s and 2090s	69
Table 3.27 GIWR of the Ma river basin under the shifting of rice to maize for the baseline period, the 2040s and 2090s	70

LIST OF FIGURES

Figure 1.1 Comparison of projected temperature from some GCMs over the research area for (a) 2040-2049; and (b) 2090-2099.....	6
Figure 1.2 Illustration of the general approach to downscaling (Wilby & Dawson, 2007).....	8
Figure 1.3 Flow of stages to determine the downscaling method (Khan et al., 2006)	11
Figure 1.4 Diagram of the soil-water balance of a crop root zone (Martin, 1993).....	14
Figure 2.1 Steps to analyze and assess climate change impacts.....	16
Figure 2.2 Ma river basin map (VAST, 2014)	17
Figure 2.3 Climate graph for Thanh Hoa, Viet Nam for the period 1975-2004.....	18
Figure 2.4 Main rivers in the Ma river basin.....	20
Figure 2.5 Land use map of the Ma river basin, Thanh Hoa province (Thanh Hoa's People Committee, 2013). Legends are translated and added based on the original map	22
Figure 2.6 Starting screen of SDSM version 4.2.9	25
Figure 2.7 Climate scenario generation of SDSM.....	26
Figure 3.1 Scatter plot of observed precipitation and (a) zonal wind at 850 hPa; (b) omegas; (c) relative humidity; (d) tcloud; (e) meridional wind at 850 hPa; (f) d4PDF temperature; (g) wind speed at 10m; (h) zonal wind at 500 hPa; (i) large-scale d4PDF precipitation; (j) meridional wind at 500 hPa	41
Figure 3.2 Scatter plot of observed temperature and (a) zonal wind at 850 hPa; (b) omegas; (c) relative humidity; (d) tcloud; (e) meridional wind at 850 hPa; (f) d4PDF temperature; (g) wind speed at 10m; (h) zonal wind at 500 hPa; (i) large-scale d4PDF precipitation; (j) meridional wind at 500 hPa	42
Figure 3.3 Observed and simulated for (a) precipitation and (b) temperature for the calibration period (1975-2004) in the Thanh Hoa station.	45
Figure 3.4: Observed downscaled (without bias correction) mean monthly values for (a) precipitation and (b) temperature during the validation period (2005-2011).....	47
Figure 3.5 Observed and downscaled mean monthly precipitation by SDSM (with bias correction) during the validation period (2005-2011)	49
Figure 3.6 Observed and simulated mean monthly precipitation by SDSM (with bias correction) for the 2040s and 2090s period in the Ma river basin.....	52
Figure 3.7 Observed and simulated mean monthly temperature by SDSM for the 2040s and 2090s period in the Ma river basin	55
Figure 3.8 Monthly NIWR between the baseline and two future periods (the 2040s and 2090s)	58
Figure 3.9 Seasonal NIWR between the baseline and two future periods (the 2040s and 2090s)	60

Figure 3.10 Percentage of IWR for each type of crop during (a) the 2040s, and (b) the 2090s	62
Figure 3.11 IWR for each type of crop in (a) the 2040s, and (b) the 2090s	65
Figure 3.12 Comparison of observed and large-scale (d4PDF) wind speed for the period 1975-2004, 2040-2049 and 2090-2099	72
Figure 3.13 Comparison of observed and large-scale (d4PDF) relative humidity for the period 1975-2004, 2040-2049 and 2090-2099	72

LIST OF ABBREVIATIONS

AGCM	Atmospheric General Circulation Model
AOGCM	Atmosphere-Ocean General Circulation Model
BC	Bias correction
CCSM	The Community Climate System Model
CGCM	Coupled General Circulation Model
CMIP5	Coupled Model Intercomparison Project Phase 5
CWR	Crop water requirements
DIAS	Data Integration and Analysis System
ECHAM	European Centre Hamburg Model
ET	Evapotranspiration
FAO	Food and Agriculture Organization
GCM	General Circulation Model
GDP	Gross Domestic Product
GFDL	Geophysical Fluid Dynamics Laboratory
GIS	Geographic Information System
GIWR	Gross Irrigation Water Requirements
GSO	General Statistics Office of Viet Nam
IHM	Viet Nam Institute of Meteorology, Hydrology and Climate Change
IPCC	Intergovernmental Panel on Climate Change
IWR	Irrigation Water Requirements
JICA	The Japan International Cooperation Agency
JMA	Japan Meteorological Agency
LS	Linear Scaling Method
MRI	Meteorological Research Institute of Japan
NCAR	National Center for Atmospheric Research
NIWR	Net Irrigation Water Requirements
NSE	Nash–Sutcliffe model efficiency coefficient
OGCM	Ocean General Circulation Model
d4PDF	Database for Policy Decision-Making for Future Climate Change
RCM	Regional Climate Model
RCP	Representative Concentration Pathway
SDSM	Statistic Downscaling Model
SE	Standard error
SRES	Special Report on Emissions Scenarios
UNEP	the United Nations Development Programme
UNESCO	The United Nations Educational, Scientific and Cultural Organisation
USDA	United States Department of Agriculture

CHAPTER 1 INTRODUCTION

1.1 Background

Climate change has been identified as one of the biggest environmental challenges facing many countries around the world nowadays. Following the Intergovernmental Panel on Climate Change (IPCC), the average temperature of Earth's surface has increased by 0.75 °C over the past century and is projected to stay rising by 2 to 4 °C, or probably even more by the end of 22nd century (Lemke et al., 2007). It is well-established scientific evidence that this global warming event has a direct relation with the concentration of greenhouse gases in the Earth's atmosphere, which has been rising steadily since the Industrial Revolution. This increase in greenhouse gases, which consist of carbon dioxide, methane, and nitrous oxide, is attributed to human activities. While carbon dioxide concentration increases due to fossil fuel burning and land use changing, nitrous oxide and methane are due to cultivation and agriculture (Lemke et al., 2007). These changes can vary sharply from regions to regions. For example, North America and Europe might see an up-rising intensity of rainfall of approximately 25 percent. Some parts of Asia with monsoon influences would even experience more significant increases, whereas South Africa, Australia, and the Mediterranean would see smaller increases. However, there are some regions that are expected to decrease in rainfall amount along with global warming, located in subtropical oceans, outside equatorial belt (Pfahl et al., 2017).

Global warming has extensive effects on every aspect of life, from global to local, ranging from climatic conditions such as temperature, rainfall, runoff, drought, wind pattern to ecosystem health (species phenology), human health and socio-economic development. The impacts of climate change also vary between regions. Many regions may be severely affected, but some parts are projected to welcome the changes, but they stay relatively small. All regions may either suffer an increase in the cost or decrease in the benefits if the mean temperature rises by more than 2-3 °C, and the developing countries are expected to experience more considerable losses in comparison to developed countries (Parry et al., 2007). The losses have significant impacts on the economy of developing countries as not only do many developing countries have naturally warmer climatic conditions, but they also depend mainly on climate-sensitive sectors such as agriculture, tourism, and forestry.

Among those sectors, agriculture is one of the most vulnerable sectors that are subject to the changes in the climate. Generally, agricultural yields are expected to decrease as the temperature increase of 1°-2 °C, especially in tropical areas (Rosenzweig et al., 2013). At the global level, there are some recent studies indicated that potential losses in some crop production due to climate change such as coffee or cacao might jeopardize the national economies and also negatively affect the surrounding area's supply chain or even bigger at the

global level of these respective industries (Bunn et al., 2015). This issue is primarily right in the areas where are currently suffering food insecurity. In South Asia and Africa, the production of maize, wheat, and sorghum are predicted to experience declines in yield of 8% by 2050, with wheat production's return decreasing to 17% in Africa (Knox et al., 2012). In Viet Nam, rice yield is projected to decrease by 0.65 tons per hectare, corresponding to 11.8% of total national rice production in the spring season and 0.1 ton per hectare (3.6%) in the summer by 2050 (The et al., 2015). Following this projection, Viet Nam will no longer be a rice-exporting country, and national food security will be threatened seriously in the future. The importance of the agriculture sector is expressed even more clearly with its contribution to the gross domestic product (GDP). For example, in Viet Nam, agriculture accounted for more than 14% of GDP in 2018, with rice exporting ranking 3rd global and bringing about 3 billion dollars in the same year (GSO, 2018). Although it is vital to economic development, agriculture also shows its fragility due to high dependence on natural conditions such as soil, weather and water resources.

Climate change can have acute effects on the water resources and water needs in agriculture uses. It is concluded to alter the "hydrologic cycle and, through it, the quantity and quality of water resources" (UNESCO, 2009). Precipitation and evapotranspiration are two vital hydrologic variables that can be altered by changing climate in general, the temperature in particular. By understanding the interaction between climate and water resources, policymakers and scientists will find a tool to help to deal with adverse impacts of climate change by applying appropriate water management approaches. There is a prediction that water resource availability will increasingly shrink in the future by climate change. Therefore, the gap between water supply and need that is already big will continue to expand. Generally, water demands tend to increase during warmer weather while water supply is anticipated to shrink. In particular, water consumption for agriculture, which takes up most of the water supply, will increase due to both depleting rainfall and increasing evapotranspiration. In water-stressed basins, where the water consumption is approaching or over water supply, the impacts of climate change can be seen more clearly. Although the effects of climate change will affect water resources and national economy in various ways, it is often marginalized in rural communities of developing countries, where local people's livelihood depends on small scale cultivation and particularly vulnerable (Morton, 2008). Therefore, there is an increasing need for impact assessment of climate change studies globally as the research communities pay attention to this problem.

1.2 Literature review

Over the past decades, there was much research on the impacts of climate change on various fields, ranging from the ecosystem (animals, plants, extinction of species), human health, economic development (industries, agriculture, tourism, culture), and so on. Several

studies have been conducted on the agriculture field since climate change and agriculture have a strong relationship and direct impacts.

1.2.1 Approaches to climate change impact assessment on agriculture

Generally, assessing the impacts of climate change can be implemented through several standard processes, including the simulation of a variety of socio-economic and physical processes (Bureau of Meteorology, 2016). Some of the processes may be well-known; some are not. Thus, the steps that researchers can follow are to consider what is known, what is not yet known, and how researchers can identify any uncertainties that occur with their knowledge.

There are two methods that researchers typically investigated their research area; these are mentioned as ‘top-down’ or ‘bottom-up’ approaches (Bureau of Meteorology, 2016). The top-down approach was primarily applied to climate impact studies over the decades and continues to happen in the future. This process commonly includes these steps: (1) Representing of different climate change scenarios; (2) global or regional climate simulation; (3) downscaling step, and; (4) assessing the outputs from the model. The bottom-up approach, on the other hand, starts with the identification of natural risks that the system may encounter under the current climate. It often takes into consideration other non-climate factors that may affect system performance and not assessed it in isolation. For example, the effects of farmers’ cultivating behaviors on agricultural water demands in the context of climate change may also be taken as one of the factors when assessing the climate change impacts on the region. However, some researches attempt to integrate two approaches into their studies. Ajay (2014) assessed climate change adaptation options using a combination of top-down and bottom-up approaches. They take into consideration stakeholders’ effects on prioritizing adaptations while applying regional climate model outputs with SRES A1B scenario to simulate river runoff using the WEAP model in Kangsabati river catchment in India (Bhave et al., 2014). Another research used the same combined method is from J. R. A (2015). They used a “novel integrated top-down and bottom-up planning approach,” focusing on multi-stakeholders’ involvement in Indonesia.

The question that arises from impact assessment studies is that which approach is suitable. In many cases, the most appropriate method is determined by the intended application of the studies. If the studies’ primary purpose is to assess the system responses under changing conditions of climate, climate model-based provides an explanatory base in testing system out. However, if the intended application is bound with real-life and mostly affected by non-climate factors, then the bottom-up approach may be better suited (Bureau of Meteorology, 2016). For this research, the intended application is to see how different the water demands for crops will be in the future due to changing climate conditions (temperature and precipitation). Thus, a top-down approach with the typical four above mentioned steps is a choice.

Over the past decade, many types of research regarding impact assessment of climate change on irrigation demands using a top-down approach have been conducted. Yano et al. (2007) modeled the regional impact of climate change on irrigation demand and crop growth in a Mediterranean environment of Turkey. This research projected climate change scenarios of the local using three global climate models (GCMs) including the second version of the Canadian Global Coupled Model (CGCM2), ECHAM4 by Max Planck Institute for Meteorology, and Meteorological Research Institute of Japan (MRI) with A2 scenario in the Special Report on Emission Scenarios (SRES). The simulation result predicted an increase in water demand for irrigation of wheat in the Mediterranean environment due to decreasing precipitation using CGCM2. However, according to this research, there were decreasing trends of evapotranspiration of crops over the calculated periods, which is in contrast to the increasing temperature of the climate change scenario. De Silva et al. (2007) studied the impacts of climate change on irrigation water requirements in the paddy field of Sri Lanka. They predicted increases of 13 to 23% of irrigation water demand due to decreases in the amount of rainfall. This research also suggests that evapotranspiration may increase by 3% with rain season ending sooner. Interestingly, not all parts of Srilanka would suffer from harmful effects of changing climate, but some parts to the far south of the country might experience a positive change of rice production during the wet season. Another research conducted by Vu et al. (2014) assessed changes in irrigation demand under the context of climate change in the Cua Dat reservoir's area in Viet Nam based on the outputs of the UK Hadley Centre for Climate Prediction and Research Model (HadCM3). This research also suggested increases in precipitation of 2%-3%, along with irrigation demand for crops rising from 5.9% to 7.6% throughout the periods of 2020s, 2050s, and 2080s. However, the researches as mentioned above applied directly the outputs of GCMs, whose resolution is relatively coarse (horizontal resolution of Had-CM3 is 3.75×2.5 degrees in longitude \times latitude, corresponding to a spacing of roughly 300 km and those of CGCM2 is 3.7×3.7 degrees longitude \times latitude). We need a finer resolution model to get a more precise simulation, especially right when working on a small research area. This is where downscaling methods started growing. Another remaining issue is that those researches only take into account one or two specific crops such as wheat, rice, or maize. A comprehensive crop pattern is necessary when dealing with climate change impacts on irrigation demands and a base for policy makings and to propose recommendations for the region to reduce any negative consequences.

1.2.2 Researches on global climate models

Global climate models or general circulation models (GCMs) are a combination of complex mathematical models representing primary components of the climate system, including ocean, land cover, atmosphere, and sea ice and their interactions (GFDL, 2014). It is

the main tool for exploring the response of climate systems to a variety of forcings, making future climate predictions over long periods of hundreds of years (Church et al., 2013). Four major components institute a climate model. These are:

- The atmospheric part simulates clouds and aerosols. This component plays a central role in the transportation of water and heat around the global model.
- The land surface component, which takes charge of simulating the characteristics of the surface, including land cover (vegetation, snow, lake, river, soil water, and carbon-storing).
- The ocean component, which simulates movements of currents and biogeochemistry, is the major storage of heat and carbon in the climate system.
- The sea ice component, which controls solar radiation absorption, air-sea fluxes, and water exchange (GFDL, 2014).

Many different types of GCMs are established by institutes, research centers, or laboratories around the world. Some of the typical GCMs whose outputs are widely used in the research community can be named as Hadley Centre Coupled Model, version 3 (HadCM3) developed by the Hadley center in the United Kingdom; Geophysical Fluid Dynamics Laboratory Coupled Model version 3 and 4 (GFDL CM3, GFDL CM4) established by the Geophysical Fluid Dynamics Laboratory, America; Meteorological Research Institute Coupled Global Climate Model version 3 (MRI-CGCM3), developed at the Meteorological Research Institute of Japan; the Community Climate System Model version 4 (CCSM4), developed at the National Center for Atmospheric Research (NCAR) under the support of the National Science Foundation (NSF), America; and recently, global climate has been simulated and freely available for access with the name “Database for Policy Decision Making for Future Climate Change” (d4PDF) (Mizuta et al., 2012).

Atmospheric (AGCMs) and oceanic GCMs (OGCMs) are two major types of GCMs. They can be combined to form an atmosphere-ocean coupled global climate model (AOGCM or CGCM). Most of AOGCMs simulate the global climate with horizontal resolution coarser than 100 km (Collins et al., 2014). These resolutions are not detailed enough to assess climate change impacts, which relates to small-scale climate events. These climate events are usually affected by local characteristics such as topography (hills, mountains), and coarse-resolution models are not suited to simulate these phenomena like tropical cyclones, monsoons, and blocking (Fowler et al., 2007). However, in some regions like Asia, tropical cyclones and monsoons play an essential role in the region’s climate pattern and leading causes of water-related problems and natural risks. Therefore, changes in these climate activities are the key to take into consideration when performing climate change impact assessment upon these regions. To resolve these issues, a high-resolution AGCM with a spacing of 60 km has been introduced to the research community (Kitoh & Endo, 2016). In this model, sea surface temperature is described as lower boundary conditions. Furthermore, a higher resolution (20 km) simulation was made with a regional climate model over Japan by the downscaling method (Kanada et al., 2012). The results of these models are now being used extensively for a variety of impact assessment of natural disasters, including flooding, storm surge, as well as impacts related to agriculture, water resources, human and ecosystem health.

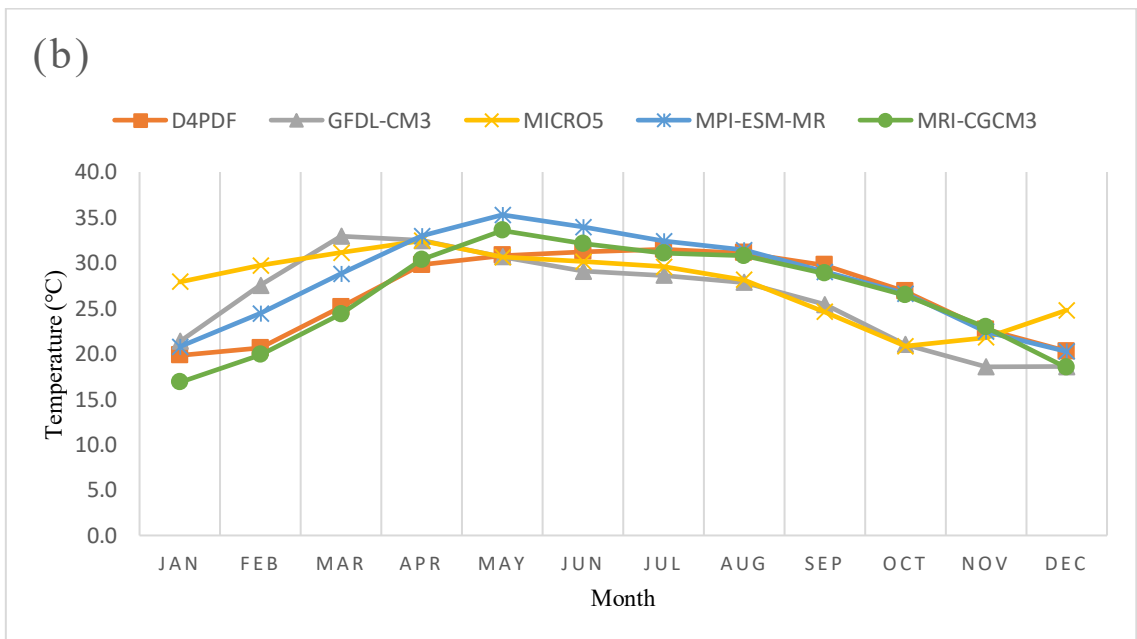
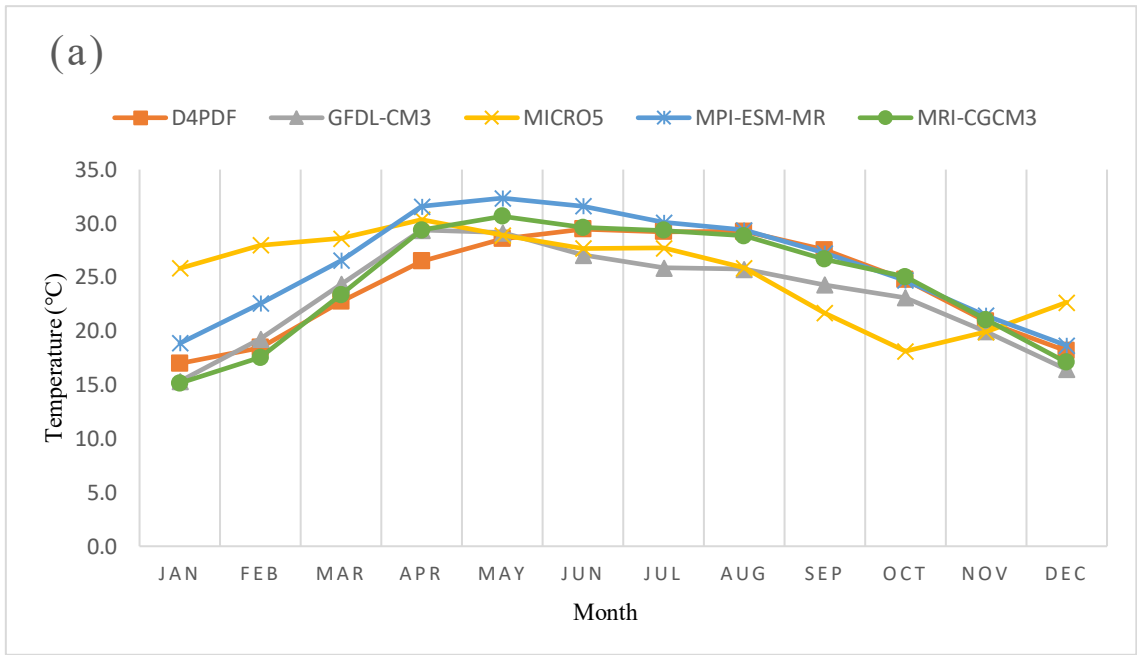


Figure 1.1 Comparison of projected temperature from some GCMs over the research area for (a) 2040-2049; and (b) 2090-2099

Figure 1.1 compares the temperature projection of d4PDF and various GCMs in Coupled Model Intercomparison Project 5 (CMIP5) for the periods 2040-2049 and 2090-2099. The input data for model comparison is obtained from the CMIP5 data portal (<https://esgf-node.llnl.gov/search/cmip5/>) and extracted to grid-site over Thanh Hoa area using Arc-Map – make netCDF table view function. It is noted that d4PDF produces average temperature among GCMs for the research area without being significantly overestimated or underestimated. With the above-mentioned advantages of d4PDF upon this research’s purpose, listed as high resolution, good representation of monsoon rainfall over Asia, and close-to-real temperature simulation of this research area, d4PDF is chosen as input GCMs.

1.2.3 Researches on downscaling methods and bias correction

Nowadays, there are increasing demands of climate information utilizing for decision makings at regional and local levels to address risks caused by changing predicted climate and its potential impacts. Climate change projections provided at the global and continental-scale are available with its simulation results to the end of the 21st century (Lemke et al., 2007). These simulations, however, do not fit the demands of sub-national adaptation activities, which require smaller scales climatic information. Although GCMs are valued predictive tools, they can not take into account the small-scale changes of climate variabilities because of their low resolution. Many landscapes such as mountains, lakes, rivers, land cover, and climate components like the tropical monsoon and convective clouds can play a role in the difference between large scale and local climate characteristics. These heterogeneities in a specific region are a key for decision-makers when they assess impacts of climate change on that area, usually at scales of 10-50 kilometers (Trzaska & Schnarr, 2014). In order to bridge the gap between small-scale resolution requirements and large-scale input data from GCMs, a process named downscaling has been developed (Mearns, 2009).

Downscaling can be implemented in the spatial and temporal processes. The spatial downscaling approach is a method to obtain a finer-resolution spatial climate from the coarser-resolution of GCMs, for example, 300 kilometers of resolution to a local scale resolution of 20 kilometers, or even to a hydrological station scale. Temporal downscaling, on the other hand, obtain fine-scale temporal climate information from the coarse-scale output of GCMs, for instance, hourly rainfall from daily or monthly rainfall information. Generally, it can be classified into two major downscaling approaches: dynamical downscaling and statistical downscaling. Each of these has its advantages and disadvantages for application. This will be discussed in the next part.

1.2.3.1 Dynamical downscaling

Dynamical downscaling techniques depend on the Regional Climate Models (RCMs) usage, which is similar to a GCM but with higher resolution. Dynamical downscaling using in RCMs takes large-scale climatic information from GCMs, and add more detail information of land covers, topography, and complex physical processes to create realistic climate information of around 20 to 50 kilometers. Because the RCMs are nested in GCMs, the quality of dynamical downscaling therefore depends on the accuracy of large-scale forcing of GCMs and usually its bias (Seaby et al., 2013). Despite supplementing the important features of the region, which may be underestimated by the GCMs, RCMs are still subject to have systematic biases, and errors occurred, and thus, they often require a bias correction following.

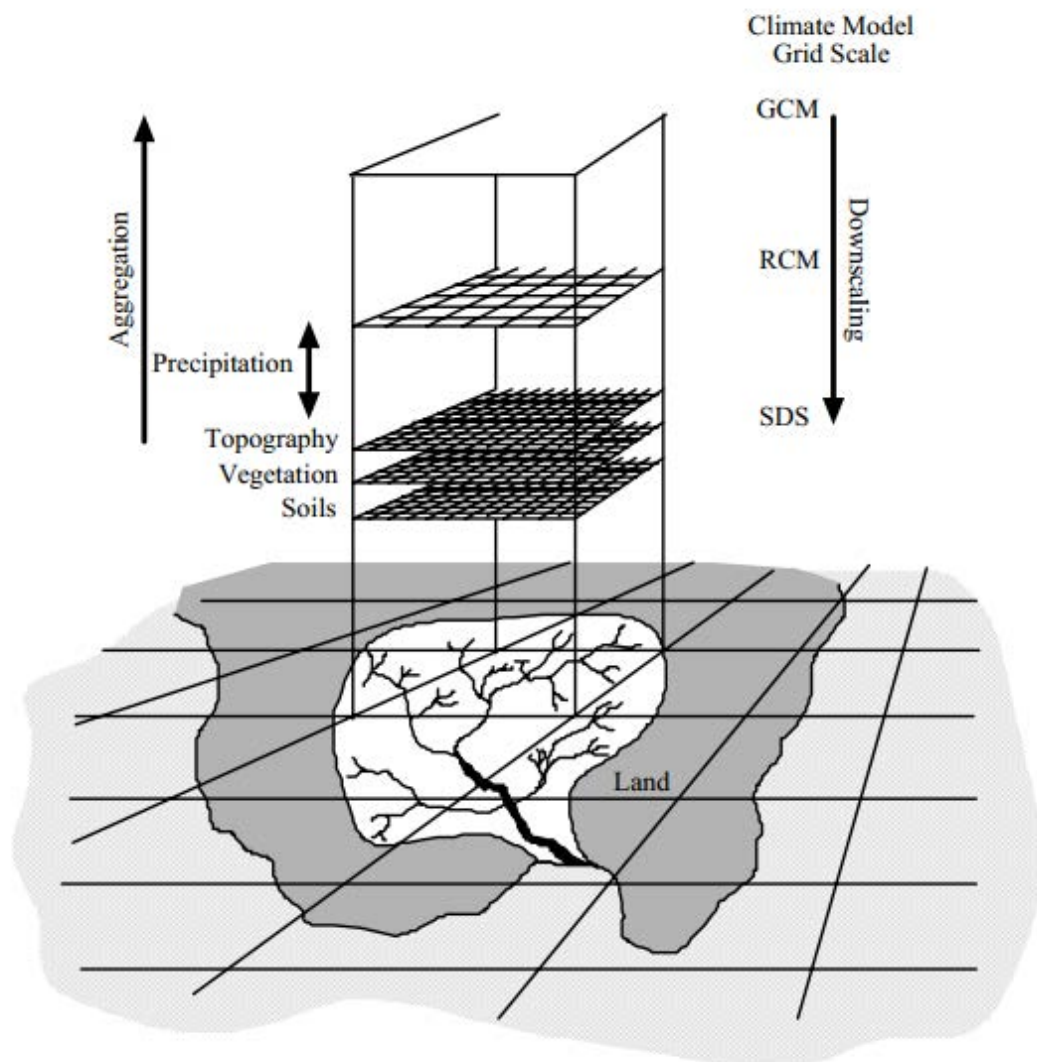


Figure 1.2 Illustration of the general approach to downscaling (Wilby & Dawson, 2007)

1.2.3.2 Statistical downscaling

The statistical downscaling method includes the formation of empirical relationships between observed historical data and large-scale climate predictors. After the connection is created and validated, the future local climate variables will be simulated based on prospective large-scale predictors from GCMs. Statistical downscaling is capable of generating climate projections at specific sites, which RCMs are unable to provide since their spatial resolution is limited to a 20 to 50 kilometers (Trzaska & Schnarr, 2014). However, this method is based on a critical assumption that the relationship of present local variables and large-scale predictors remains valid in the future (Zorita & von Storch, 1999).

1.2.3.3 Comparison of statistical and dynamical downscaling

As mentioned, two downscaling methods have their own merits and drawbacks. The table below summarizes the principal strength and weakness of two types of downscaling approaches, statistical and dynamical downscaling.

Table 1.1 Comparison of statistical and dynamical downscaling

	Statistical downscaling	Dynamical downscaling
Strengths	<ul style="list-style-type: none"> Downscaling to the station-scale climate information from large-scale GCM output Low cost, do not require heavy computing resources and easily transferable Uncertainty analyses are permitted through ensembles of climate change scenarios Generally applicable for any predictand-predictor 	<ul style="list-style-type: none"> 10–50 km resolution climate information from large-scale GCMs outputs Based on physical processes that are treated consistently upon different external forcings. A good representation of complex atmospheric processes including precipitation Consistency with GCMs
Weakness	<ul style="list-style-type: none"> Dependent on the reliability of GCM boundary forcings Results affected by area size and location Requires long term and high-quality data for model calibration Predictor–predictand connections are usually non–stationary Choice of predictors affects results Choice of empirical transfer equation affects results Always applied off-line; therefore, the host GCMs do not get feedback from users 	<ul style="list-style-type: none"> Dependent on the reliability of GCM boundary forcings Results affected by area size and location Requires significant computing capability and resources Ensembles of climate change scenarios are hardly generated Initial boundary conditions affect results Scheme of cloud/ convection affects precipitation results New regions are not ready to be transferred. Typically applied off-line; therefore, the host GCMs do not usually get feedback from users

Generally, statistical downscaling methods have several practical benefits over dynamical downscaling approaches. Specifically, in situations where local climate change impacts need fast assessments with low cost, statistical downscaling appears a more promising option. Due to their low computational requirement and expense, statistical downscaling techniques become popular among climate change impact assessments (Khan et al., 2006). Figure 1.3 shows stages that we could follow to determine which downscaling method is suitable for the research area.

1.2.3.4 A combination of downscaling and bias correction

The systematic biases of GCMs impede their application in climate-change effect analysis, such as downscaling, and lead to errors. As a response, bias correction (BC) has become a necessary prerequisite for climate change research. Many bias correction methods ranging from the simple process of scaling techniques to the complicated distribution mapping techniques, have been built to correct biases from GCMs and relevant climate models (Teutschbein & Seibert, 2012). Generally, a linear or non-linear method, which adjusts climate variables based on the differences between observed and simulated mean, is included in the scaling approach.

Mahmood. (2012) introduced a combination of statistical downscaling method and bias correction to simulate future precipitation and temperature in Jhelum basin and showed an excellent performance with R^2 reaching 0.89 for rainfall and 0.99 for temperature during validation. The bias correction method used in Mahmood's research was the linear scaling method (LS) discussed further in Salzmann et al., (2007). This LS method applies constant corrected factors that are calculated by the difference between observations and GCM simulations for each month. This approach can adjust the climate factors when monthly average values are involved. In this method, the temperature is corrected by adding a constant, and precipitation is adjusted by a multiplier.

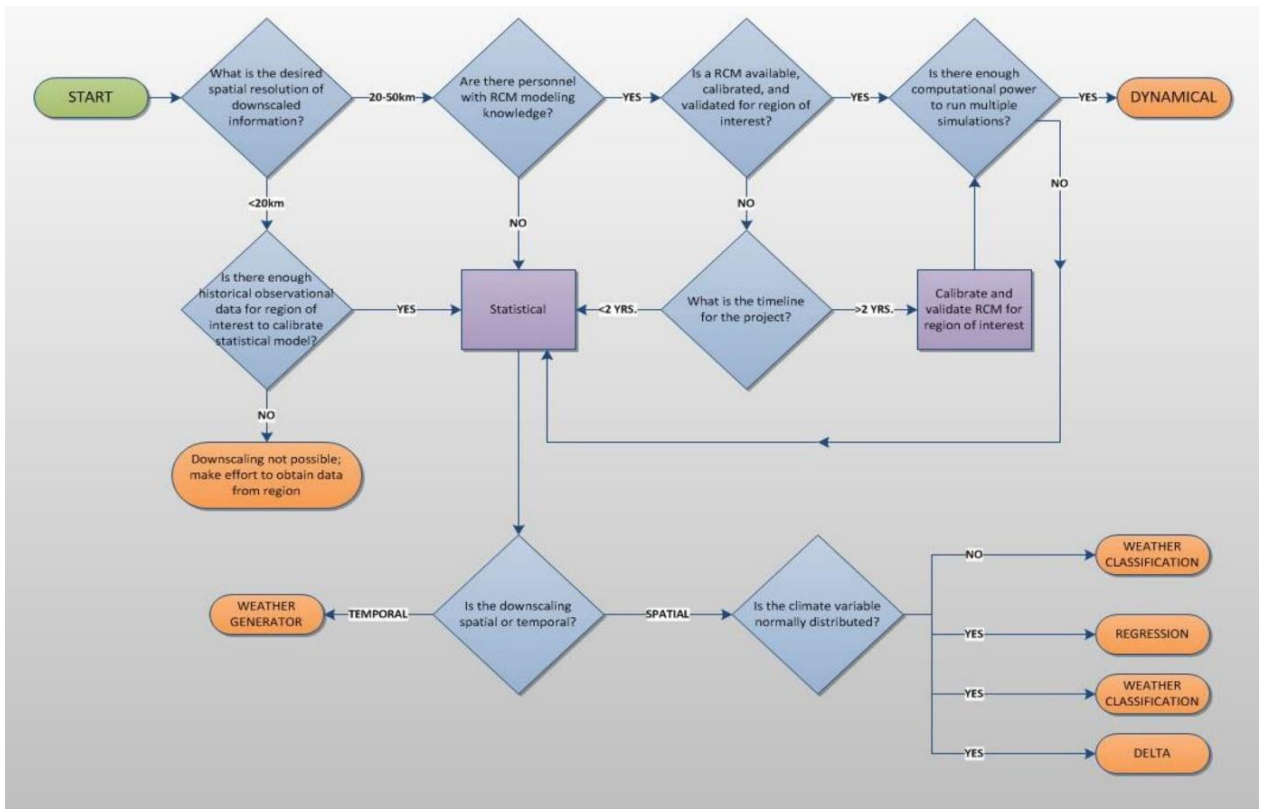


Figure 1.3 Flow of stages to determine the downscaling method (Khan et al., 2006)

1.2.4 Researches on irrigation requirements

Agriculture nowadays is facing new challenges that require advanced approaches in management compared to conventional ways. Formerly, irrigated agriculture relies mainly on rainfall and water supply through small-scale manual water pumpings and channels. However, present issues include limited water resources with many competing users, water quality and quantity degradation's risk, as well as weak economic development planning, put this sector on a need for change. Overcoming these challenges requires enhanced prediction of irrigation water requirements.

Irrigation water requirements are defined as the amount of water (or quantity or depth) in addition to precipitation needed for crops to produce desired quality and yield, and to maintain acceptable salt balance in the root zone (Martin, 1993). The quantity of water is required for uses in irrigation scheduling at a specific field and design water demands for management, planning, and development of agriculture. Generally, the precipitation timing and amount have a strong influence on irrigation water requirements in agriculture. For example, in arid regions, annual precipitation is usually less than 10 inches (254 cm), irrigation is a requirement to grow crops fully. However, in the humid areas, where typically receive more than 30 inches (762 mm) of annual rainfall, irrigation may not be a must for cultivation since the amount of rainfall normally exceeds evapotranspiration in most of the time. Nonetheless, in some exceptions, drought may occur, reducing yield or even causing crop loss, especially for crops cultivated on shallow and sandy soil (Martin, 1993). In other regions with climatic conditions ranging between those regions above, irrigation may or may not be required depending on the climate characteristics of the areas. For instance, in semiarid regions (frequently receive from 15-20 inches, corresponding to 381-508 mm), crops can develop without being watered but are subject to droughts, which reduce crop yield and may lead to crop failure. Subhumid regions (20-30 inches or 508-762 mm rainfall per year) are characteristically recognized by short and dry periods. Irrigation may be necessary for short periods of cultivation in these regions, relying on the available capacity of soil water storage and crop rooting depth.

The primary purpose of irrigation is to provide crops with sufficient water to achieve optimum yields and designed harvested products. The requirement of timing and quantity of irrigated water is decided by the existing climatic conditions, crop patterns, and its growing stages, soil properties, and the rooting information. Each crop has a critical growth period in which a small moisture deficiency can negatively impact crop yields. Critical water demands periods change from crop to crop. Soil moisture during crop's critical water demands should be sufficiently maintained to prevent the crops from lack of water. To avoid a reduction in quality or yield, irrigation should be supplemented to the plant before available water in the root zone becomes depleted.

Maintaining the soil water within the acceptable range requires information about the addition and extraction of water to the root zone. The main process of soil-water balance is demonstrated in Figure 1.4. The field water balance can be written generally as:

$$F_g = ET_c + D_p + RO - P - GW + SDL - \Delta SW \quad (1-1)$$

F_g = gross irrigation required during the period

ET_c = amount of crop evapotranspiration during the period

D_p = deep percolation from the crop root zone during the period

RO = surface runoff that leaves the field during the period

P = total precipitation during the period

GW = groundwater contribution to the crop root zone during the period

SDL = spray and drift losses from irrigation water in air and evaporation off of plant canopies

ΔSW = change in soil water in the crop root zone during the period

Equation (1-1) is the basis for the Water Balance development process. Figure 1.4 shows the diagram of the soil-water balance of a crop root zone

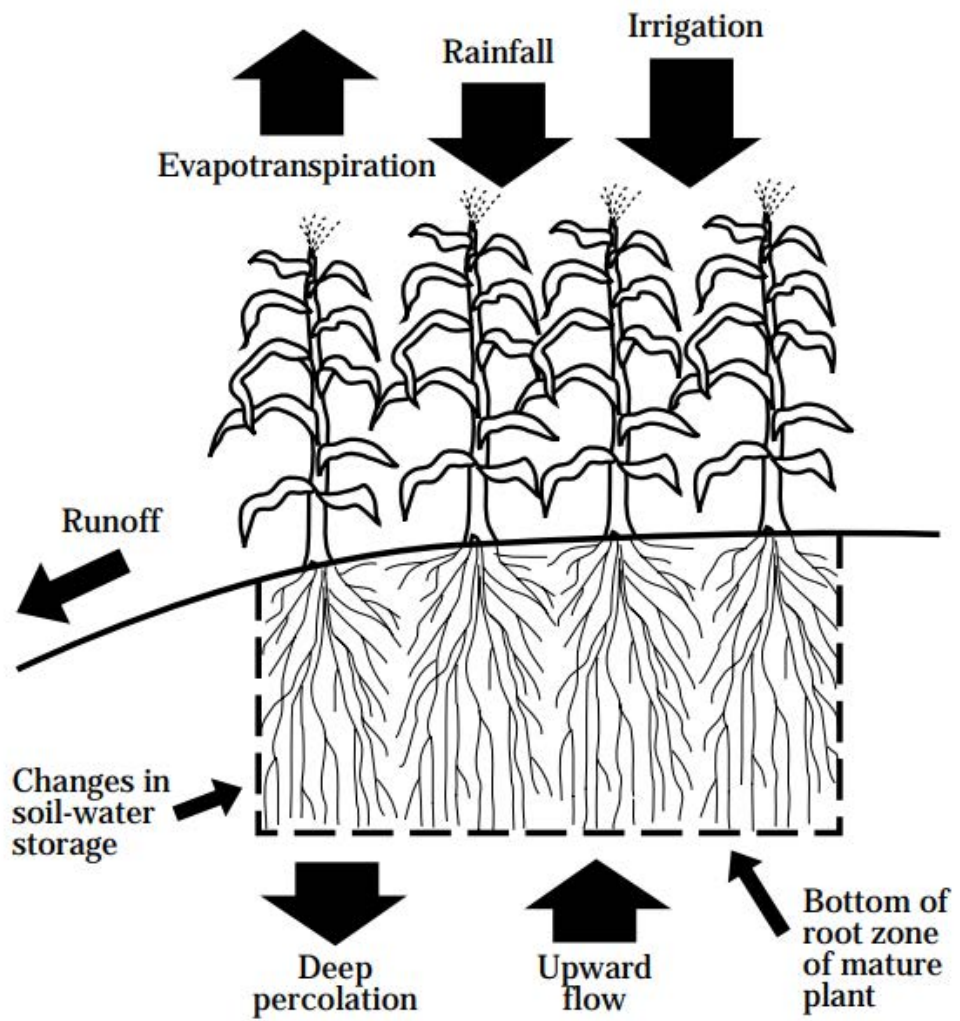


Figure 1.4 Diagram of the soil-water balance of a crop root zone (Martin, 1993).

1.3 Objectives of this study

As mentioned in the literature review, many existing studies assess the impacts of climate changes on irrigation water requirements using the inputs of GCMs directly. However, the resolution of most GCMs is relatively coarse (200-300 km), which might inaccurately represent the small-scale climate of the research area. On the other hand, to comprehensively assess climate change's impacts on irrigation water requirements, all primary crops in the regions should be involved. To overcome these issues, this research uses a high-resolution GCMs of 60 km to downscale to climate station site, and irrigation water requirements of a total of eight major crops are calculated for the region.

The overall objective of this research is to assess the impacts on irrigation water requirements due to changing precipitation and temperature in the future using Statistical Downscaling with high-resolution d4PDF inputs and CROPWAT model. Specifically, for the selected area of the Ma river basin, which belongs to Thanh Hoa province, Viet Nam, the study objectives were:

- Apply the SDSM tool to project precipitation and temperature changes for the Ma river basin based on selected climate change scenarios of the d4PDF model.
- Calculate Crop water requirements for each type of crop in the region for current and future periods using CROPWAT.
- Compare the current and future irrigation water requirements to assess changes in climate.
- Give recommendations to reduce these potential impacts in the future.

CHAPTER 2 METHODS AND MATERIALS

2.1 Introduction

The methods, models, and data needed that were used in this research are discussed. Projection of precipitation and temperature used Statistical Downscaling Model (SDSM), and irrigation water requirement is calculated using the CROPWAT model. Figure 2.1 illustrates the steps that were carried out to assess climate change impacts.

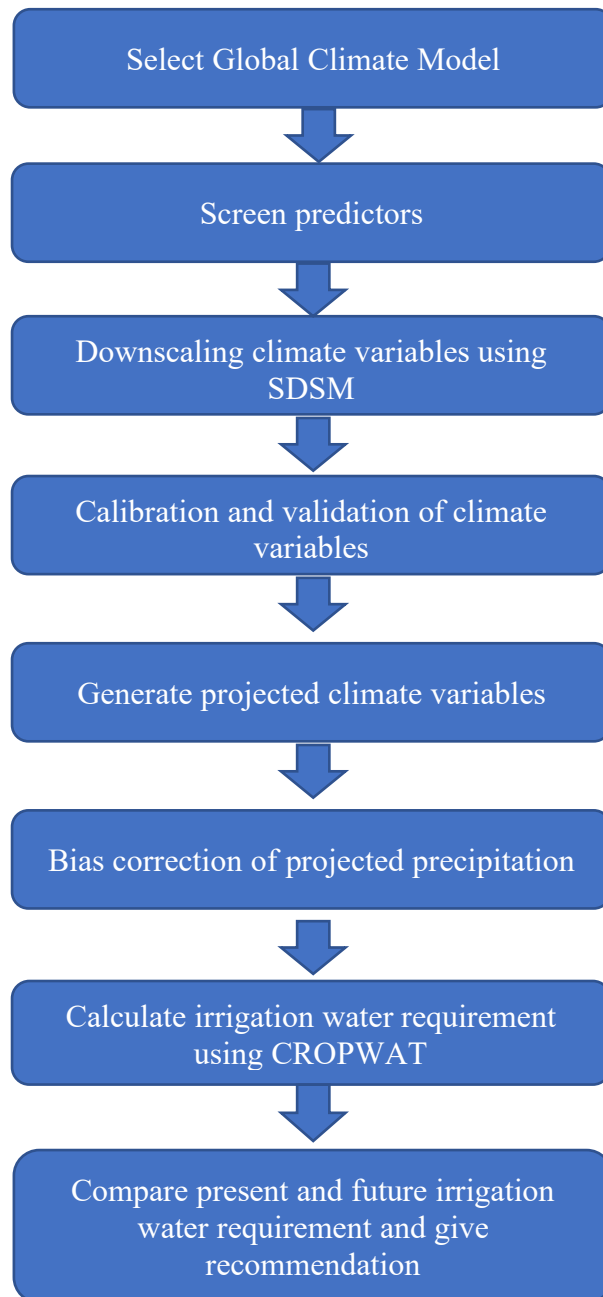


Figure 2.1 Steps to analyze and assess climate change impacts

2.2 Study area

2.2.1 Location

Ma river is the largest river in the Middle of Viet Nam. Its whole basin ranges from the North-Western part of Viet Nam (upper part of the basin), through the territory of Lao People's Democratic Republic to the Middle part of Viet Nam (lower part of the basin). The research area is the lower part of the Ma river basin, which belongs to Thanh Hoa province, Viet Nam. The coordinate was measured as 19°18'N - 20°40'N and 104°22'E - 106°05'E, corresponding to the area of 11.129,48 km² (Ngo, 2007). This is a relatively large area located in the North Central Coast region of Viet Nam, which ranks fifth in the area and third in population among 63 central administrative subdivisions. Due to the transitional characteristics of the region, it appears as a transition from the North to the Middle of Viet Nam in terms of geology, climate, administrative division, and local culture.

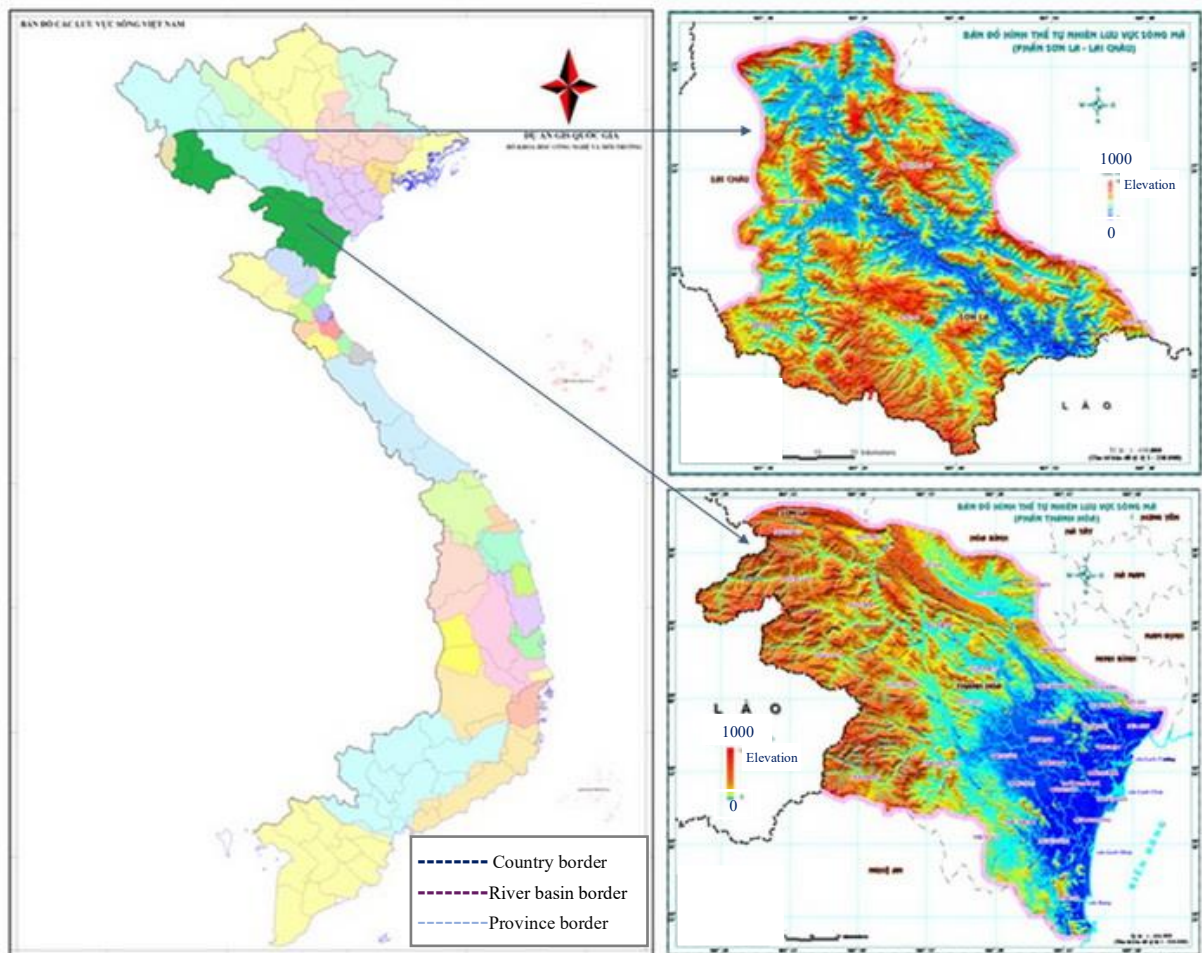


Figure 2.2 Ma river basin map (VAST, 2014)

2.2.2 Climate

The typical climate in the region is tropical monsoon with four distinct seasons. Distribution of rainfall is uneven throughout the year, with total rainfall from May to October takes up approximately 70% of the total amount of rainfall during the year. The average annual rainfall is about 1600-2300 mm, with roughly 90 to 130 rainy days.

The temperature in the region varies following topographical locations, with lower temperatures to the mountainous area (North-West) and higher temperatures to the Delta and Coastal area (South-East). The average temperature is 23-24 °C, with the average number of sunny hours ranging between 1600 and 1800 hours per year, and relative humidity is from 85% to 87%.

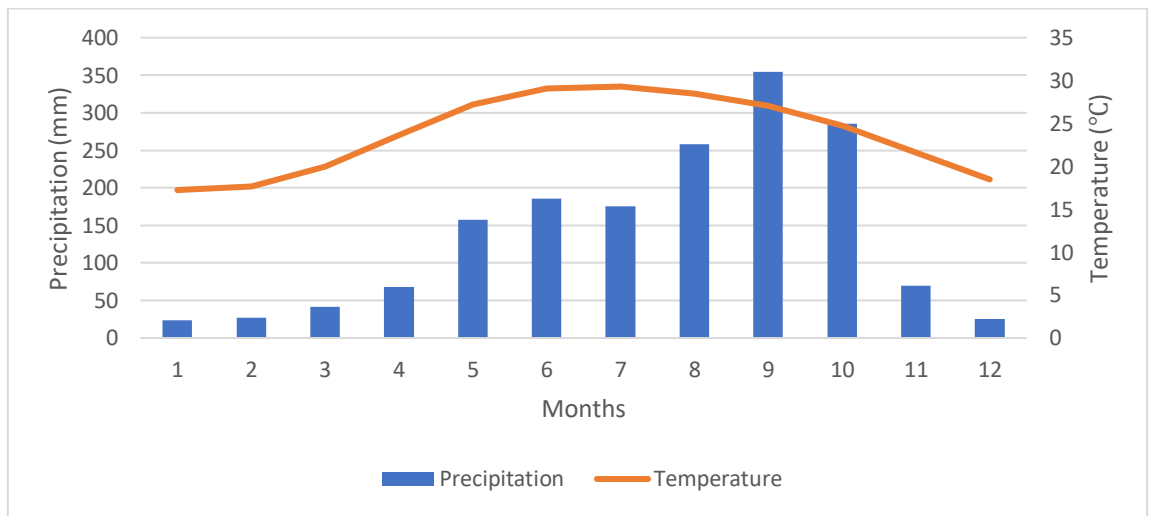


Figure 2.3 Climate graph for Thanh Hoa, Viet Nam for the period 1975-2004

2.2.3 Water Resources

2.2.3.1 Surface water

In the Ma river basin, the irrigation water primarily comes from surface water, which is the flow of the Ma river system including the Ma river (main river) and two major river branches namely Chu river and Buoi river. The total annual amount of runoff generated in the Ma river system is 13.2 billion m³. The Ma river mainstream – the largest river has a capacity of 9.1 billion m³ of annual runoff, Chu river and Buoi river take up a lower amount of runoff (3.2 billion m³ and 0.89 billion m³ annually). Table 2.1 shows the mean monthly river discharge of major rivers in the Ma river basin from 1975 to 2004 (Hoang, 2009).

The surface runoff's quantity of Ma river is not so abundant (4200 m³/ person), approximately at the country's average level, and slightly higher than the world average (4000 m³/ person) (Hoang, 2002).

Table 2.1 Mean monthly discharge of main rivers in the Ma river basin for the period 1975-2004 (Hoang, 2009)

Month	1	2	3	4	5	6	7	8	9	10	11	12
Buoi river	6	5	13	14	20	26	35	59	75	61	20	11
Chu river	40	34	37	38	37	113	144	167	162	271	122	69
Ma river	118	106	109	135	166	367	413	767	757	327	138	121
Ma river system	164	144	159	188	224	506	592	993	995	659	280	201

Unit: m³/s

Surface water in the Ma river basin is used primarily for socio-economic development activities and environmental purposes. Sectors that consume water are domestic use, industry, livestock, and environmental flow (Hoang, 2009), as shown in Table 2.2.

Table 2.2 Water consumption by sectors in the Ma river basin (Hoang, 2009)

Month	1	2	3	4	5	6	7	8	9	10	11	12
Domestic use	24	24	24	24	24	24	24	24	24	24	24	24
Industry	33	33	33	33	33	33	33	33	33	33	33	33
Livestock	24	24	24	24	24	24	24	24	24	24	24	24
Environmental flow	246	223	246	238	246	238	246	246	238	246	238	246

Unit: Mm³

There are lakes and reservoirs in the basin. Their main functions are to control floodings, water supplies, and generate electricity to meet people's demands. The peak runoff usually is during September and October due to the rainy season. Furthermore, there are some lakes and reservoirs which are used for other purposes such as fisheries and recreation.

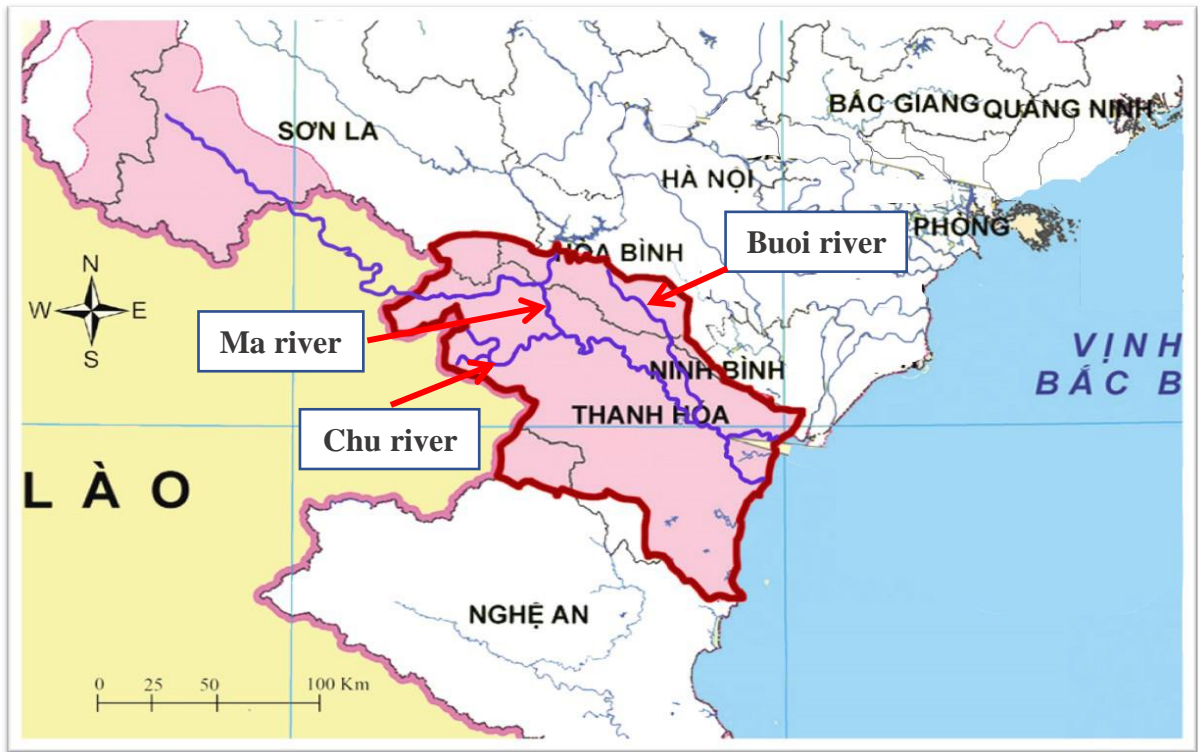


Figure 2.4 Main rivers in the Ma river basin

2.2.3.2 Groundwater

The reserve of groundwater resources is plentiful due to abundant rainfall, concentrated on some main aquifers. 80% of groundwater is exploited by unconsolidated quaternary sediments in the delta area.

Currently, the amount of underground water used for domestic use accounts for the largest proportion of the total amount of underground water extracted annually. This amount of water is withdrawn by households' wells or public water treatment facilities. Due to the high content of iron in the water, this water is usually treated before being put into use. The exploited capacity in this area is about 9000 m³ per day (Hoang, 2002).

2.2.3.3 Land

Thanh Hoa has a natural area of 1,112,033 ha, of which agricultural land is 369,284 ha; forestry production land 454,865 ha; aquaculture land 10,157 ha; unused land of 128,737 ha with groups of land suitable for developing food crops, forestry trees, industrial crops, and fruit trees.

Thanh Hoa has diverse terrain, lower from the West to the East, divided into 3 distinct regions:

- The mountainous and midland area accounts for 75.44% of the province area, the average elevation of the mountainous region is from 600 to 700 m, the slope is over 25°; midland has an average elevation of 150-200 m with a slope of 15 -20°.

- The delta region accounts for 14.61% of the province's area, deposited by the Ma, Song Bang, Yen, and Hoat systems. The average elevation of 5-15 m. This area is the third-largest delta after the Mekong River Delta and the Red River Delta.

- The coastal area covers an area of 110,655 ha, accounting for 9.95% of the province's area, with a 102 km long coastline and relatively flat terrain. The coastal sandy area has an average elevation of 3-6 m, with large tracts of land favorable for aquaculture and development of industrial parks and marine economic services.

Figure 2.5 shows the primary land use in the region. The main cultivated area is located in the Delta, which is relatively flat in terrain and suitable soil for farming rice (in yellow color). The major irrigated crops are rice, groundnut, sugarcane, soybean, maize, potato, and perennial crops.

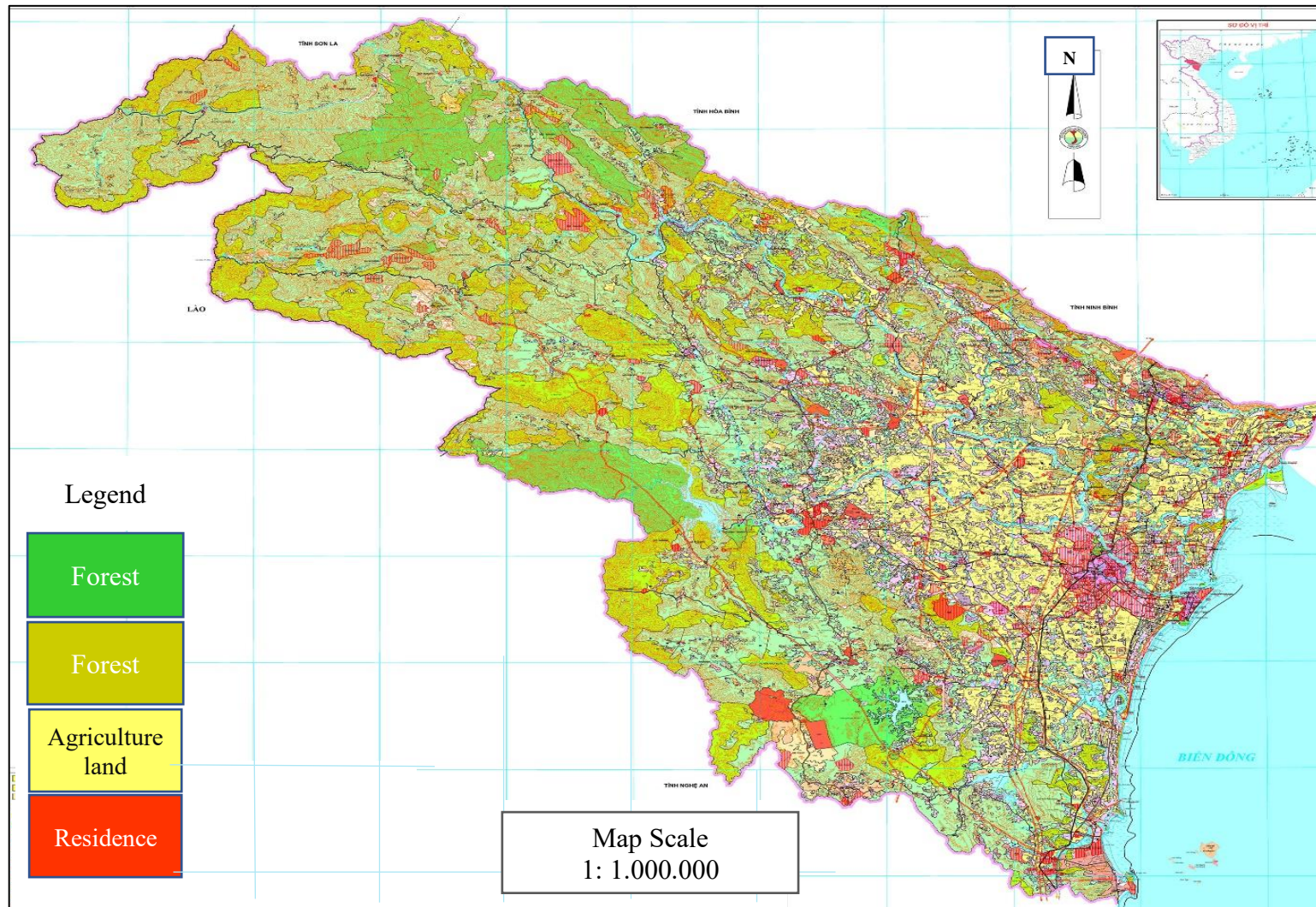


Figure 2.5 Land use map of the Ma river basin, Thanh Hoa province (Thanh Hoa's People Committee, 2013). Legends are translated and added based on the original map

2.3 Methods

2.3.1 Global Climate Model

Database for Policy Decision making for Future climate change (d4PDF) was used as input predictors to simulate the future climatic conditions of the Ma river basin. As mentioned in the literature review, impact assessment of changing climate requires a relatively fine-resolution to obtain a good result, especially the research area belongs to those regions affected by specific phenomena like monsoons and tropical cyclones. With the need for impact assessment research, d4PDF has been formed with 60 km of resolution globally, which is able to represent tropical cyclones, alongside with a dynamical downscaling using the 20 km regional climate model (RCM) over the Japan, which provides sufficient information to simulate heavy precipitation and topographical effects. The d4PDF is formed with the intention of contributing to climate change impact assessment studies. This AGCM used in this model is from the Meteorological Research Institute AGCM, version 3.2 (MRI-AGCM3.2), initially based on the numerical weather prediction model at the Japan Meteorological Agency (JMA, 2007). The model has 640×320 grid cells corresponding to a triangular truncation of 319 with a linear Gaussian grid (TL319) in the horizontal (Mizuta et al., 2012). Its vertical layers consist of 64 levels, ranging from 1000 hPa to 0.01 hPa. There are previous researches that show the capability of AGCM in simulating local climate. Further information can be seen at Kusunoki and Mizuta (2003) for East Asian summer monsoon, and in Endo et al. 2017 for monsoon rainfall.

The experimental structure of d4PDF includes four sets of experiments: a historical climate simulation, a +4-K future climate simulation, a +2-K future climate simulation, and a non-warming simulation for the past (Mizuta et al., 2016). The lower boundary of this model is the sea surface temperature, sea ice concentration, and sea ice thickness. The external forcings (climate forcings) involve greenhouse gas concentration, three-dimensional allocation of aerosols and ozone. Each experiment has 60 years in length and 90 to 100 ensemble members. In the 2-K climate scenario, the surface-mean temperature of the globe is set to be warmer 2 Kelvin than the preindustrial period, starting from 2031 to 2090. For the 4-K scenario, the simulating year starts later, from 2051 to 2110, corresponding to the temperature of the end of the 21st century in the representative concentration pathway 8.5 (RCP8.5)- a scenario of CMIP5. Notably, in these future simulations, the amplitude of warming remained ‘constant’ over the 60 years of simulation (Mizuta et al., 2016). That means the temperature and relevant climate variables in this model are expressed differently in trend in comparison to ‘so-called emission scenario simulations’ of other GCMs in CMIP5 in which the phase of global warming is changing during the simulating period. In other GCMs under the CMIP5, the climate change scenarios use radiative forcings as their input data in which the radiative forcing level increases

over time and reaches 2.6, 4.5 and 8.5 W/m² by 2100 corresponding to the Representative Concentration Pathway 2.6 (RCP 2.6), RCP 4.5 and RCP 8.5 scenarios. Radiative forcing is a “measure of the combined effect of greenhouse gases, aerosols, and other factors that can influence the climate to trap additional heat” (Zeke Hausfather, 2019). With this change in model settings of d4PDF, a large sample size can be obtained (Mizuta et al., 2016).

The d4PDF products are available for 60 years in each of 2031-2090 and 2051-2110. In this research, only the period from 2040-2049 and 2090-2099 are used for simulation. There are two reasons for that. Firstly, the greenhouse gases in d4PDF for 2031-2090 and 2051-2110 is set to values of 2040 and 2090 of RCP8.5, according to the d4PDF experimental setting. The chosen periods (the 2040s and 2090s) in this research aim to represent that setting of d4PDF with respect to RCP 8.5, and hence, comparable results can be made. Secondly, there are little changes in mean temperature within one d4PDF simulation (2031-2090 and 2051-2110) since the mean temperature is set to increase by 2K and 4K for the whole simulation period (Mizuta et al., 2016). This research chose periods from 2040-2049 and 2090-2099 to distinguish with RCP8.5 in which the temperature changes through time.

2.3.2 Statistical downscaling model

The statistical downscaling model was used in this research to obtain future local precipitation and temperature from large-scale predictors of d4PDF. In this process, regressions models were established between local observations and predictors with 60 km of resolution of the d4PDF model. These regression models were then calibrated and validated before being used to simulate future climate scenarios of the Ma river basin.

The SDSM, as comprehensively described in the SDSM User Guide (Wilby et al., 2002), is designed as a decision support tool for evaluating the impacts of local climate change using a robust statistical downscaling technique. SDSM facilitates the development of scenarios of daily climatic variables under current and future climate forcing with several advantages such as low-cost, multiple, and single-site scenarios. Also, the software performs additional tasks of data quality control and transformation, predictor screening, automatic model calibration, necessary diagnostic testing, statistical analyses, and graphing of climate data.

Following downscaling techniques, the structure and operation of SDSM are designed with seven major tasks: 1) quality control and data transformation; 2) screening of potential downscaling predictor variables; 3) model calibration; 4) generation of current weather data using observed predictor variables; 5) statistical analysis of observation and climate change scenarios; 6) graphing of model output; 7) generation of ensembles of *future* weather data using GCM predictors. Figure 2.6 shows the starting screen of SDSM, and Figure 2.7 describes the production of climate change scenarios within SDSM.

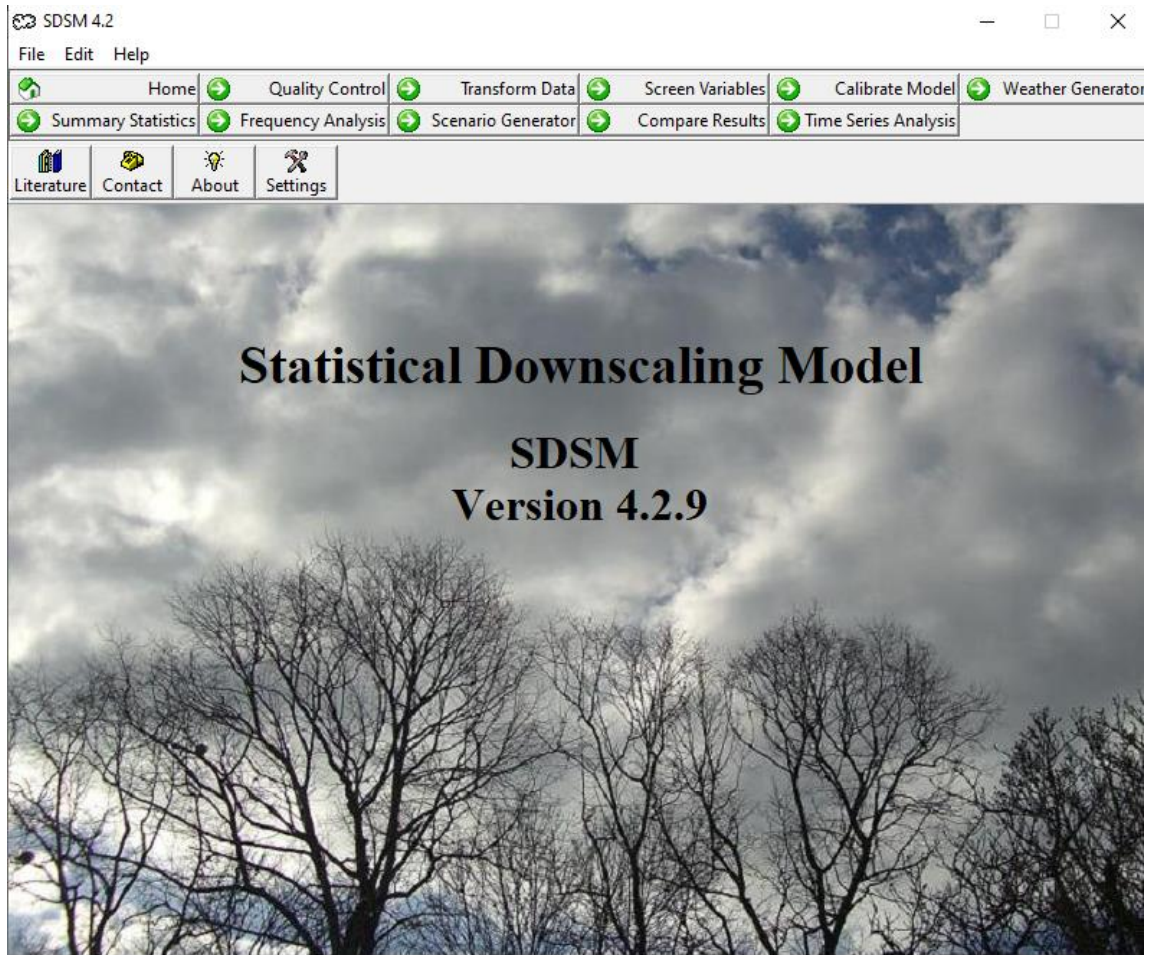


Figure 2.6 Starting screen of SDSM version 4.2.9

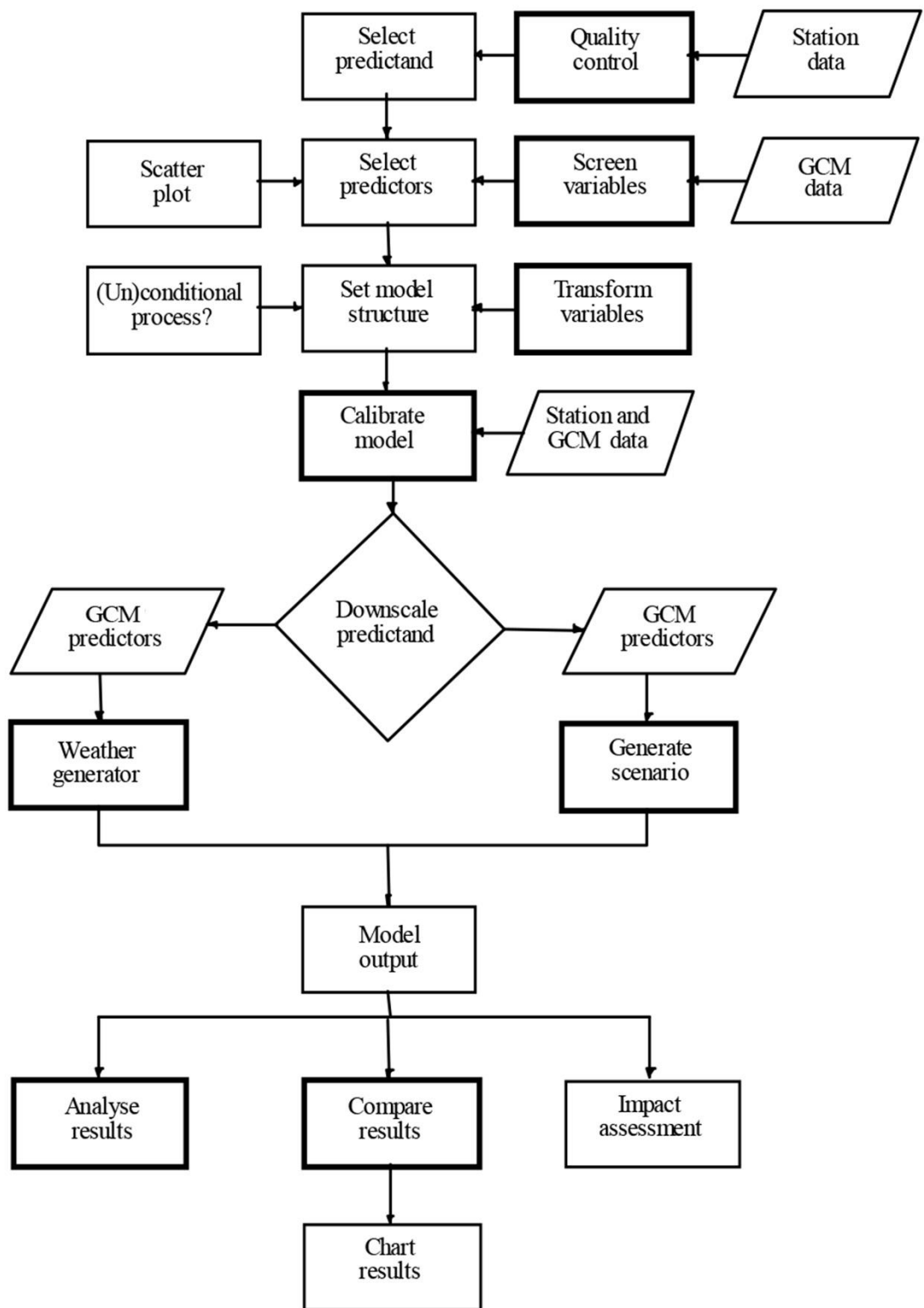


Figure 2.7 Climate scenario generation of SDSM

2.3.2.1 Quality control and data transformation

There are few climate stations that have 100% complete or entirely accurate sets of observation data. In most practical cases, data may be lost or missing for some reason. Therefore, handling of those data is necessary before moving on to the main process. The Quality Control function in SDSM checks the general data errors, missing data, and any data lying outside of the research period. In some cases, the predictors or predictand may need to be transformed before model calibration using transformation (logarithm, inverse, power, etc.). In this study, the transformation facility was not applied since precipitation and temperature are under standard conditions.

2.3.2.2 Selection of predictors for downscaling

Establishing the relationships between large-scale predictors (such as gridded relative humidity) and local predictands (such as station temperature) is essential to most statistical downscaling methods. The main purpose of this process is to support users from selecting downscaling predictors. This process stays one of the most challenging steps in the evolution of any statistical downscaling model since the selection of predictors largely affects the character of downscaled scenarios. In this study, the empirical relationships of predictors-predictands were examined by using the Backward-Forward Stepwise method (Borboudakis & Tsamardinos, 2017). The backward selection process begins with a model in which all candidate variables have been included. For each step, one variable that gives the least significant is removed from the model (probability value is a criterion in this process). The process continues until there is no nonsignificant remaining. Forward selection, on the other hand, starts with no candidate in the model. The highest R-Squared will be selected for the first candidate. At each stage, the candidate variable that increases R-Squared the most is selected and added to the model. The process terminates when no significant variables are remaining (SCSS, 2007). The most effective predictor is the predictor that satisfies and ranks highest in both backward and forward selection.

2.3.2.3 Calibration and validation

The calibration of model function takes a predictand (e.g., precipitation or temperature) together with predictor variables. SDSM will compute the parameters of multiple linear regression equations using the efficient dual simplex algorithm (Wilby & Dawson, 2007). The model structure can be a monthly, seasonal, or annual model specified by the user.

Based on the availability of observed daily data, the dataset of 1975-2004 is used for calibration of precipitation and temperature. It is also recommended by the IPCC for using 30

years as the baseline because it is considered long enough to define local climate conditions as it is likely to have all wet, dry, warm, and cold periods (Gebremeskel et al., 2004). In this research, SDSM is established with selected d4PDF predictors using the monthly model. The Nash–Sutcliffe model efficiency coefficient (NSE) and standard error are used to evaluate the performance of SDSM (Huang et al., 2011).

With the created models, precipitation and temperature are simulated for 1975-2004 using historical d4PDF predictors. The SDSM outputs are compared to observed data by using NSE and standard error for precipitation and temperature for the calibration and validation periods. NSE shows the accuracy of SDSM in data prediction and standard error is used to observe the variability of data predicted by SDSM. In order to observe the pattern and variation of data, many SDSM users choose to plot observed and simulated data (Dibike & Coulibaly, 2005; Wilby et al., 2002). In this study, the monthly mean simulated precipitation and temperature computed by SDSM using historical d4PDF predictors are plotted against the observed data for each year of the calibration period. Following this, the mean monthly simulated temperature and precipitation are then graphically compared with observed data for the validation period.

In this research, the bias correction (BC) method, which is explained in detail below, is applied for downscaled precipitation attained by the SDSM using d4PDF predictors to obtain a more realistic and unbiased future climate data. BC was first validated for the period of 2005-2011 before applying it to the future downscaled data. In this method, the mean biases for each month, which need to be adjusted in the validation period, are obtained from the period of 1975-2004 by using downscaled data of SDSM and observed data. These biases are then adjusted to the downscaled data for the period of 2005-2011. The corrected downscaled data (precipitation) is compared with observed data by using the same abovementioned indicators, and only corrected downscaled data is graphically plotted. After successful validation, BC is applied to the future downscaling of the precipitation with their respective months.

2.3.2.4 Data analysis

Both derived SDSM simulations and observed climate data can be analyzed with this mean. The data analysis is based on selected criteria such as monthly/seasonal/annual means, maximum, minimum, sums, and variances. Once analyzed, data will be available for the next stage – comparison.

2.3.2.5 Scenario generation

The Generate Scenario function produces ensembles of synthetic daily weather given the atmospheric predictors from d4PDF. The calibrated and validated parameters from the calibration and validation processes are used in this scenario generation. The scenarios in this research are determined according to the future simulations of d4PDF, but suitable periods are selected for simulation. In d4PDF, two scenarios are available. One scenario includes the 2K simulation in which global mean temperature increase 2 Kelvin than the preindustrial period and the greenhouse gas concentration corresponding to the value in 2040 of the RCP8.5 scenario in the Coupled Model Intercomparison Project 5 (CMIP5). This 2K simulation starts from 2031 to 2080. The other future simulation is 4K simulation, which assumes global mean temperature increase by 4 Kelvin and greenhouse gases equivalent to the value of 2090 of the same RCP) starting from 2051 to 2110. In both scenarios, the amplitude of warming is kept constant throughout 60 years of simulation. In other words, the mean temperature remains the same within a simulation period (2031-2080 and 2051-2110), and these two scenarios are designed not to see changes of climate through the time as a continuous period, but see the differences among periods to periods (present and two future periods). This setting of d4PDF is different compare to other conventional climate models in CMIP5, with the purpose of “obtaining a large sample size under the same specified stage of global warming” (Mizuta et al., 2016). Therefore, to avoid misunderstandings, the scenario in this research is set to two periods: the 2040s simulation from 2040-2049 and the 2090s simulation from 2090 to 2099. The precipitation and temperature are simulated by SDSM for the 2040s and 2090s periods using validated parameters.

2.3.2.6 Bias correction

The linear scaling method (LS) is applied in this research to eliminate the bias coming from the daily time series of downscaled data (Sharma et al., 2007). This bias correction method applied to this research is mainly similar to the technique discussed in Mahmood (2012). In this method, the biases are attained by dividing (precipitation case) and subtracting (temperature case) the long-term monthly mean observed data (for the calibrated period of 30 years) with the simulated data generated by SDSM. However, for this particular case, LS is used for only the case of precipitation simulation since it shows a strong bias compare to the temperature case.

$$Pbc_future = Psi_future \times \frac{Pob_{1975-2004}}{Psi_{1975-2004}} \quad (2-1)$$

Where:

Pbc_future is the bias-corrected daily time series of precipitation for the future periods (the 2040s and 2090s)

Psi_future is the downscaled precipitation of scenario in the future (generated by SDSM for the 2040s and 2090s).

$Pob_{1975-2004}$ is the long-term average monthly observed of precipitation (for the period 1975-2004).

$Psi_{1975-2004}$ is the long-term average monthly downscaled of precipitation generated by SDSM (for the period 1975-2004).

Precipitation variability is mainly affected by two factors: frequency and intensity (Sharma et al., 2007). The application of this method in this study is to correct the amount of precipitation rather than frequency and to remove any systematic errors that belong to SDSM in the downscaling process. The research assumed that the frequency is accurately simulated by SDSM (Mahmood, 2012).

2.3.2.7 FAO Irrigation requirement calculation

Once the future climatic condition of the Thanh Hoa station is determined, this will be input data beside crop and soil features to calculate irrigation water requirement (IWR) of the research area. In this research, the CROPWAT model is used to compute crop water requirement (CWR) and IWR following the guidelines of FAO in FAO Irrigation and drainage paper No. 56 (Allen et al., 1998). To calculate CWR, information of reference evapotranspiration (ET_o), which is evapotranspiration of crop under reference condition is needed. In this research, the monthly average temperature of the climate station, relative humidity, wind speed, and sunshine duration is required as input data for calculation of ET_o using the Penman-Monteith method proposed by FAO in 1990.

$$ET_o = \frac{0.408\Delta(R_n - G) + \gamma \frac{900}{T + 273} u_2 (e_s - e_a)}{\Delta + \gamma(1 + 0.34u_2)} \quad (2-2)$$

where:

ET_o reference evapotranspiration [mm day⁻¹],

R_n net radiation at the crop surface [MJ m⁻² day⁻¹],

G soil heat flux density [MJ m⁻² day⁻¹],

T mean daily air temperature at 2 m height [$^{\circ}\text{C}$],

u_2 wind speed at 2 m height [m s^{-1}],

e_s saturation vapour pressure [kPa],

e_a actual vapour pressure [kPa],

$e_s - e_a$ saturation vapour pressure deficit [kPa],

Δ slope vapour pressure curve [$\text{kPa } ^{\circ}\text{C}^{-1}$],

γ psychrometric constant [$\text{kPa } ^{\circ}\text{C}^{-1}$].

The net radiation at the crop surface R_n is the difference between the net shortwave radiation (R_{ns}) and the net longwave radiation (R_{nl})

$$R_n = R_{ns} - R_{nl} \quad (2-3)$$

R_{ns} : Net shortwave radiation [$\text{MJ m}^{-2} \text{ day}^{-1}$]

R_{nl} : Net longwave radiation [$\text{MJ m}^{-2} \text{ day}^{-1}$]

The net shortwave radiation (R_{ns}) is the balance between incoming and reflected solar radiation, as shown in Equation (2-4)

$$R_{ns} = (1 - \alpha)R_s \quad (2-4)$$

α : albedo or canopy reflection coefficient, which is 0.23 for the hypothetical grass reference crop [dimensionless]

R_s : the incoming solar radiation [$\text{MJ m}^{-2} \text{ day}^{-1}$].

The incoming solar radiation R_s is calculated with the Angstrom formula which includes solar radiation to extraterrestrial radiation and relative sunshine duration, as shown in Equation (2-5)

$$R_s = (a_s + b_s \frac{n}{N}) R_a \quad (2-5)$$

where

n actual duration of sunshine [hour],

N maximum possible duration of sunshine or daylight hours [hour],

n/N relative sunshine duration,

R_a extraterrestrial radiation [$\text{MJ m}^{-2} \text{ day}^{-1}$],

a_s regression constant, expressing the fraction of extraterrestrial radiation reaching the earth on overcast days ($n = 0$),

$a_s + b_s$ fraction of extraterrestrial radiation reaching the earth on clear days ($n = N$).

The extraterrestrial radiation, R_a , for each day of the year and for different latitudes can be estimated from the solar constant, the solar declination and the time of the year by Equation (2-6)

$$R_a = 24 (60) \frac{24(60)}{\pi} G_{sc} d_r [\omega_s \sin(\varphi) \sin(\delta) + \cos(\varphi) \cos(\delta) \sin(\omega_s)] \quad (2-6)$$

where

R_a extraterrestrial radiation [$\text{MJ m}^{-2} \text{ day}^{-1}$],

G_{sc} solar constant = $0.0820 \text{ MJ m}^{-2} \text{ min}^{-1}$,

d_r inverse relative distance Earth-Sun,

ω_s sunset hour angle [rad],

φ latitude [rad],

δ solar declination [rad].

The net longwave radiation R_{nl} is calculated by the Stefan-Boltzmann law, as described in Equation (2-7)

$$R_{nl} = \sigma \left(\frac{T_{max,K}^4 + T_{min,K}^4}{2} \right) (0.34 - 0.14\sqrt{e_a}) \left(1.35 \frac{R_s}{R_{so}} - 0.35 \right) \quad (2-7)$$

where

σ Stefan-Boltzmann constant [$4.903 \cdot 10^{-9} \text{ MJ K}^{-4} \text{ m}^{-2} \text{ day}^{-1}$],

$T_{max,K}$ maximum absolute temperature during the 24-hour period [$\text{K} = ^\circ\text{C} + 273.16$],

$T_{min,K}$ minimum absolute temperature during the 24-hour period [$\text{K} = ^\circ\text{C} + 273.16$],

e_a actual vapour pressure [kPa],

R_s/R_{so} relative shortwave radiation (limited to ≤ 1.0),

R_s measured or calculated solar radiation [$\text{MJ m}^{-2} \text{ day}^{-1}$],

R_{so} calculated clear-sky radiation [$\text{MJ m}^{-2} \text{ day}^{-1}$].

The clear-sky radiation (or cloudless radiation) R_{so} is calculated by Equation (2-8)

$$R_{so} = (a_s + b_s) R_a \quad (2-8)$$

where

a_s+b_s fraction of extraterrestrial radiation reaching the earth on clear-sky days ($n = N$).

The soil heat flux, in other hands, is small compared to R_n . Specifically, when the surface is covered by vegetation and the time steps for calculation are longer than one day, the soil heat flux is calculated based on the idea that the soil temperature follows air temperature, as shown in Equation (2-9)

$$G = c_s \frac{T_i - T_{i-1}}{\Delta t} \Delta z \quad (2-9)$$

G soil heat flux [$\text{MJ m}^{-2} \text{ day}^{-1}$],

c_s soil heat capacity [$\text{MJ m}^{-3} \text{ }^\circ\text{C}^{-1}$],

T_i air temperature at time i [$^\circ\text{C}$],

T_{i-1} air temperature at time $i-1$ [$^\circ\text{C}$],

Δt length of time interval [day],

Δz effective soil depth [m].

It is noted that humidity and wind speed have less influence on ET_o and IWR, as discussed in Acharjee et al. (2017). Due to their fewer influences on IWR, wind speed and humidity are assumed to be the same in the future. The sunshine is also assumed unchanged in the simulation periods.

The evapotranspiration of crop under standard condition (ET_c) is then calculated by multiplying ET_o with crop coefficient (K_c), which varies depends on types of plants and determined through practical experiment. This ET_c is calculated based on the crop coefficient approach (Allen et al., 1998).

$$ET_c i = K_c i * ET_o \quad (2-10)$$

Where:

$ET_c i$: Evapotranspiration of crop i under standard condition (mm)

$K_c i$: Crop coefficient of the given crop i

Beside ET_c , rainfall data is also needed to identify how much water crops need to grow completely. However, not one hundred percent of rainwater is available for crops, but some are lost through runoff and deep percolation process. The amount of available water for crops is called effective rainfall, and it is calculated in this research using the USDA Soil Conservation Service Method (Allen et al., 1998), which is incorporated in CROPWAT software. The CWR

is defined as the difference between ETc_i and effective rainfall. CWR for a given crop, i , are defined as:

$$CWR_i = ETc_i - P_{eff} \quad (2-11)$$

Where:

CWR_i is crop water requirement for crop i

ETc_i is evapotranspiration of crop i (mm)

P_{eff} : effective rainfall (mm)

Each crop has its own CWR. Thus, the net irrigation water requirement (NIWR) of a region is thus the sum of individual crop water requirement (CWR_i).

$$NIWR = \frac{\sum_{i=1}^n CWR_i \cdot S_i}{S} \quad (2-12)$$

Where:

$NIWR$ is net irrigation water requirement (mm)

S_i is the cultivated area of crop i (ha)

S is the total cultivated area (ha)

Gross irrigation water requirement (GIWR) is lastly calculated, taking into consideration of irrigation efficiency. This is the amount of water to be extracted (by pumping, diversion) and applied to the irrigation system (Frenken, K. and Faurès, 1997).

$$GIWR = \frac{NIWR}{E} \text{ (mm)} \quad (2-13)$$

E is the global efficiency of the irrigation system

The GIWR is compared to the discharge of the river to see the availability of water in the research area. Based on that, recommendations are made to manage irrigation water better.

2.4 Data preparation

In this research, datasets from global climate model d4PDF, observed data (precipitation and temperature), crop data (types of crops, cultivated area, growing and harvesting date), and soil characteristics are required.

2.4.1 Global climate data

“Database for Policy Decision-Making for Future Climate Change” (d4PDF) was used as large-scale predictors in this research. This data has been made open for publicity since 2015 and freely accessible through the Data Integration and Analysis System (DIAS-http://www.miroc-gcm.jp/~pub/d4PDF/index_en.html). A total of fourteen daily predictors available in d4PDF are extracted for the calibration period of 1975-2004 (Table 2.3). After calibration and validation, only predictors which show the highest simulating performance are used for future simulation of 2K and 4K scenarios.

Table 2.3 Predictor description of d4PDF

No.	Predictor	Description
1	pre	Precipitation (mm)
2	rh	Surface Air Relative Humidity at 2m (%)
3	tcloud	Total cloud amount (%)
4	temp	Surface Air Temperature at 2m (K)
5	wind10	Surface Air Wind Speed at 10m (m/s)
6	zwind5	Zonal velocity at 1000 hPa (m/s)
7	zwind8	Zonal velocity at 850 hPa (m/s)
8	zwind5	Zonal velocity at 500 hPa (m/s)
9	mwinds	Meridional velocity at 1000 hPa (m/s)
10	mwind8	Meridional velocity at 850 hPa (m/s)
11	mwind5	Meridional velocity at 500 hPa (m/s)
12	omegas	Vertical pressure velocity at 1000 hPa (Pa/s)
13	omega8	Vertical pressure velocity at 850 hPa (Pa/s)
14	omega5	Vertical pressure velocity at 500 hPa (Pa/s)

For the simulation of future climate, predictors that have been selected for downscaling temperature and precipitation are downloaded according to the periods of simulation (2K scenario is from 2040 to 2049 and 4K corresponding to the period of 2090 to 2099)

2.4.2 Observed data

Daily observed precipitation (mm), temperature (°C), relative humidity (%), wind speed (m/s) and sun hours from 1975-2004 and 2004-2011 at Thanh Hoa climate station are provided

by the Institute of Meteorology, Hydrology and Climate change (IMHEN) in Viet Nam. The period 1975-2004 is chosen for calibration since there are no missing data in this period, and it has been widely used in climate studies of Thanh Hoa province. The observed mean monthly precipitation, temperature, humidity, wind speed and sunshine for the period 1975 to 2004 are given in Table 2.4.

Table 2.4 Observed mean monthly climate data for the period 1975-2004 at Thanh Hoa climate station

Month	Temperature	Humidity	Wind speed	Sunshine duration	Rainfall
	°C	%	m/s	hours	mm
January	17.2	78	2.0	3.6	23.7
February	17.7	88	2.1	3.8	27.2
March	20	88	1.5	2.0	41.3
April	23.7	87	1.7	3.5	68.0
May	27.2	86	2.3	5.2	157.6
June	29.1	74	1.7	6.3	185.4
July	29.3	82	1.7	5.6	175.1
August	28.5	85	1.3	6.0	258.4
September	27	83	1.9	4.6	354.8
October	24.8	84	1.6	4.4	285.5
November	21.6	76	2.1	4.2	69.5
December	18.5	82	1.7	2.9	25.2

2.4.3 Crop data

Eight main crops are cultivated in the research area in which rice takes up more than 60% of the total cultivated area with two growing seasons in a year. Other crops are maize (14%), sugarcane (8%). Potato, soybean, groundnut, and perennial crop account for the remaining 10%.

Information on crops including types of plants, cultivated area (ha), planting, and harvesting date are provided by the local Department of Statistics in Thanh Hoa province (Thanh Hoa's Department of Statistic, 2017). The detail is provided as Table 2.5 follow.

Table 2.5 Crop information in Thanh Hoa province

	Area (ha)	Percentage	Planting date (day/month)	Harvesting date (day/month)
Winter rice (winter-spring)	122,224	33	25/11	22/2
Summer rice (summer - autumn)	128,259	35	05/8	02/11
Maize	50,521	14	15/5	16/9
Sugarcane	28,875	8	10/5	09/5
Potato	7,510	2	24/4	31/8
Soybean	2,565	1	24/4	17/7
Groundnut	11,528	3	24/4	31/8
Perennial crop	17,802	4	05/5	04/5
Total cultivated area	369,284	100		

Source: Thanh Hoa's Department of Statistic, 2017

The crop coefficient (K_c) varies with the growth stage of the crop and among crops. It is identified by experimental practice in the field. K_c is studied and applied for the research area based on the Ma river basin's water resources planning.

Table 2.6 Crop coefficients for wet crops (rice) with different growth stages

Number of days	10	20	30	40	50	60	70	80	90	100	110	120
K_c	1.04	1.04	1.04	1.08	1.15	1.25	1.30	1.38	1.35	1.25	1.10	0.95

Source: People Committee, 2006

Table 2.7 Crop coefficients for dry crops

Crop	Initial K_c	Middle K_c	Late K_c
Maize	0.30	1.20	1.05
Potato	0.50	1.10	0.50
Groundnut	0.55	1.15	0.90
Sugarcane	0.40	1.25	0.95
Soybean	0.40	1.15	0.75
Perennial crop	0.7	0.65	0.7

Source: People Committee, 2006

2.4.4 Soil characteristics

The soil types in the Ma river basin are classified based on the FAO/UNESCO methodology conducted by the Department of Natural Resources and Environment of Thanh Hoa province (Department of Natural Resources and Environment, 2017). The main soils in this region are Fluvisols concentrating on delta area (17.2%) and Acrisols, which distribute on the mountainous area (64.6%). Since the agricultural land is dominantly located in the delta area, the type of soil applied for cultivation is set to Fluvisol.

Table 2.8 Soil characteristic in the region

Soil name	Soil characteristic	Value
Fluvisols	Total available soil moisture -TAM(mm/m)	290
	Maximum rain infiltration rate (mm/day)	40
	Maximum rooting depth (cm)	900
	Initial soil moisture depletion (as percentages of TAM)	0

Source: Default values for soils (Allen et al., 1998)

CHAPTER 3 RESULTS AND DISCUSSION

3.1 Introduction

The changes in the future climate, corresponding irrigation water requirement, as well as analysis of scenarios using the SDSM and CROPWAT model, are presented in this chapter. For this research, two climate change simulations are conducted based on two future simulations described in d4PDF (2K and 4K simulations). The results of projections were compared to the baseline period (1975-2004) to see general changes in precipitation and temperature, and these results were applied to obtain future irrigation water requirement of the region with respect to two projections. A comparison of gross irrigation water requirement and total water supplied capacity within the area was also made in this chapter.

3.2 Screening of predictors

The selected predictors for precipitation and temperature are shown in Table 3.1 and Table 3.2, respectively. For the backward selection of predictors for precipitation, five predictors are satisfied with p-values less than 0.05 including mwind8 (meridional velocity at 850 hPa), rh (relative humidity), temp (large-scale temperature), wind10 (win speed at 10m), zwind5 (zonal velocity at 500 hPa), and zwind8 (zonal velocity at 800 hPa). In the forward selection process, zwind5 ranks the most effective predictors for precipitation with the highest R squared value among predictors (0.325). In combination, zwind5 is chosen as the predictor for precipitation. It is noted that large-scale precipitation from d4PDF is also one of the most effective predictors for local precipitation, but it is not chosen. As discussed in Eden & Widmann (2014), large scale precipitation is considered to contain predictive information of all relevant climate variables since it uses large scale circulation, humidity and temperature as an input. Furthermore, large scale precipitation may comprise model-inherent error and bias of the GCMs of which it has been calibrated.

For screening of predictors for temperature, backward selection results in 9 predictors, which are remaining in the model (mwind5, mwind8, omegas, rh, tcloud, temp, wind10, zwind5, and zwind8). In the forward selection, temp is the most effective predictor for temperature since it shows the highest R squared value (0.804). The final predictor for temperature is thus determined as “temp” (large-scale temperature). The scatter plots of observed data and predictors are shown in Figure 3.1 and Figure 3.2.

Table 3.1 Backward and forward selection for precipitation

	Backward selection		Forward selection
	<i>t Stat</i>	<i>P-value</i>	R^2
mwind5	-1.48	0.15	0.003
mwind8	-4.01	0.00	0.001
omegas	0.23	0.82	0.000
rh	3.01	0.00	0.078
tcloud	0.39	0.78	0.043
temp	2.07	0.04	0.188
wind10	3.39	0.00	0.064
zwind5	-10.50	0.00	0.325
zwind8	3.49	0.00	0.055
pre	-0.96	0.34	0.158

Table 3.2 Backward and forward selection for temperature

	Backward selection		Forward selection
	<i>t Stat</i>	<i>P-value</i>	R^2
mwind5	5.138	0.000	0.067
mwind8	6.943	0.000	0.019
omegas	-5.620	0.000	0.021
rh	8.013	0.000	0.390
tcloud	5.272	0.000	0.285
temp	33.319	0.000	0.804
wind10	7.927	0.000	0.499
zwind5	-75.585	0.000	0.067
zwind8	29.836	0.000	0.022
pre	-0.446	0.656	0.570

*Note: *t Stat* or *t Statistic* is the ratio of the estimated value to its standard error. *P-value* or probability value is a probability measure of finding the observed or more extreme results when the null hypothesis of a given statistical test is true. R^2 is the coefficient of determination.

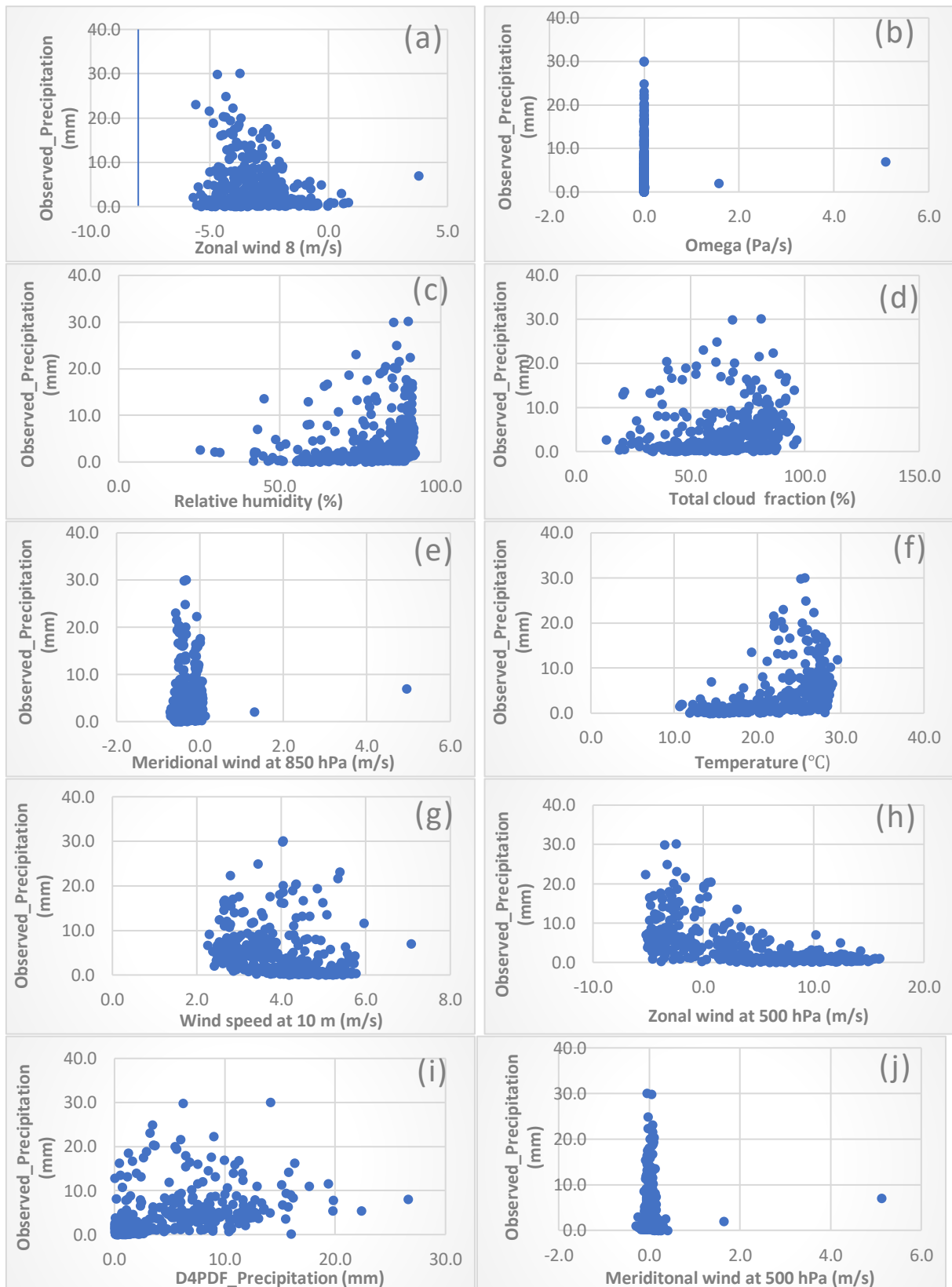


Figure 3.1 Scatter plot of observed precipitation and (a) zonal wind at 850 hPa; (b) omegas; (c) relative humidity; (d) teloud; (e) meridional wind at 850 hPa; (f) d4PDF temperature; (g) wind speed at 10m; (h) zonal wind at 500 hPa; (i) large-scale d4PDF precipitation; (j) meridional wind at 500 hPa

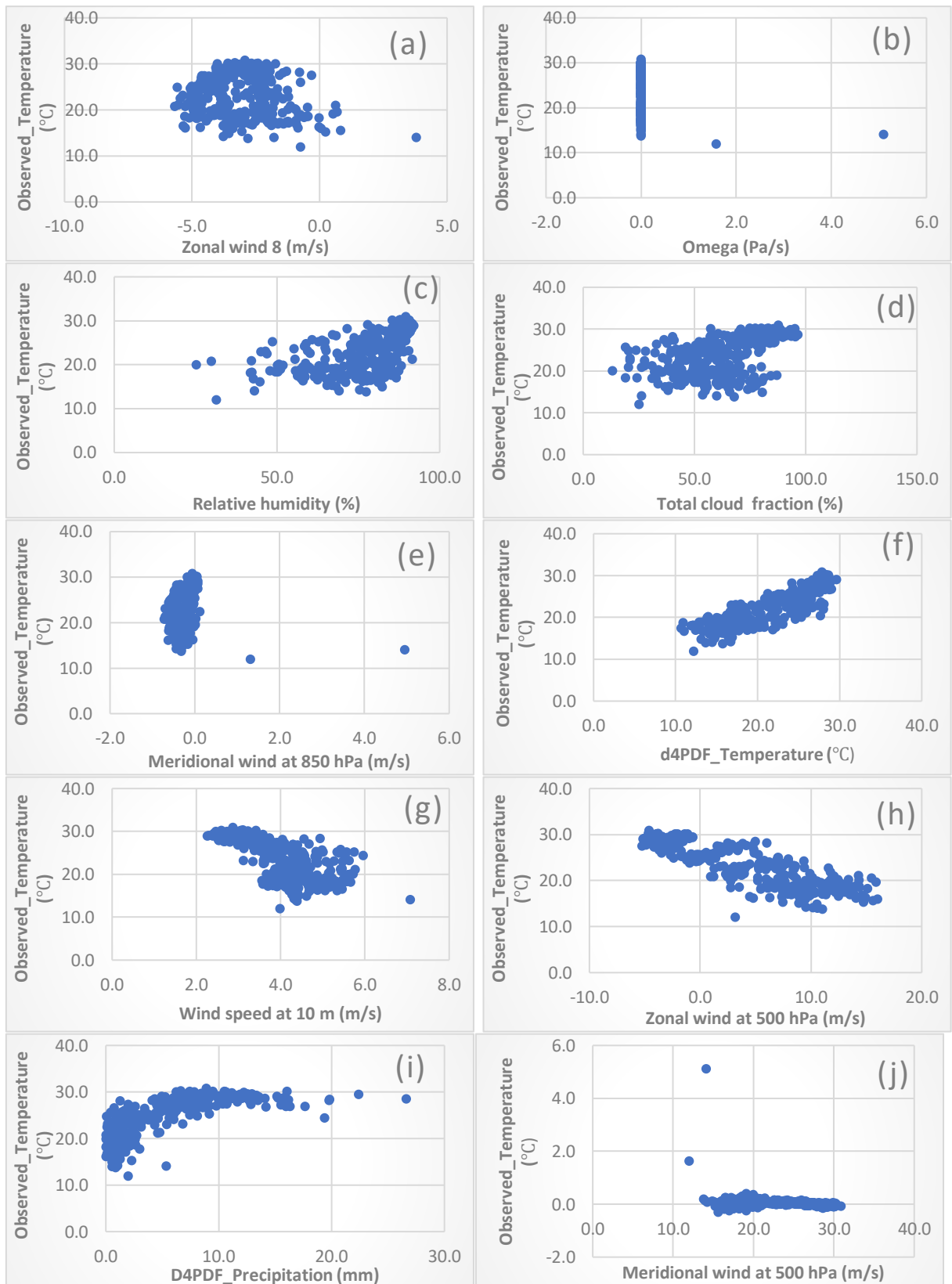


Figure 3.2 Scatter plot of observed temperature and (a) zonal wind at 850 hPa; (b) omegas; (c) relative humidity; (d) tcloud; (e) meridional wind at 850 hPa; (f) d4PDF temperature; (g) wind speed at 10m; (h) zonal wind at 500 hPa; (i) large-scale d4PDF precipitation; (j) meridional wind at 500 hPa

3.3 Calibration of SDSM

The regression models for temperature and precipitation are calibrated for the period 1975-2004. Parameters of regression models for temperature are provided in Table 3.3, while those for precipitation are listed in Table 3.4.

Table 3.3 Parameters for monthly regression model of temperature

Month	Intercept	Coefficient	SE (°C)	R ²
1	17.69	-0.03	3.16	0.001
2	17.29	0.02	3.24	0.001
3	19.20	0.04	2.94	0.003
4	20.68	0.12	2.60	0.024
5	22.57	0.17	2.11	0.027
6	26.50	0.09	1.87	0.003
7	24.12	0.19	1.55	0.012
8	23.61	0.18	1.43	0.016
9	23.98	0.12	1.49	0.019
10	22.30	0.11	2.00	0.023
11	19.29	0.12	2.60	0.024
12	16.40	0.13	3.03	0.023

Table 3.4 Parameters for monthly regression model of precipitation

Month	Intercept	Coefficient	SE (mm)	R ²
1	4.7	-0.2	4.06	0.02
2	5.1	-0.2	5.44	0.01
3	3.5	-0.1	6.89	0.00
4	13.6	-1.1	11.75	0.04
5	12.8	-0.4	18.32	0.00
6	12.4	-1.6	25.32	0.01
7	7.1	-2.0	26.90	0.01
8	21.6	1.0	29.42	0.00
9	28.1	1.0	40.60	0.00
10	22.8	-0.8	44.23	0.00
11	14.0	-1.5	21.96	0.02
12	2.7	0.3	9.80	0.01

The results shown in Table 3.5 are comparable to some previous research (Huang et al., 2011; Mahmood, 2012; Wilby et al., 2002). The coefficient of determination (R²) for precipitation is much lower than that for temperature. As studied by Wilby et al. (2002), precipitation is a “heterogeneous climate variable and is difficult to simulate accurately.” Besides, the proportion of explained variance for temperature is most likely more than 70 %, while precipitation is most likely smaller than 40 % (Mahmood, 2012).

Table 3.5 Coefficient of determination (R^2) and standard error (SE) of the yearly model during calibration (1975-2004)

Variable	R^2	SE (mm or °C)
Precipitation	0.325	0.303
Temperature	0.800	0.255

Precipitation and temperature are simulated and compared to the calibration period (1975-2004), as shown in Table 3.6. As can be seen that SDSM performed well in case of temperature, reflected by the Nash Sutcliffe coefficient (NSE reaches 0.84). In the case of precipitation, the NSE is lower, at 0.65. It is noted that the standard deviation (SD) of precipitation increases during the rainy season (May – October) with decreases in the dry season (November – April), and peaks in September.

Table 3.6 Comparison of observed and downscaled monthly mean precipitation and temperature by SDSM during the calibration period (1975-2004)

Month	NSE		Standard deviation	
	Precipitation	Temperature	Precipitation (mm)	Temperature (°C)
January			3.00	9.49
February			3.92	10.32
March			6.08	12.41
April			6.59	14.60
May			12.99	15.51
June	0.65	0.84	10.70	15.72
July			11.72	15.63
August			17.06	15.40
September			33.64	14.82
October			29.32	13.72
November			10.92	11.97
December			2.66	10.57

The monthly simulated mean of SDSMs is plotted against the observed data in Figure 3.3. In the case of precipitation, there are overestimations in most of the months during the calibrated year except July. Temperature simulated by SDSM is slightly underestimated from June to February and overestimated in March and April.

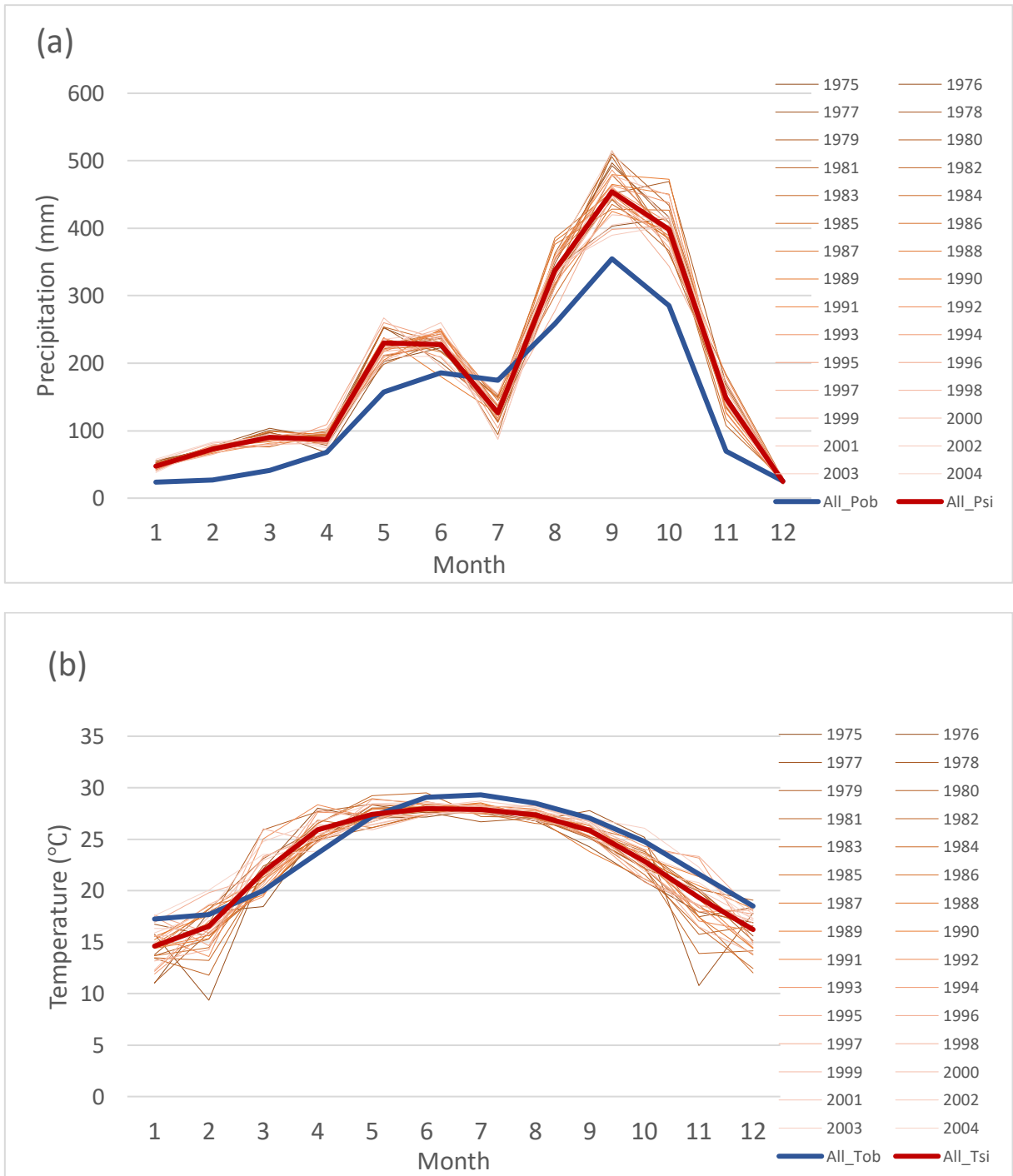


Figure 3.3 Observed and simulated for (a) precipitation and (b) temperature for the calibration period (1975-2004) in the Thanh Hoa station.

*Note: All_Pob and All_Tob is the average observed precipitation and temperature, respectively; All_Psi and All_Tsi is the average simulated precipitation and temperature, respectively. All average observed and simulated lines are for 30 years of calibration

3.4 Validation of SDSM without bias correction

To validate SDSM, precipitation and temperature are generated from 2005 to 2011 using the same d4PDF predictors. The results are presented in Table 3.7. It is seen that the NSE is higher in both cases (precipitation and temperature) compared to the calibration period (1975-2004). For precipitation, the NSE reaches 0.71 while NSE of temperature is much higher, at 0.97. This validation indicates that SDSM produces reasonable simulated results insofar, although there remains a concern in precipitation simulations.

The simulated mean monthly precipitation and temperature are graphically compared with observed data for the validation period (2005-2011), as shown in Figure 3.4. SDSM generally captures the pattern of mean monthly observed precipitation; however, there are still some great overestimations and underestimations that happened throughout the validation period. Figure 3.4(a) indicates that SDSM overestimates precipitation from September to June, and underestimates in July and August. However, the observed mean monthly temperature is well represented by this model, as suggested in Figure 3.4(b). These results indicate a robust application of SDSM to downscale temperature under future d4PDF forcings.

Table 3.7 Comparison of observed and downscaled monthly mean precipitation and temperature by SDSM (without bias correction) during the validation period (2005-2011)

Month	NSE		Standard deviation	
	Precipitation	Temperature	Precipitation (mm)	Temperature (°C)
January			3.43	2.56
February			14.13	1.65
March			5.97	1.41
April			9.91	1.05
May			15.14	0.48
June	0.71	0.97	11.11	0.34
July			14.89	0.19
August			23.60	0.43
September			34.43	0.80
October			43.77	1.73
November			45.43	1.56
December			2.66	0.54

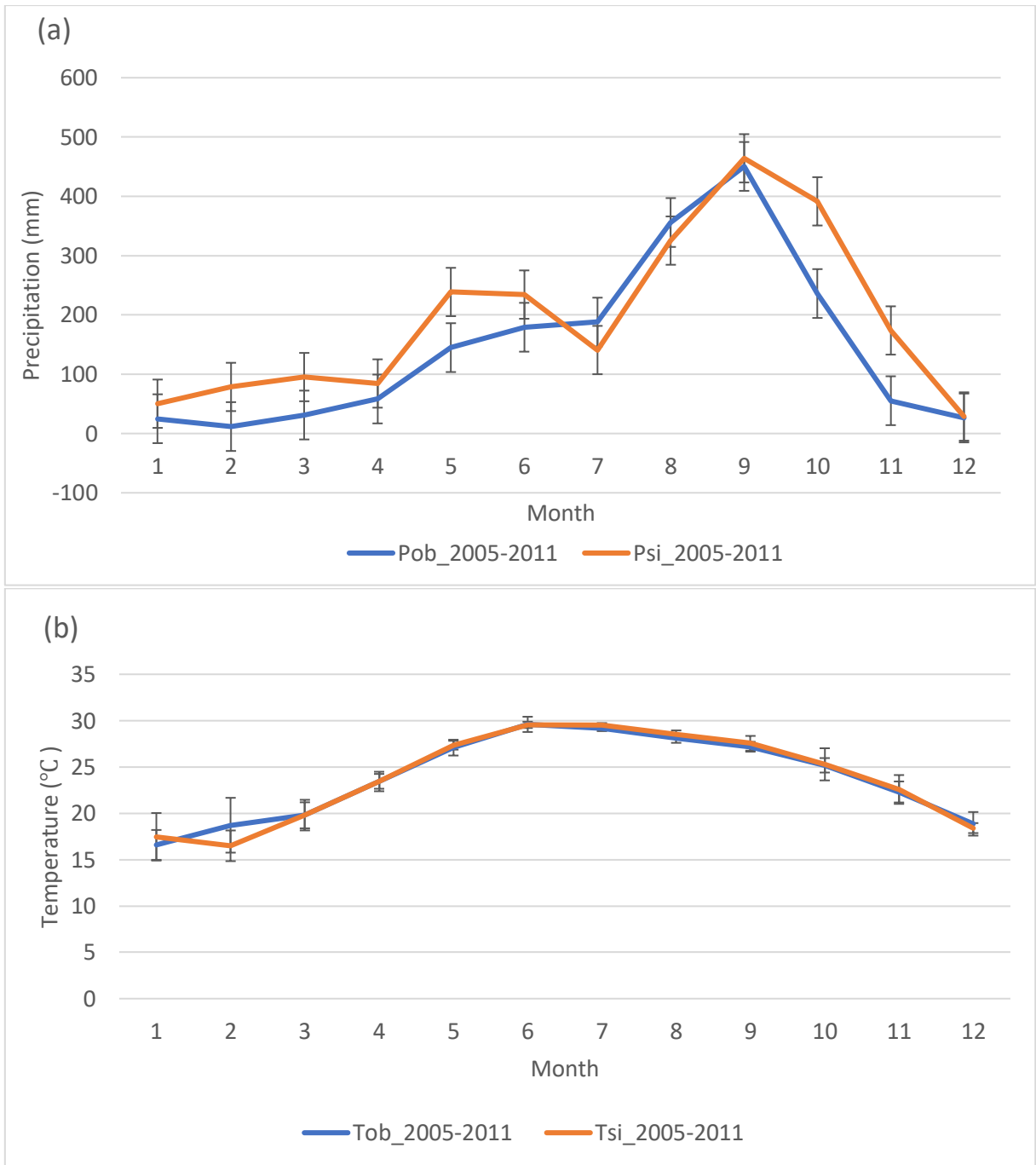


Figure 3.4: Observed downscaled (without bias correction) mean monthly values for (a) precipitation and (b) temperature during the validation period (2005-2011)

3.5 Validation of SDSM with bias correction in downscaling precipitation

As indicated in section 3.4, there are some significant biases in terms of precipitation simulation, which should be removed to improve the results of the validation. This research applies a simple linear scaling bias correction using the bias correction coefficient $P_{ob1975-2004}/\Psi_{1975-2004}$ discussed in Salzman et al. (2007).

Precipitation is downscaled and corrected for biases for the validation period (2005-2011). The results of NSE and standard deviation are described in Table 3.8. Downscaled corrected precipitation is then graphically compared to the observed precipitation, as shown in Figure 3.5. The NSE value after bias-corrected has significantly improved from 0.71 (without bias correction) to 0.86 (with bias correction). Also, the patterns and variations of simulated precipitation are far enhanced through most of the months, although there are still some underestimations in August and September. These results indicate favorable applicability of SDSM with a supplementary bias correction method to downscaled precipitation in Thanh Hoa region.

Table 3.8 Downscaled monthly mean precipitation with bias correction for the validation period (2005-2011)

Month	NSE	Standard deviation (mm)
January		1.72
February		10.19
March		2.99
April		7.54
May		10.44
June	0.86	10.85
July		20.79
August		18.11
September		26.81
October		31.57
November		12.54
December		2.50



Figure 3.5 Observed and downscaled mean monthly precipitation by SDSM (with bias correction) during the validation period (2005-2011)

3.6 Climate projection

SDSM is used to simulate precipitation and temperature for the future periods of the 2040s (2040-2049), and the 2090s (2090-2099) using input predictors from the future 2K and 4K simulation of d4PDF respectively. The downscaled precipitation is corrected for biases. The simulated temperature and corrected precipitation are compared to the observed data of the baseline period (1975-2004) to analyze potential future changes in the 2040s and 2090s in the Ma river basin, and the results are shown in Table 3.9 and Table 3.11. Observed precipitation and temperature are denoted as P_{ob} and T_{ob}; simulated precipitation and temperature are denoted as P_{si} and T_{si}, and bias-corrected precipitation is denoted as P_{bc}.

3.6.1 Precipitation

Table 3.9 presents the percentage change in monthly and annual mean precipitation in the 2040s and 2090s compared to the baseline period (1975-2004) under 2K and 4K simulation of d4PDF downscaled by SDSM. The changes in precipitation projected by SDSM in both periods of 2040s and 2090s have similar increasing trends. In particular, annual mean precipitation increases in both periods, with a growing rate of the 2090s (13.4 %) far higher than that of the 2040s (4.8%). There are also similar changing patterns for monthly mean precipitation among the two future periods, in which precipitation increases from April to October (rainy season) and decreases from November to March (dry season), with changing magnitude higher in the 2090s compared to the 2040s. The mean monthly precipitation for the 2040s and 2090s are graphically compared to observed data of baseline period in Figure 3.6.

Table 3.9 Future changes in precipitation (with bias correction) in comparison with the baseline period (1975-2004)

Month	1975-2004		2040-2049			2090-2099		
	P _{ob} _1975-2004	SD	P _{bc} _2040-2049	SD	Changes (%)	P _{bc} _2090-2099	SD	Changes (%)
1	24	21.2	22	2.0	-8.3	21	1.6	-12.5
2	27	25.1	25	58.3	-7.4	26	50.7	-3.7
3	41	31.3	37	2.3	-9.8	45	2.7	9.8
4	68	49.4	78	6.5	14.7	92	8.7	35.3
5	158	74.7	185	11.2	17.1	184	9.8	16.5
6	185	135.9	194	93.2	4.9	220	8.5	18.9
7	175	112.6	193	15.9	10.3	209	13.3	19.4
8	258	147.7	280	17.0	8.5	308	24.7	19.4
9	355	229.4	393	28.7	10.7	397	31.2	11.8
10	286	223.1	256	18.7	-10.5	330	14.1	15.4
11	69	83.5	69	6.8	0.0	48	5.6	-30.4
12	25	26.2	20	2.2	-20.0	15	2.7	-40.0
Total	1671	37.9	1752	6.2	4.8	1896	7.8	13.5

- Pob_1975-2004: Observed precipitation for 1975-2004
- Pbc_2040-2049 and Pbc_2090-2099: Bias corrected precipitation for 2040-2049 and 2090-2099
- SD: standard deviation
- Changes (%) are differences between Pbc_2040-2049 and Pbc_2090-2099 in a comparison with Pob_1975-2004

The precipitation means of period 2040-2049 and 2090-2099 are statistically tested if they are significantly different compared to the baseline period (1975-2004) using t-statistic given two significance levels 0.05 and 0.01, as shown in Table 3.10.

Table 3.10 Statistical test for precipitation for the period 2040-2049 and 2090-2099 in comparison with the baseline

	2040-2049		2090-2099	
significance level	0.05	0.01	0.05	0.01
t-statistic	-0.14	-0.14	-0.36	-0.36
t-critical	2.07	2.82	2.08	2.83

The t-critical value is the cutoff between retaining or rejecting the null hypothesis.

It is recognized that precipitation in both periods 2040-2049 and 2090-2099 have the t-statistic values falling into the range of t-critical values in both significant levels ($|-0.14| < |2.07|$, $|-0.14| < |2.82|$, $|-0.36| < |2.08|$, $|-0.36| < |2.83|$). It can be said that there are no significant differences between the average precipitation of 2040-2049 and 2090-2099 in comparison with 1975-2004.

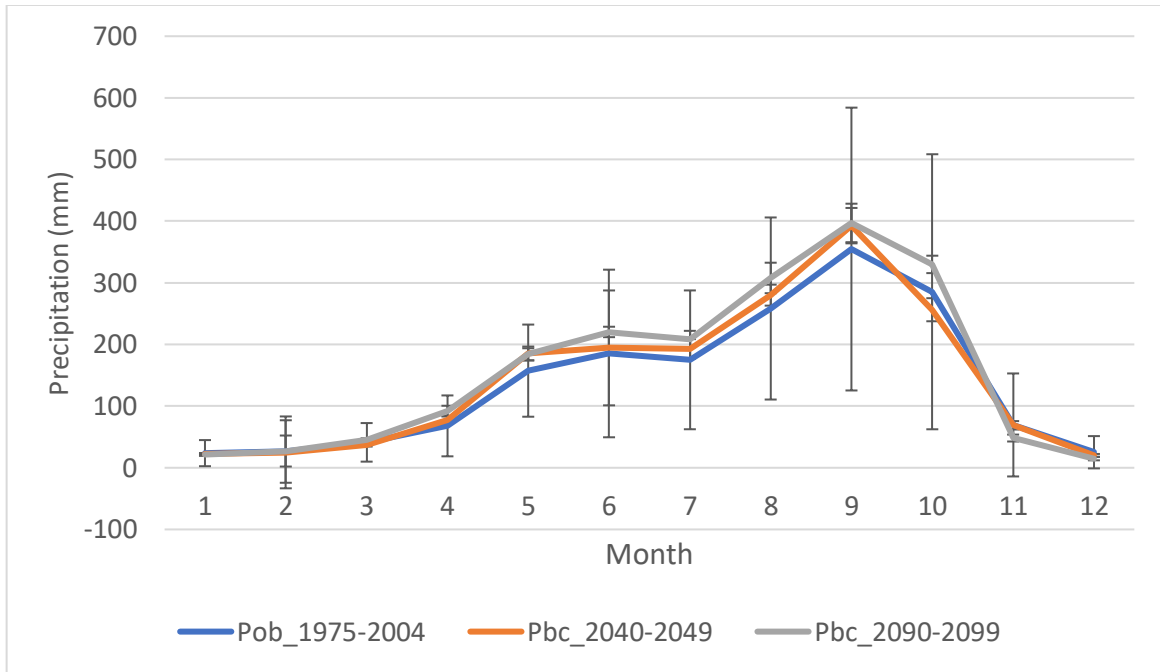


Figure 3.6 Observed and simulated mean monthly precipitation by SDSM (with bias correction) for the 2040s and 2090s period in the Ma river basin

3.6.2 Temperature

Table 3.11 shows the changes in temperature in the 2040s and 2090s compared to the baseline period (1975-2004) under the 2K and 4K simulation of d4PDF downscaled by SDSM. It is seen that the temperature projected by SDSM in two future periods is different in magnitude but similar in pattern. Under the downscaling of SDSM, the mean annual temperature is predicted to increase by 1.7 °C during the 2040s. The temperature increases the most in December, January, and February, with changes ranging from 2.1 to 2.8 °C. From March to July, changes in temperature is seen lower in intensity, with changing values from 0.8 to 1.4 °C. In the 2090s, the mean annual temperature is projected to rise by 4 °C, with the most significant temperature changes seen in January (6.1 °C) and December (4.6 °C). The remaining months could experience a higher mean temperature of approximately 4 °C compared to the period 1975 to 2004. Both simulations suggest that the Ma river basin could experience warmer weather during all months of the 2040s and 2090s, and this warming could be seen most manifest in the winter season. Observed and simulated mean monthly temperature for two future periods are plotted with the baseline period for comparison, as shown in Figure 3.7.

Table 3.11 Future changes in temperature in comparison with the baseline period (1975-2004)

Month	1975-2004		2040-2049			2090-2099		
	Tob_1975-2004	SD	Tsi_2040-2049	SD	Changes (%)	Tsi_2090-2099	SD	Changes (%)
1	17.2	1.73	20.1	2.14	2.8	23.4	1.61	6.1
2	17.7	2.52	19.7	1.95	2.1	22.1	1.75	4.4
3	20	1.58	20.8	1.66	0.8	23	2.13	3
4	23.7	1.64	24.2	1.67	0.5	27.2	1.21	3.5
5	27.2	1.71	28.4	0.43	1.2	30.6	1.15	3.4
6	29.1	1.51	30.6	0.35	1.6	32.5	0.54	3.4
7	29.3	1.37	30.7	0.30	1.4	33.1	0.39	3.8
8	28.5	1.53	30.4	0.39	2	32.4	0.53	3.9
9	27	1.27	28.8	0.50	1.7	31.1	0.51	4.1
10	24.8	1.94	26.8	1.16	2	29.1	1.59	4.3
11	21.6	3.25	23.4	2.11	1.8	25.3	2.18	3.7
12	18.5	1.97	20.7	1.09	2.2	23.2	2.44	4.6
Total	23.7	0.77	25.4	0.35	1.7	27.7	0.56	4

- Tob_1975-2004: Observed temperature for the period 1975-2004
- Tsi_2040-2049 and Tsi_2090-2099: Simulated temperature for the period 2040-2049 and 2090-2099
- SD is standard deviation
- Changes (%) are differences between Tsi_2040-2049 and Tsi_2090-2099 in comparison with Tob_1975-2004

Table 3.12 Statistical test for temperature for the period 2040-2049 and 2090-2099 in comparison with the baseline

	2040-2049		2090-2099	
Significance level	0.05	0.01	0.05	0.01
t-Stat	-0.91	-0.91	-2.25	-2.25
t-Critical	2.07	2.82	2.07	2.82

Table 3.12 shows statistical test results of mean temperature for future periods in comparison with the baseline. For the mean temperature of 2040-2049, the t-Stat values fall within the range of t-Critical values in both significance levels ($|-0.91| < |2.07|$ and $|-0.91| < |2.82|$), which means there are no significant differences between the mean temperature of the 2040s and the baseline. For the 2090s situation, the t-Stat value lies between t-Critical values of -2.82 and 2.82 for the significance level of 0.01 but stay outside the t-Critical range of significance level of 0.05. Therefore, there is probably no significant difference in the mean temperature of the 2090s and the baseline.

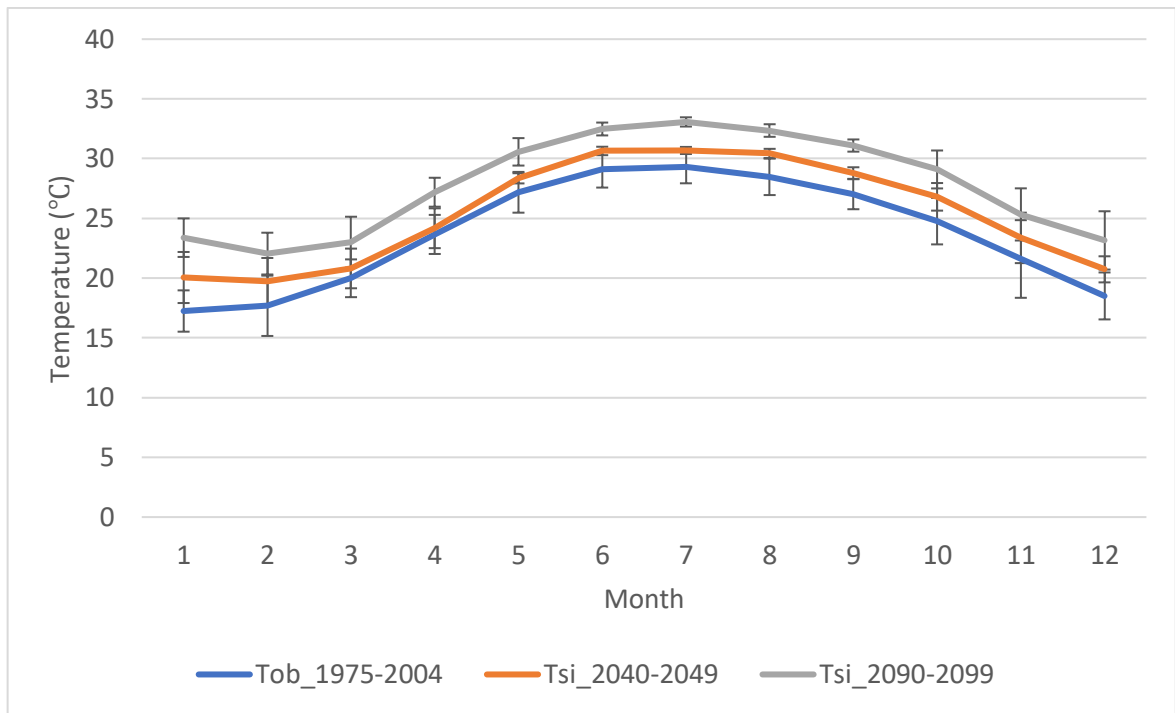


Figure 3.7 Observed and simulated mean monthly temperature by SDSM for the 2040s and 2090s period in the Ma river basin

3.7 Irrigation water requirement

3.7.1 Net irrigation water requirement (NIWR)

3.7.1.1 Reference evapotranspiration and effective rainfall

Table 3.13 shows reference evapotranspiration (ET_o) of Thanh Hoa area during simulation periods. It is noted that the reference evapotranspiration increases throughout the periods, as a result of increasing the temperature. Table 3.10 shows rainfall and effective rainfall of Thanh Hoa area for the same simulation periods using the USDA Soil Conservation Service Method presented in section 2.3.2.7.

Table 3.13 Reference Evapotranspiration of Thanh Hoa area in the periods 1975-2004, 2040-2049, and 2090-2099

Month	ET _o (mm/day)		
	1975-2004	2040-2049	2090-2099
January	2.13	2.33	2.58
February	2.04	2.21	2.4
March	2.09	2.17	2.29
April	2.84	2.87	3.1
May	3.71	3.81	4.06
June	4.58	4.74	4.96
July	4.21	4.35	4.61
August	4.08	4.27	4.49
September	3.55	3.72	3.94
October	2.97	3.14	3.34
November	2.74	2.89	3.05
December	1.95	2.06	2.19
Average	3.08	3.21	3.42

Table 3.14 Rainfall and effective rainfall of Thanh Hoa area in the periods 1975-2004, 2040-2049, and 2090-2099

	1975-2004		2040-2049		2090-2099	
	Rain (mm)	Effective rain (mm)	Rain (mm)	Effective rain (mm)	Rain (mm)	Effective rain (mm)
January	23.7	22.8	22.0	21.2	21.0	20.3
February	27.2	26.0	25.0	24.0	26.4	25.3
March	41.3	38.6	36.8	34.6	45.1	41.8
April	68.0	60.6	77.7	68.0	91.9	78.4
May	157.6	117.9	185.4	130.4	184	129.8
June	185.4	130.4	194.4	133.9	220.3	142.6
July	175.1	126	192.7	133.3	208.9	139.1

August	258.4	150.8	280	153	307.9	155.8
September	354.8	160.5	392.7	164.3	397.1	164.7
October	285.5	153.6	256.4	150.6	329.9	158
November	69.5	61.8	68.9	61.3	48.3	44.6
December	25.2	24.2	20.2	19.5	14.8	14.4
Total	1671.7	1073.1	1752.2	1094.3	1895.6	1114.9

3.7.1.2 Changes in monthly, seasonal and annual net irrigation water requirement

Table 3.15 presents monthly and yearly NIWR of the baseline (1975-2004), the 2040s and 2090s period, and the percentage of changes between these two future periods with respect to the baseline. It is seen that the annual NIWR is predicted to increase through periods of simulation, from 189.1 mm/year for the period 1975-2004 to 201 and 220.4 mm/year for the 2040s and the 2090s, respectively. The percentage of changes in NIWR is not the same for two future periods, which is 6.3 % higher for the 2040s and 16.6 % greater for the 2090s in comparison with the baseline period. In particular, November to March may experience positive increases in terms of NIWR, with the changes ranging from 14 – 44 %, while there may be slight changes in the remaining months of the future periods. NIWR is predicted to increase the most in November, December, and January, with the number of changes reaching 10.2 mm (14.9 %), 8.4 mm (44.4 %) and 7.7 mm (34.7 %) by the 2090s compared to 1975-2004. NIWRs among periods are illustrated in Figure 3.8.

Table 3.15 Changes of monthly and annual NIWR between the 2040s and 2090s with respect to the baseline period (1975-2004)

Month	1975-2004		2040-2049			2090-2099		
	NIWR (mm/ha/month)	SD	NIWR (mm/ha/month)	SD	Changes (%)	NIWR (mm/ha/month)	SD	Changes (%)
1	22.2	7.3	26	2.3	17.1	29.9	1.6	34.7
2	12.2	6.0	14.6	4.3	19.7	16.3	5.0	33.6
3	1.7	1.1	2.2	0.4	29.4	1.8	0.4	5.9
4	0.7	0.2	0.4	0.2	-42.9	0.1	0.1	-85.7
5	0	0.0	0	0.0	0	0	0.0	0
6	0.1	0.0	0.2	0.2	100.0	0.1	0.1	0
7	46.5	11.1	46.2	0.5	-0.6	46.5	0.7	0
8	18.3	15.3	18.5	0.4	1.1	19.7	0.7	7.7
9	0	0.0	0	0.0	0	0	0.0	0
10	0	0.0	0	0.0	0	0	0.0	0
11	68.5	11.7	70	2.6	2.2	78.7	1.6	14.9
12	18.9	9.5	22.9	1.9	21.2	27.3	2.8	44.4
Annual	189.1	33.8	201	4.7	6.3	220.4	7.4	16.6

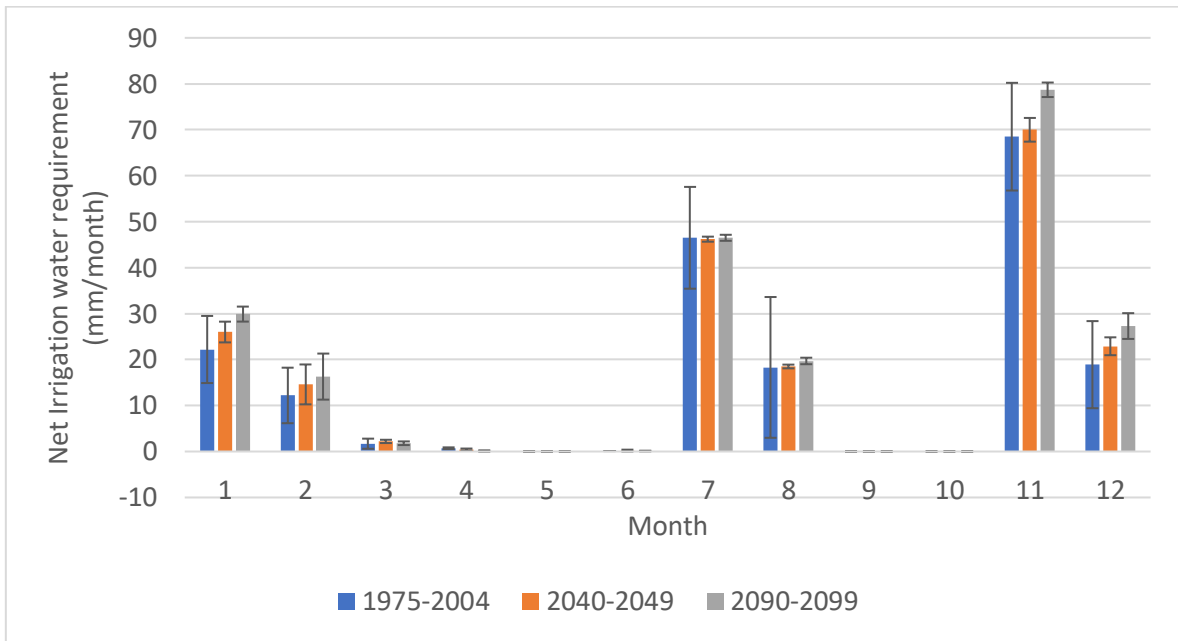


Figure 3.8 Monthly NIWR between the baseline and two future periods (the 2040s and 2090s)

The seasonal changes of NIWR are shown in Table 3.16. Generally, the irrigation water requirements for the dry season (November to April) are predicted to increase while the rainy season could remain almost the same throughout three periods. According to the result analysis, the total irrigation water requirement for the whole dry season is likely to increase by 9.6 % by 2040s and 24.1 % by the 2090s. However, irrigation water requirements for the rainy season might be relatively stable, with no change during the 2040s and a small increase of 2.2 % by the end of the 21st century. Figure 3.9 illustrates the predicted changing trend of seasonal NIWR from the 1975-2004 period to the 2040s and 2090s.

Table 3.16 Changes of seasonal NIWR between the 2040s and 2090s with respect to the baseline period (1975-2004)

Period	1975-2004		2040-2049			2090-2099		
	NIWR	SD	NIWR	SD	Changes (%)	NIWR	SD	Changes (%)
Dry season	124.2	17.5	136.1	4.5	9.6	154.1	6.7	24.1
Rainy season	64.9	28.8	64.9	0.8	0.0	66.3	1.3	2.2

NIWR unit: (mm/season)

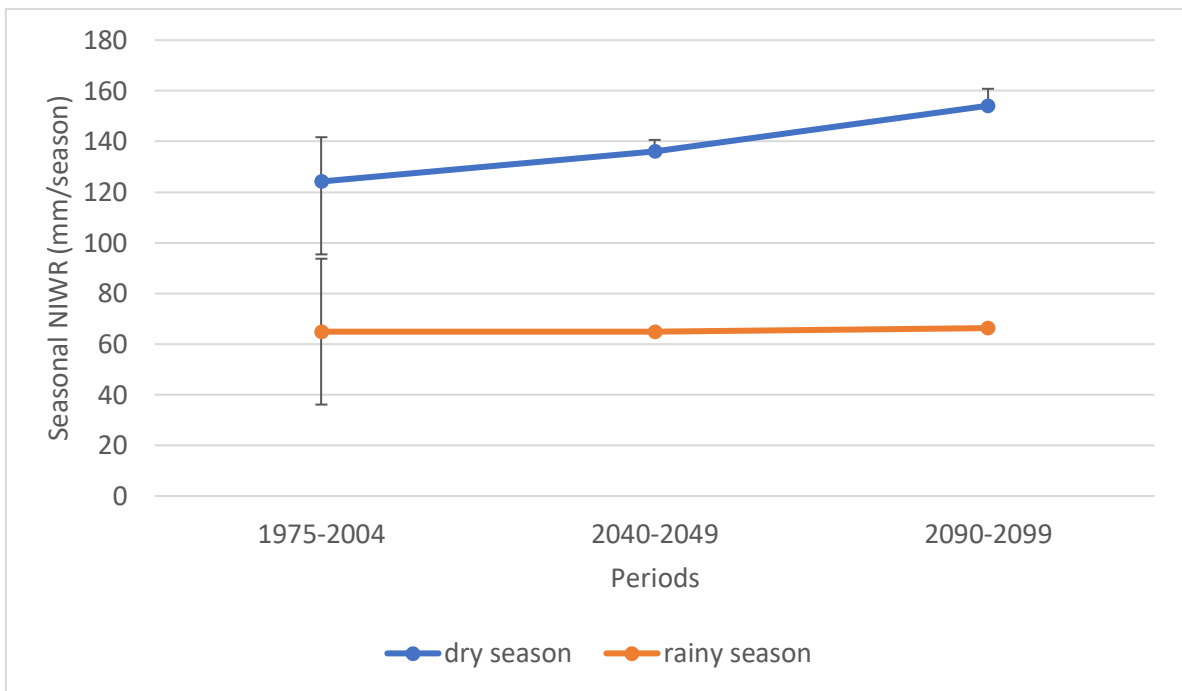


Figure 3.9 Seasonal NIWR between the baseline and two future periods (the 2040s and 2090s)

3.7.1.3 Changes in IWR for each type of crops

Table 3.17 shows the annual IWR for each cultivated crops in the Ma river basin from 2040 to 2049 and 2090 to 2099, respectively. It is recognized that the IWR of winter rice (grown from winter to spring) and summer rice (cultivated from summer to autumn) could take up more than 90 % of total IWR in the region for both periods. It is because rice requires a large amount of water (high crop water requirement) to grow, and the cultivated areas of both seasons of rice are large (33 % per total cultivated area for winter rice and 35 % for summer rice) compared to other crops in the region. Sugarcane takes up between 7 and 8 % of total IWR for the region and other crops (maize, potato, soybean, groundnut, and perennial crops) share the remaining less than 3 % of area's IWR, as shown in Figure 3.10.

Table 3.17 Annual IWR for each type of crop in the Ma river basin for the 2040s and 2090s

Periods	2040s		2090s	
	IWR (mm/yr)	%	IWR (mm/yr)	%
1. Rice1	117.9	58.7	132.6	60.1
2. Rice2	66.1	32.9	67.3	30.5
3. Maize (Grain)	0.2	0.1	0.4	0.2
4. Sugarcane (Ratoon)	15.5	7.7	18.2	8.3
5. Potato	0.0	0.0	0.0	0.0
6. Soybean	0.1	0.0	0.1	0.0
7. Groundnut	0.3	0.1	0.3	0.1
8. Perennial crops	0.9	0.5	1.6	0.7
Total	200.9	100	220.5	100

It is recognized that both future periods may experience a general increasing trend in terms of monthly IWR for each type of crop, as shown in Table 3.18, Table 3.19, and Figure 3.11. Winter rice requires a large amount of water for its growth during four months of the dry season (November to February), while summer rice takes a comparative amount of water in July and August. There is almost no irrigation water needed for April to June and September to October, although some crops such as soybean, groundnut, potato and maize being cultivated in these months. No water requirement happens when the evapotranspiration of these crops does not exceed the effective rainfall during these months.

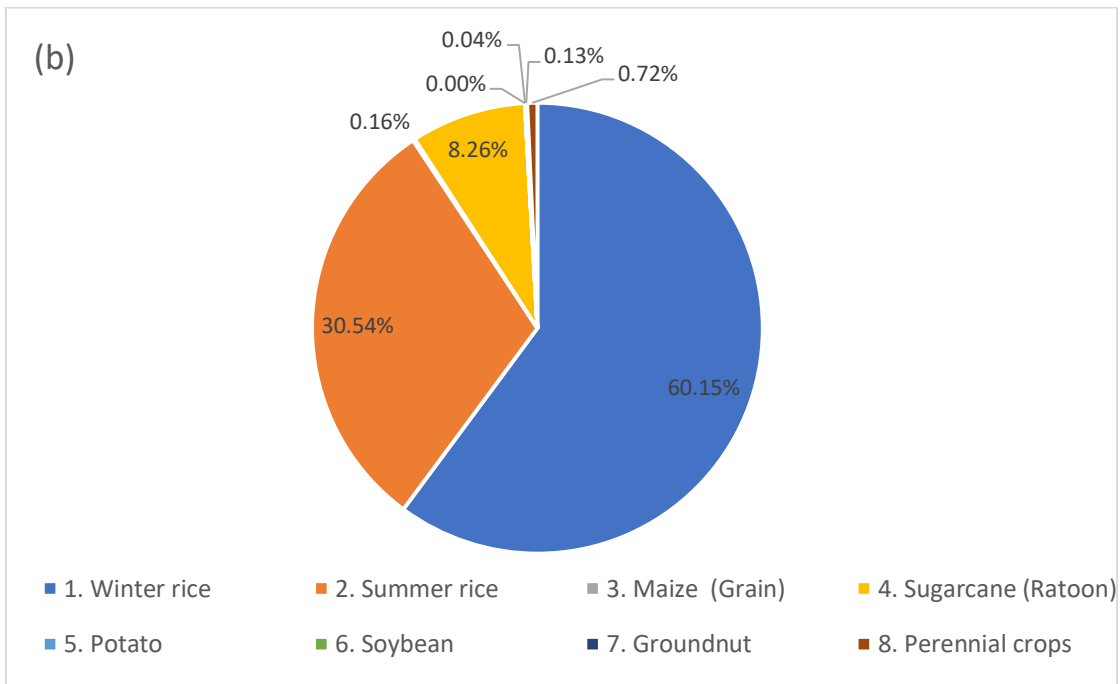
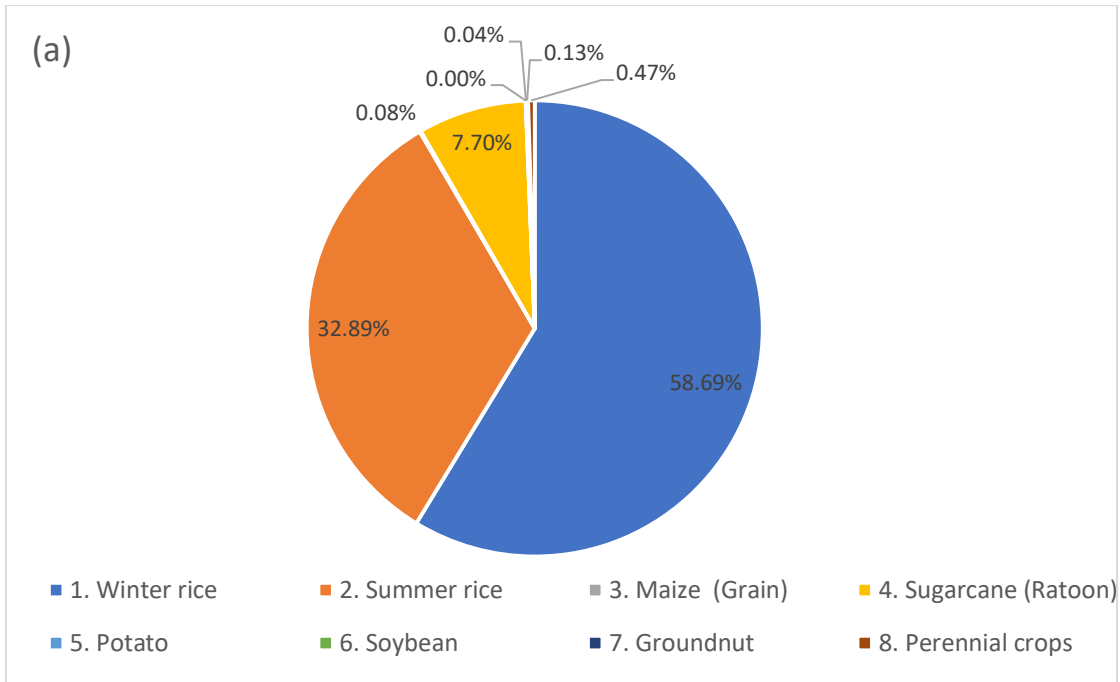


Figure 3.10 Percentage of IWR for each type of crop during (a) the 2040s, and (b) the 2090s

Table 3.18 Irrigation water requirements (mm) for each type of crop during the 2040s

	January	February	March	April	May	June	July	August	September	October	November	December
1. Winter rice	21.52	11.35	0	0	0	0	0	0	0	0	66.3	18.78
2. Summer rice	0	0	0	0	0	0	45.92	18.52	0	0	1.65	0
3. Maize (Grain)	0	0	0	0	0	0	0.17	0	0	0	0	0
4. Sugarcane (Ratoon)	4.1	2.98	2.21	0.42	0	0	0	0	0	0	2.02	3.76
5. Potato	0	0	0	0	0	0	0	0	0	0	0	0
6. Soybean	0	0	0	0	0	0.08	0	0	0	0	0	0
7. Groundnut	0	0	0	0	0	0.1	0.16	0	0	0	0	0
8. Perennial crops	0.35	0.24	0.02	0	0	0	0	0	0	0	0	0.32

Table 3.19 Irrigation water requirements (mm) for each type of crop during the 2090s

	January	February	March	April	May	June	July	August	September	October	November	December
1. Winter rice	24.69	12.67	0	0	0	0	0	0	0	0	73.06	22.21
2. Summer rice	0	0	0	0	0	0	45.92	19.67	0	0	1.75	0
3. Maize (Grain)	0	0	0	0	0	0	0.35	0	0	0	0	0
4. Sugarcane (Ratoon)	4.74	3.29	1.76	0.14	0	0	0	0	0	0	3.74	4.54
5. Potato	0	0	0	0	0	0	0.008	0	0	0	0	0
6. Soybean	0	0	0	0	0.02	0.06	0	0	0	0	0	0
7. Groundnut	0	0	0	0	0	0.07	0.22	0	0	0	0	0
8. Perennial crops	0.51	0.3	0	0	0	0	0	0	0	0	0.19	0.59

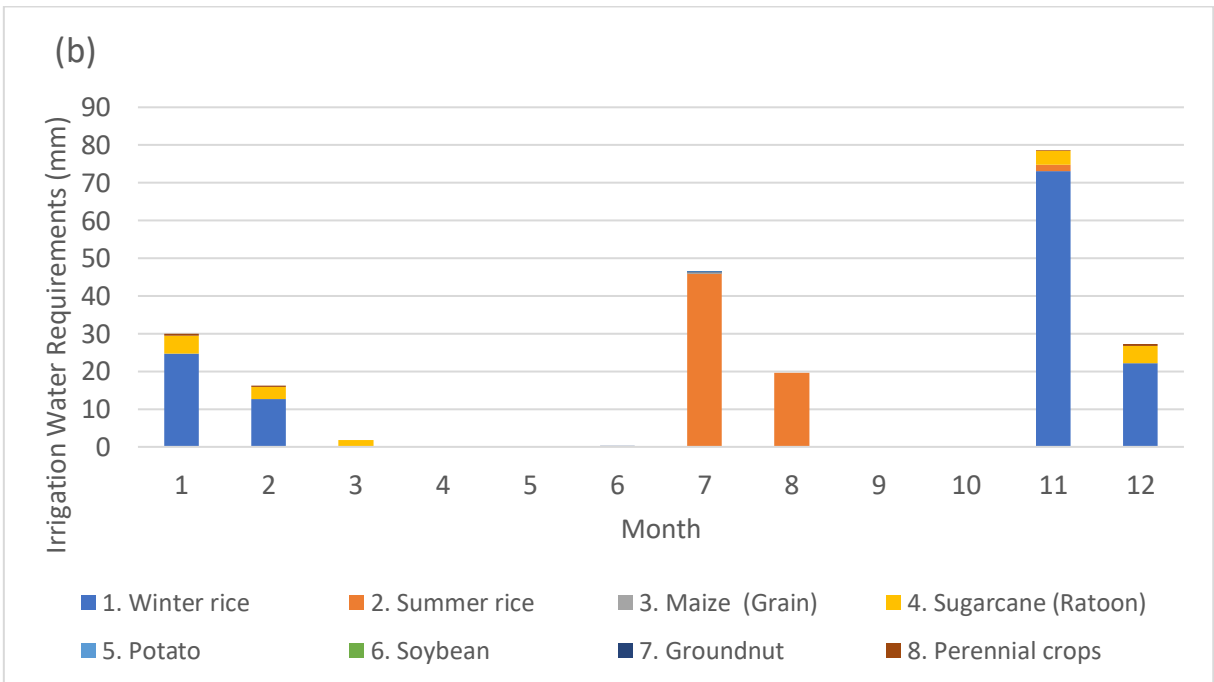
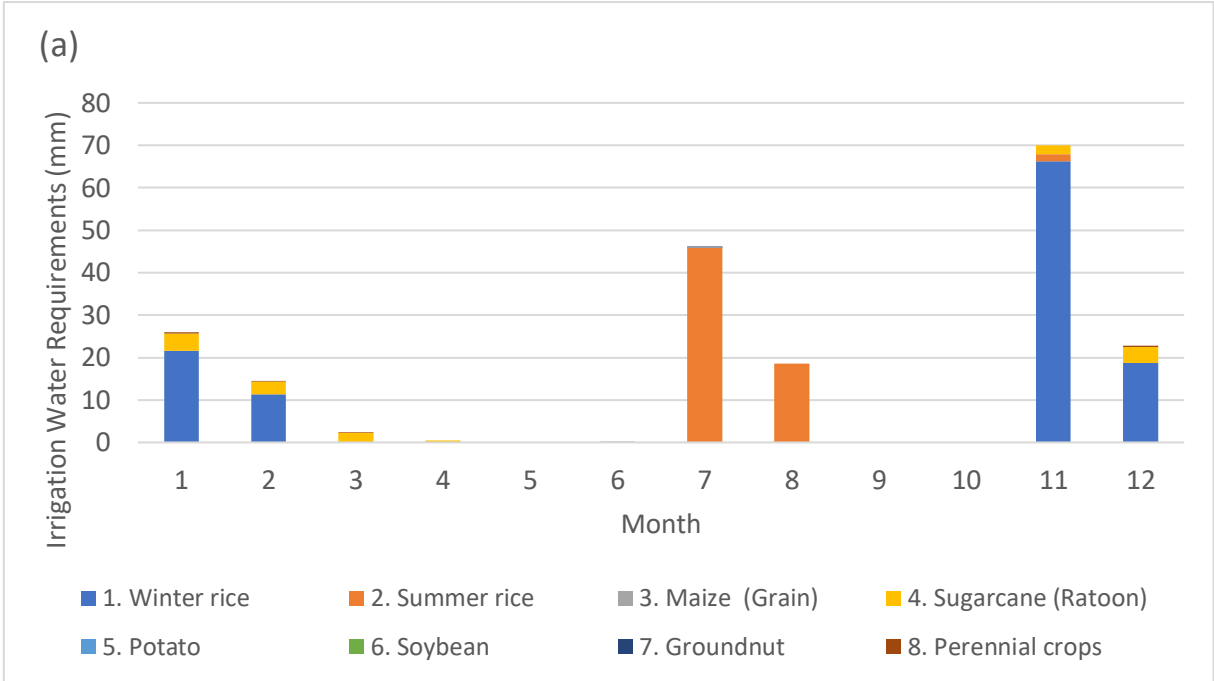


Figure 3.11 IWR for each type of crop in (a) the 2040s, and (b) the 2090s

3.7.2 Gross irrigation water requirement (GIWR)

Table 3.20, Table 3.21, and Table 3.22 show the monthly and yearly GIWR for the period 1975-2004, the 2040s and 2090s, taking into account an irrigation efficiency (E) of 65%. The volume of GIWR is obtained by multiplying GIWR by the irrigated areas. This GIWR is the actual quantity of water needed for crop growth in the region.

Table 3.20 Monthly GIWR in Ma river basin for the period of 1975-2004

	1	2	3	4	5	6	7	8	9	10	11	12	Total
NIWR (mm)	22.2	12.2	1.7	0.7	0	0.1	46.5	18.3	0	0	68.5	18.9	189.1
Irrigation efficiency (%)	65	65	65	65	65	65	65	65	65	65	65	65	
GIWR (mm/month)	34.2	18.8	2.6	1.1	0.0	0.2	71.5	28.2	0.0	0.0	105.4	29.1	290.9
Irrigated area (ha)	369,284												
GIWR (Mm³/month)	126.1	69.3	9.7	4.0	0.0	0.6	264.2	104.0	0.0	0.0	389.2	107.4	1074.3

Table 3.21 Monthly GIWR in Ma river basin for the period of 2040 to 2049

	1	2	3	4	5	6	7	8	9	10	11	12	Total
NIWR (mm)	26	14.6	2.2	0.4	0	0.2	46.2	18.5	0	0	70	22.9	201
Irrigation efficiency (%)	65	65	65	65	65	65	65	65	65	65	65	65	
GIWR (mm/month)	40.0	22.5	3.4	0.6	0.0	0.3	71.1	28.5	0.0	0.0	107.7	35.2	309.2
Irrigated area (ha)	369,284												
GIWR (Mm³/month)	147.7	82.9	12.5	2.3	0.0	1.1	262.5	105.1	0.0	0.0	397.7	130.1	1141.9

Table 3.22 Monthly GIWR in Ma river basin for the period of 2090 to 2099

	1	2	3	4	5	6	7	8	9	10	11	12	Total
NIWR (mm)	29.9	16.3	1.8	0.1	0	0.1	46.5	19.7	0	0	78.7	27.3	220.4
Irrigation efficiency (%)	65	65	65	65	65	65	65	65	65	65	65	65	
GIWR (mm/month)	46.0	25.1	2.8	0.2	0.0	0.2	71.5	30.3	0.0	0.0	121.1	42.0	339.1

	1	2	3	4	5	6	7	8	9	10	11	12	Total
Irrigated area (ha)													369,284
GIWR (Mm³/month)	169.9	92.6	10.2	0.6	0.0	0.6	264.2	111.9	0.0	0.0	447.1	155.1	1252.2

The total irrigation water requirement for Thanh Hoa area is predicted as 1141.9 Mm³ per year for the period 2040 to 2049, and 1252.2 Mm³ per year for the period 2090 to 2099.

The irrigation water requirements for each type of crop, evapotranspiration of crops, crop characteristics (rooting depth, crop coefficient Kc) and are presented in the appendix A for the 2040s and appendix B for the 2090s.

3.8 Discussion

The monthly gross irrigation water requirements (GIWR) for three simulation periods are compared to the monthly mean discharge of Ma river basin (1975-2004), with the presence of water use of other sectors in the region including domestic use, industry, livestock, and environmental flow. This comparison enables the assessment of water availability in the area and could be a base for recommendations. The present Ma river's discharge, water for domestic use, industry, livestock and environmental flow are obtained from Hoang (2009). The future discharge of the Ma river is derived from Nohara et al. (2006). They use 19 coupled atmosphere-ocean general circulation models based on the Special Report on Emissions Scenarios A1B scenario to simulate the total annual discharge of Southeast Asia including Thanh Hoa area by 2090s. The total annual river discharge is projected to increase by 10 % over the research area. Table 3.19 and 3.20 shows water supply requirements for the baseline period and the 2090s.

Table 3.23 Water supply requirements for the baseline period (1975-2004) in the Ma river basin

Month	1	2	3	4	5	6	7	8	9	10	11	12
GIWR	126	69	10	4	0	1	264	104	0	0	389	107
Water for domestic use	24	24	24	24	24	24	24	24	24	24	24	24
Water for industry	33	33	33	33	33	33	33	33	33	33	33	33
Water for livestock	24	24	24	24	24	24	24	24	24	24	24	24
Environmental flow	246	223	246	238	246	238	246	246	238	246	238	246
Total water requirements	454	373	338	324	328	320	592	432	320	328	709	435
Ma river discharge	426	374	412	486	579	1312	1535	2574	2578	1708	726	520
Water supply requirements	28	0	0	0	0	0	0	0	0	0	0	0

Unit: Mm³/month

Table 3.24 Water supply requirements for the 2090s in the Ma river basin

Month	1	2	3	4	5	6	7	8	9	10	11	12
GIWR	170	93	10	1	0	1	264	112	0	0	447	155
Water for domestic use	28	28	28	28	28	28	28	28	28	28	28	28
Water for industry	38	38	38	38	38	38	38	38	38	38	38	38
Water for livestock	28	28	28	28	28	28	28	28	28	28	28	28
Environmental flow	246	223	246	238	246	238	246	246	238	246	238	246
Total water requirements	511	410	351	334	341	334	605	453	333	341	780	496
Ma river discharge	468	411	454	535	637	1443	1689	2831	2836	1879	798	572
Water supply requirements	43	0	0	0	0	0	0	0	0	0	0	0

Unit: Mm³/month

It is recognized that the total water requirements in the Ma river basin are generally higher during the dry season (November to April), and lower in the rainy season (May to October). The results suggest a water deficit of 28 Mm³/month in January during 1975-2004, and the shortage of water will be likely to continue expanding by 2090s corresponding to the increases of gross irrigation water requirements. The 2090s may experience a total water shortage of 43 Mm³ per year in the area, while total water requirements would reach close to the water supply capacity of the river during the dry season. The results are calculated based on mean monthly input data. If extreme weather such as drought and heatwave happen, the situation might be further worse.

It is seen that the irrigation water requirements mostly come from winter rice and summer rice, as discussed in Section 3.7.1.3. To reduce water irrigation requirements in the region, it is possible to shift the planting date of rice toward the rainy season, when more rainfall is available. This research proposes a scenario of changing the planting date of rice, as shown in Table 3.25 and Table 3.26

Table 3.25 Proposal of shifting planting time for rice in the Ma river basin

	Original		Proposal	
	Planting date day/month	Harvesting date day/month	Planting date day/month	Harvesting date day/month
Winter rice	25/11	22/02	25/05	22/08
Summer rice	05/08	02/11	05/09	03/12

Table 3.26 GIWR of the Ma river basin under the shifting of rice's planting date for the baseline period, the 2040s and 2090s

Periods	1975-2004		2040-2049		2090-2099	
Month	GIWR	GIWR after shifting	GIWR	GIWR after shifting	GIWR	GIWR after shifting
1	126.1	13.7	147.7	16.2	169.9	19.6
2	69.3	9.6	82.9	11.8	92.6	13.3
3	9.7	6.3	12.5	8.1	10.2	6.6
4	4.0	2.6	2.3	1.5	0.6	0.4
5	0.0	231.9	0.0	229.7	0.0	234.1
6	0.6	35.8	1.1	38.0	0.6	36.9
7	264.2	43.6	262.5	40.6	264.2	45.8
8	104.0	176.9	105.1	177.3	111.9	179.5
9	0.0	65.0	0.0	65.7	0.0	66.5
10	0.0	0.0	0.0	0.0	0.0	0.0
11	389.2	41.7	397.7	50.2	447.1	85.7
12	107.4	11.8	130.1	15.9	155.1	21.8
Total	1074.3	638.9	1141.9	655.1	1252.2	710.1
Water-saving (%)		40.5		42.6		43.3

Unit: Mm³/month

Table 3.26 shows the GIWR of the Ma river basin after shifting cultivated time of rice. If winter rice is planted six months later, and summer rice is shifted one month later, the GIWR will likely decrease by 40.5 % for the baseline, 42.6 % for the 2040s and 43.3 % for the 2090s. There would be less water needed for irrigation since the rainfall is much more abundant during shifting rice's growth.

Another possibility is to change rice to short-term crops such as maize, which require less water during their growths while boosting economic benefits. Table 3.27 presents GIWR of the Ma river basin if maize is grown instead of winter rice. Obviously, GIWR significantly decreases in all periods, with the amount of water-saving reaching 62.3 % (670 Mm³/year) for the baseline period, 60.9 % (695 Mm³/year), and 61.9 % (774 Mm³/year) for the 2040s and 2090s.

It is noted that these proposals solely take into account the possibility of reducing GWIR for the Ma river basin based on science's aspects. However, bringing the crop shifting into practice requires taking into consideration many other aspects, such as farmer's preference, food security, or agricultural development planning and strategy of the local government. Thus, this proposal should only be played as a reference to the decision-makers in the region.

Table 3.27 GIWR of the Ma river basin under the shifting of rice to maize for the baseline period, the 2040s and 2090s

Period	1975-2004		2040-2049		2090-2099	
Month	GIWR	GIWR crop-type shifting	GIWR	GIWR crop-type shifting	GIWR	GIWR crop-type shifting
1	126.1	56.5	147.7	68.3	169.9	80.5
2	69.3	47.3	82.9	58.3	92.6	64.6
3	9.7	29.2	12.5	38.4	10.2	29.9
4	4.0	2.6	2.3	1.5	0.6	0.7
5	0.0	0.0	0.0	0.0	0.0	0.0
6	0.6	0.4	1.1	0.7	0.6	0.4
7	264.2	171.7	262.5	171.0	264.2	172.1
8	104.0	67.6	105.1	68.3	111.9	72.4
9	0.0	0.0	0.0	0.0	0.0	0.0
10	0.0	0.0	0.0	0.0	0.0	0.0
11	389.2	11.8	397.7	13.7	447.1	21.8
12	107.4	17.7	130.1	26.6	155.1	35.1
Total	1074.3	404.7	1141.9	446.8	1252.2	477.5
Water-saving (%)		62.3		60.9		61.9

Unit: Mm³/month

This research used the outputs from GCM d4PDF to downscale precipitation and temperature for the future in the Ma river basin. The results of downscaled precipitation and temperature were consistent with the changing tendencies of respective d4PDF climate, in which the mean ratio of monthly total precipitation (mm/month)/monthly mean temperature (°C) is approximately 3. In other words, precipitation will likely increase by 3 mm for every degree increase in temperature in the future (Mizuta et al., 2016). However, downscaling results of this research basically rely on the quality input of GCM d4PDF that is taken as input data. The closer the GCM represents the climate of the region, the better downscaling the research can obtain. Hence, a comparison of downscaling results with input data from various GCMs would give a comprehensive view of future climate patterns in this region.

It is noted that large-scale climate variable that significantly affects precipitation in the region is determined as zonal velocity at 500 hPa, which flow in the west-east direction. In Thanh Hoa area, the tropical monsoon dominantly affects the local climate since it brings enormous rain every year. In summer, tropical monsoon blows from the Pacific Ocean to the land, carrying a humid air to the Thanh Hoa region while winter wind brings about dry and cold air.

For the assessment of climate change impacts on the irrigation water requirement of the region, the research assumed that local wind speed, humidity, and sunshine would not change for the simulation period. Only precipitation and temperature will change under the GCM climate forcings. A cross-checking of observed local wind speed and humidity with respective future d4PDF climate is implemented to explore if this assumption remains valid in the future. There are great differences between observed and large-scale d4PDF wind speed, as shown in Figure 3.12. However, the changing tendencies of wind speed simulated by d4PDF remain relatively stable throughout future periods (2040-2049 and 2090-2099), and these stable tendencies support the assumption that wind speed remain the same in the future. Relative humidity, on the other hand, shows notable changes among historical (1975-2004) and future simulations of d4PDF (2040-2049 and 2090-2099), but harmony between observed and future large-scale humidity, as shown in Figure 3.13. This harmony suggests an applicable assumption of current relative humidity to the future. The research also assumes that sunshine duration remains unchanged in the future. The validation of this assumption stays unclear so far since there is a lack of data from d4PDF to compare. Hence, this assumption remains a source of uncertainty in this research, as it affects the irrigation water requirements.

Further assumptions of the study are that the cropping patterns, including the area of cultivation, types of crops and soil characteristics of the irrigated area, would remain the same in the future. These assumptions might not be strictly correct; however, they enable the separation of the impacts of climate change from other potential changes in the region. While this research shows the possible effects of climate change on irrigation water requirements, it must be understood within the context of the study's assumptions. It should be noted that there may be more or less crop cultivated in the future. Crop shifting and rotating may also happen as a result of climate change, and soil characteristics probably change due to degradation or erosion. Therefore, the results of this research should be interpreted in a general context in which increasing precipitation and temperature will lead to the rise of irrigation water requirements in this region.

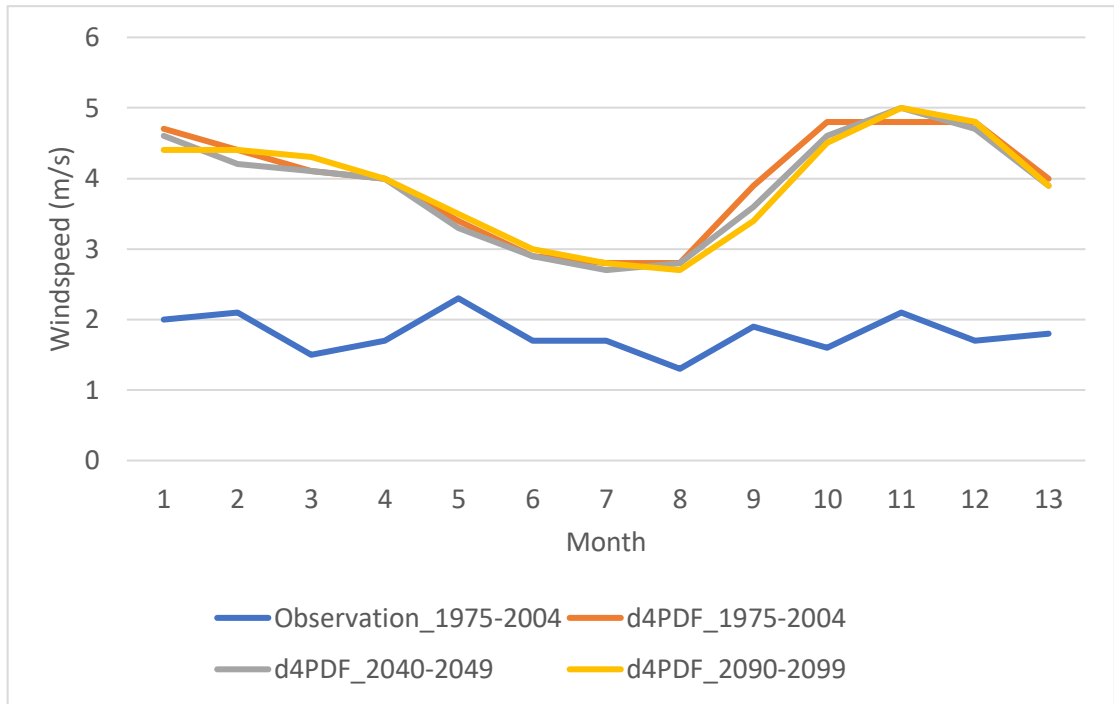


Figure 3.12 Comparison of observed and large-scale (d4PDF) wind speed for the period 1975-2004, 2040-2049 and 2090-2099

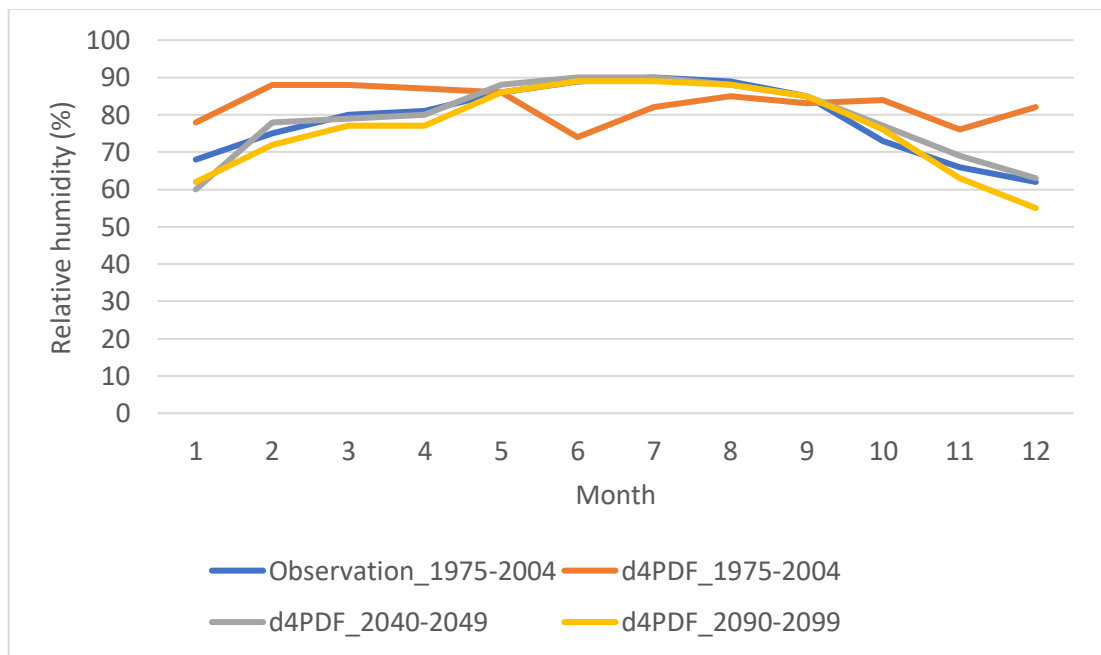


Figure 3.13 Comparison of observed and large-scale (d4PDF) relative humidity for the period 1975-2004, 2040-2049 and 2090-2099

CHAPTER 4 CONCLUSIONS

4.1 Summary of the findings

In this research, two models (SDSM and CROPWAT) were used to find the potential impacts of climate change on irrigation water requirements in the Ma river basin in Thanh Hoa, Viet Nam. The first model SDSM downscaled local precipitation and temperature based on the outputs of GCM d4PDF. The SDSM was calibrated, validated, and bias-corrected with existing data sets for the Ma river basin and then used to explore the changes in two future scenarios of monthly mean precipitation and temperature of the basin. The second model CROPWAT used climate projections from SDSM to compute irrigation water requirements for the region. A total of eight crops was calculated for crop water requirements, and the irrigation water requirements were calculated by the sum of individual crop water requirements for their cultivated areas. The research computes the gross irrigation water requirement for two future simulations by applying a local irrigation efficiency, and finally, conclusions and recommendations were made to reduce the negative impacts of climate change on irrigation water requirements for the region based on results and discussions.

This research implemented the backward-forward stepwise method to screen for effective predictors from d4PDF. The results of screening showed that zonal velocity at 500 hPa was the most effective predictor for precipitation, while the large-scale temperature was selected as the useful predictor for temperature. The regression models of SDSM between these predictors and precipitation and temperature were calibrated and validated for the period of 1975 to 2004 and 2005 to 2011. The results of calibration and validation indicated a reasonable simulation of the local climate, although there are some underestimations and overestimations in the case of precipitation. The downscaled precipitation was then corrected for bias using the linear scaling bias correction method. The validation of bias correction showed an improvement in simulating precipitation and indicated strong applicability of this method for simulation of precipitation of the region in the future.

Two climate scenarios (the 2040s and 2090s) based on d4PDF's future simulations 2K and 4K were generated for precipitation and temperature in the Ma river basin. Based on the results of the two scenarios generated, the trends of climate change are similar in pattern but different in magnitude. Warmer and wetter climates are anticipated for the region with the mean changes ranging from 1.7 to 4 °C for temperature and 4.8 to 13.4 % for precipitation.

Precipitation projected using two climate change scenarios increased precipitation in the region. Based on the 2040s simulation, the precipitation is projected to increase for the months from April to September, between 4.9 and 17.7 %, and to decrease for the remaining months

between -0.9 to -19.7 %. The 2090s scenario, as compared to the 2040s, showed more increases of precipitation from April to September, and more significant decreases in rainfall for other months.

Temperature simulated based on climate change scenarios 2K and 4K of d4PDF showed a general increasing trend in the region. Results of the 2040s simulation suggested increases in temperature for all months, with the most significant changes in December, January, and February (2.1 to 2.8 °C). The 2090s scenarios projected similar changes in trend, but a more considerable increase, with the biggest rises of 6.1 °C in January. The effects of these changes in climate on irrigation water requirements of the Ma river basin were analyzed using the CROPWAT model.

The results of the CROPWAT model showed rising tendencies of irrigation water requirements in the region over the two future periods compared to the baseline. Net irrigation water requirement increased from 189.1 during the baseline period (1975-2004) to 201 and 220.4 mm/month for the period of 2040-2049 and 2090-2099, respectively. Seasonal irrigation water requirements were also projected to change. Dry season's irrigation water requirements are likely to increase through simulated periods while the wet season remains the same. The first and second water-needed crops were projected as winter rice (winter to spring) and summer rice (summer to autumn), which requires water from November to February and July to August. Other crops were predicted to require less than 10 % of the total irrigation water requirement of the region.

4.2 Recommendations

The results of this research showed overall increases in irrigation water requirements in Thanh Hoa throughout the 2040s and 2090s in which the demands for irrigation water could increase the most during the dry season. These changes pose a significant threat to crop growth, food security, and water balance in the region, especially during the period when extreme weather such as drought and heatwave happen. The situation could be even worse for places where crops are planted in the hilly or mountainous area so that the local irrigation system cannot reach. Based on the current situation of the locality and the results of this research, some recommendations are proposed to reduce the potential negative impacts of climate changes on Thanh Hoa's agriculture.

(1) Improvement of irrigation efficiency

Improving irrigation efficiency aims to minimize the water used for agriculture, reduce water loss while maintaining optimal crop productivity. The irrigation efficiency (E) in the Ma river basin is currently categorized as a "bad irrigation management system," with E equal 65%

(JICA. 2010). The primary sources of irrigation water come from the surface flow of the Ma river, which is led to the field by channel and then electrically or manually pumped to the specific fields. The water loss along the way is relatively high (35%). One of the proposed ways to effectively reduce this water loss and hence improve irrigation efficiency is to control the water release so that the crops receive only the amount needed. For example, more efficient irrigation could include a pressurized irrigation system (drip irrigation). A drip irrigation system delivers water by dripping water to the specific crop at very slow rates. Only parts of the soil that the root grows is irrigated, and hence, it minimizes deep percolation, reduces surface runoff and evapotranspiration from the soil. This innovative irrigation method can save up to 50% water usage and increase crop yields by 40% compared to the conventional irrigation system. However, it requires a relatively high initial cost of \$1,200 to \$3,000 per hectare (Smith, 2015), which may be inaccessible to small-scale farmers in the Ma river basin. Therefore, subsidy mechanisms are also required to support farmers for drip irrigation's installation. It is noted that the drip irrigation system is suitable for row crops such as vegetables, soft fruit and tree crops where one or more emitters can be provided for each plant. Perennial crops in the Ma river basin is a potential application of this irrigation method. Another recommendation to reduce the amount of water loss is to regularly monitor the equipment and repair damages/leakages in the irrigation system (pipe or channel).

(2) Construction of new exploitation works and upgrading the current irrigation system

There is a lack of water reservoirs in the mainstream of Ma rivers since most water constructions are built on the river branches. The need to construct new exploitation work along the mainstream to regulate and store water for multiple purposes, including irrigation, emerges with future climate-driven. Also, upgrading irrigation pumping stations and canals on the South of the Ma river basin are necessary to improve the irrigation situation in the whole region. A remaining difficulty in irrigation supply in this area is that the irrigation system cannot cover hilly and mountainous cultivated regions. Terraced water exploitation works might be a solution to this problem.

(3) Crop rotation and shifting

As can be seen in the results of this research, IWR peaks during the dry season (November to April) and July to August. Altering farming practices such as crop rotation (grow crops according to the seasons and soil condition) could help reduce irrigation requirement pressure in months whose water demands are already high. For example, winter rice (winter to spring), whose IWR ranks the highest in total IWR of the region, could be planted six months later (rotate from late November to late May), and summer rice could be cultivated one month later (from August to September) to avoid dry season while maintaining double cropping.

Another possible recommendation for this region is crop shifting, which refers to the changes from one crop to another crop. A successful model was created in the Mekong river delta in which rice is changed to short-term crops to shorten the crop cycle, reduce water used while improving economic benefits (Seed. 2018). In this region, rice could be partly replaced with corn or other short-term leafy vegetables such as cucumber and hot pepper, which require less water consumption and deliver higher profits.

(4) Crop breeding

The future projection of this research suggests drier-hotter weather during the dry season and wetter-hotter for the rainy season. Developing crop varieties that can withstand drought stresses while producing a reliable yield is needed. This could be possible by crop breeding. Many new drought-resistant crop seeds are being developed by conventional and advanced breeding. There are already examples of drought-tolerant crops such as maize, soybean, and rice variety that farmers in Thanh Hoa can apply for a better adaptation to future climate change.

(5) Healthy soil

Healthy soil and biodiversity are essential to ecological approaches to helping farming more drought-tolerant and increasing resilience to extreme weather in Thanh Hoa. An appropriate practice of soil management makes soil hold moisture better and reduce erosion in the field. Building healthy soil in the irrigated areas is thus a crucial factor in making farms cope with water stresses and drought. There are many applicable practices that farmers in Thanh Hoa can apply to build healthy soils. Cover the field with crop residues that protect the land from wind and being eroded is one among many possible ways of building healthy soils. Other ideas could be the application of manure and compost to increase organic matter in the soil, enhance soil structure, help water infiltration, and make nutrients more accessible to the crops.

4.3 Suggestions for future work

For future work, an improvement to the research would be to project the future runoff of the Ma river using projected rainfall in this research. Since irrigation water of the area mostly comes from rivers, a comparison of future irrigation water requirements and simulated discharge of the river using the same input data (precipitation) could draw a clearer picture of irrigation water requirement and hence, more specific recommendations could be made based on that. Another improvement might be to include other GCMs as input data for the simulation of future conditions. Improvements could also take into consideration the changes in wind speed, humidity, and sunshine in the future to have a broader and comprehensive simulation of future local climatic conditions based on various GCM sources, not only one d4PDF model. Hence, comparisons can be made among GCMs to see which GCMs better simulate the local climate.

Further improvement could be to include the estimates of uncertainty in types of changes of cropping patterns (area of crops, variety of plants, and planting date) and soil characteristics that might be in the future. The major limitation of current climate prediction, especially precipitation, is the lack of variability's prediction of the future climate. Without the ability to simulate climate variability, studies such as this one can only indicate general tendencies.

ACKNOWLEDGMENTS

Foremost, I would like to express my deepest and sincere gratitude to my supervisor Prof. Michiaki Sugita for his continuous support of my Master's study and research; for his patience, enthusiasm, motivation, and immense knowledge. His guidance helped me throughout all the time of my research, making presentations, and writing this thesis. He has taught me the methodology to research an academic way and explore every side of the study as clearly as possible. I also would like to thank him for his empathy for every mistake that I made during the research and extra working time during weekends to give me insightful advice and comments. It would be a great honor and privilege to work and study under his guidance. I could not have imagined having a better supervisor for my Master's study.

I would like to thank my advisors, Prof. Maki Tsujimura and Prof. Asanuma Jun for their encouragement and precious comments. My sincere thank also goes to Prof. Tsutomu Yamanaka for his enthusiasm, dedication, and open-minded questions during the Joint seminar.

I thank the Project for Human Resource Development by Japanese Grant Aid for valuable financial supports during two years of studying. My appreciation also goes to the Japanese International Cooperation Center and my coordinator Ms. Emi Takabe for their consistent and continuous support to me during the time in Japan. I would like to thank Dr. Nguyen Toan Thang – Director of Center for Responding to Climate Change, for allowing my absence at work to study here in Tsukuba.

I thank my fellows in Sugita lab: Iuma Bani, Abdul Jabbar, Kawase, Kotaro, Youssef Mohammed, and Zang Chao for useful discussions and for the late-night we are working together, and for all the fun we have had during the last two years. I also thank my friends at the University of Tsukuba and the Vietnamese student association for their support and entertaining activities.

Last but not least, I am incredibly grateful to my family for their unconditional love, caring, prayers, and sacrifices for educating and supporting me for my future. I am very much thankful to my sister, who consistently helps me with my research proposal, preparation for scholarships, and actively inspires me to study abroad. A sincere appreciation to my wife for her love, sacrifices, understanding, and mental support during all the far-from-home journeys.

REFERENCES

- Acharjee, T. K., Ludwig, F., van Halsema, G., Hellegers, P., & Supit, I. (2017). Future changes in water requirements of Boro rice in the face of climate change in North-West Bangladesh. *Agricultural Water Management*, *194*, 172–183. <https://doi.org/https://doi.org/10.1016/j.agwat.2017.09.008>
- Allen, R., Pereira, L., Raes, D., & Smith, M. (1998). FAO Irrigation and drainage paper No. 56. *Rome: Food and Agriculture Organization of the United Nations*, *56*, 26–40.
- Bhave, A. G., Mishra, A., & Raghuvanshi, N. S. (2014). A combined bottom-up and top-down approach for assessment of climate change adaptation options. *Journal of Hydrology*, *518*, 150–161. <https://doi.org/https://doi.org/10.1016/j.jhydrol.2013.08.039>
- Borboudakis, G., & Tsamardinos, I. (2017). *Forward-Backward Selection with Early Dropping*.
- Bunn, C., Läderach, P., Ovalle Rivera, O., & Kirschke, D. (2015). A bitter cup: climate change profile of global production of Arabica and Robusta coffee. *Climatic Change*, *129*(1), 89–101. <https://doi.org/10.1007/s10584-014-1306-x>
- Bureau of Meteorology, Department of the Environment, A. G. (2016). *Climate change in Australia*. <https://www.climatechangeinaustralia.gov.au/>
- Church, J., Clark, P., Cazenave, A., Gregory, J., Jevrejeva, S., Levermann, A., Merrifield, M., Milne, G., Nerem, R., Nunn, P., Payne, A., Pfeffer, W., Stammer, D., & Alakkat, U. (2013). Climate Change 2013: The Physical Science Basis. Contribution of Working Group I to the Fifth Assessment Report of the Intergovernmental Panel on Climate Change. *Sea Level Change*, 1138–1191.
- Collins, M., Knutti, R., Arblaser, J., Dufresne, J.-L., Fichet, T., Friedlingstein, P., Gao, X., Gutowski, W., Johns, T., Krinner, G., Shongwe, M., Tebaldi, C., Weaver, A., & Wehner, M. (2014). *Long-term Climate Change: Projections, Commitments and Irreversibility* (pp. 1029–1136).
- Department of Natural Resources and Environment. (2017). *Classifications of soil in Thanh Hoa*.
- Dibike, Y. B., & Coulibaly, P. (2005). Hydrologic impact of climate change in the Saguenay watershed: comparison of downscaling methods and hydrologic models. *Journal of Hydrology*, *307*(1), 145–163. <https://doi.org/https://doi.org/10.1016/j.jhydrol.2004.10.012>
- Eden, J. M., & Widmann, M. (2014). Downscaling of GCM-Simulated Precipitation Using Model Output Statistics. *Journal of Climate*, *27*(1), 312–324. <https://doi.org/10.1175/JCLI-D-13-00063.1>
- Endo, H., Kitoh, A., Mizuta, R., & Ishii, M. (2017). Future Changes in Precipitation Extremes in East Asia and Their Uncertainty Based on Large Ensemble Simulations with a High-Resolution AGCM. *SOLA*, *13*, 7–12. <https://doi.org/10.2151/sola.2017-002>
- Fowler, H., Ekström, M., Blenkinsop, S., & Smith, A. (2007). Estimating change in extreme European precipitation using a multimodel ensemble. *Journal of Geophysical Research*, *112*. <https://doi.org/10.1029/2007JD008619>
- Frenken, K. and Faurès, J. M. (1997). Irrigation Potential in Africa: A Basin Approach. In *FAO*

Land and Water Bulletin, Vol. 4, Food & Agriculture Organization (Vol.4, p. 177).

- Gebremeskel, S., Liu, Y. B., de Smedt, F., Hoffmann, L., & Pfister, L. (2004). Analysing the effect of climate changes on streamflow using statistically downscaled GCM scenarios. *International Journal of River Basin Management*, 2(4), 271–280. <https://doi.org/10.1080/15715124.2004.9635237>
- GFDL. (2014). *Climate Modeling – Geophysical Fluid Dynamics Laboratory*. <https://www.gfdl.noaa.gov/climate-modeling/>
- GSO. (2018). *Statistical Yearbook of Vietnam*.
- Hoang, Q. (2002). *Management, exploitation, use and protection of water resources and environment in Ma River basin, 2002* [Water Resources University]. <http://luanan.nlv.gov.vn/luanan?a=d&d=TTbFlGutQvce2002.1.1&e=-----vi-20--1--img-txIN----->
- Hoang, Q. (2009). Water Balance in the lower section of Ma river basin in Thanh Hoa province. *Journal of Hydrology and Meteorology*, 1, 19–25. <http://tapchikttv.vn/article/351>
- Huang, J., Zhang, J., Zhang, Z., Xu, C., Wang, B., & Yao, J. (2011). Estimation of future precipitation change in the Yangtze River basin by using statistical downscaling method. *Stochastic Environmental Research and Risk Assessment*, 25(6), 781–792. <https://doi.org/10.1007/s00477-010-0441-9>
- JICA. (2010). *Prediction of Water demand in 14 river basins*. https://openjicareport.jica.go.jp/pdf/11740727_03.pdf
- JMA. (2007). *Outline of the operational numerical weather prediction at the Japan Meteorological Agency, Appendix to WMO Technical Progress Report on the Global Data-processing and Forecasting System (GDPFS) and Numerical Weather Prediction (NWP) Research*.
- Kanada, S., Nakano, M., & Kato, T. (2012). Projections of Future Changes in Precipitation and the Vertical Structure of the Frontal Zone during the Baiu Season in the Vicinity of Japan Using a 5-km-mesh Regional Climate Model. *Journal of the Meteorological Society of Japan*, 90A, 65–86. <https://doi.org/10.2151/jmsj.2012-A03>
- Khan, M. S., Coulibaly, P., & Dibike, Y. (2006). Uncertainty analysis of statistical downscaling methods. *Journal of Hydrology*, 319(1), 357–382. <https://doi.org/https://doi.org/10.1016/j.jhydrol.2005.06.035>
- Kitoh, A., & Endo, H. (2016). Future Changes in Rainfall Extremes Associated with El Niño Projected by a Global 20-km Mesh Atmospheric Model. *SOLA, 12A(Special_Edition)*, 1–6. <https://doi.org/10.2151/sola.12A-001>
- Knox, J., Hess, T., Daccache, A., & Wheeler, T. (2012). Climate change impacts on crop productivity in Africa and South Asia. *Environmental Research Letters*, 7, 34032. <https://doi.org/10.1088/1748-9326/7/3/034032>
- Lemke, P., Ren, J. F., Alley, R., Allison, I., Carrasco, J., Flato, G., Fujii, Y., Kaser, G., Mote, P., Thomas, R., & Zhang, T. (2007). IPCC, 2007. Climate Change 2007. Synthesis Report. Contribution of Working Groups I, II & III to the Fourth Assessment Report of the Intergovernmental Panel on Climate Change. Geneva. In *IPCC*. <https://doi.org/10.1017/CBO9780511546013>

- Mahmood, R. (2012). Evaluation of SDSM developed by annual and monthly sub-models for downscaling temperature and precipitation in the Jhelum basin, Pakistan and India. *Theoretical and Applied Climatology*, 113. <https://doi.org/10.1007/s00704-012-0765-0>
- Martin, D. L. (University of N. at L. J. R. G. (Iowa S. U. at A. (1993). Irrigation Water Requirements. In *the National Engineering Handbook, Part 623* (pp. 2-1-2–281). the Technical Publishing Team, SCS National Cartography and GIS Center, Fort Worth, TX. <https://www.wcc.nrcs.usda.gov/ftpref/wntsc/waterMgt/irrigation/NEH15/ch2.pdf>
- Mearns, L. O. (2009). *Methods of Downscaling Future Climate Information and Applications*. 30.
- Mizuta, R., Murata, A., Ishii, M., Shiogama, H., Hibino, K., Mori, N., Arakawa, O., Imada, Y., Yoshida, K., Aoyagi, T., Kawase, H., Mori, M., Okada, Y., Shimura, T., Nagatomo, T., Ikeda, M., Endo, H., Nosaka, M., Arai, M., ... Kimoto, M. (2016). Over 5,000 Years of Ensemble Future Climate Simulations by 60-km Global and 20-km Regional Atmospheric Models. *Bulletin of the American Meteorological Society*, 98(7), 1383–1398. <https://doi.org/10.1175/BAMS-D-16-0099.1>
- Mizuta, R., Yoshimura, H., Murakami, H., Matsudea, M., Endo, H., Ose, T., Kamiguchi, K., Hosaka, M., Sugi, M., Yukimoto, S., Kusunoki, S., & Kitoh, A. (2012). Climate Simulations Using MRI-AGCM3.2 with 20-km Grid. *Journal of the Meteorological Society of Japan. Ser. II*, 90A, 233–258. <https://doi.org/10.2151/jmsj.2012-A12>
- Morton, J. (2008). The Impact of Climate Change on Smallholder and Subsistence Agriculture. *Proceedings of the National Academy of Sciences of the United States of America*, 104, 19680–19685. <https://doi.org/10.1073/pnas.0701855104>
- Ngo, K. (2007). *Overview of Thanh Hoa*. <http://thanhhoa.gov.vn/portal/Pages/2007-01-26/TONG-QUAN-VE-THANH-HOA-4c00cd833c63f09.aspx>
- Nohara, D., Kitoh, A., Hosaka, M., & Oki, T. (2006). Impact of Climate Change on River Discharge Projected by Multimodel Ensemble. *Journal of Hydrometeorology*, 7(5), 1076–1089. <https://doi.org/10.1175/JHM531.1>
- Parry, M. L., Canziani, O., Palutikof, J. P., van der Linden, P., & Hanson, C. E. (2007). Climate Change 2007: Impacts, Adaptation and Vulnerability. In *Contribution of Working Group II to the Fourth Assessment Report of the Intergovernmental Panel on Climate Change*.
- People Committee. (2006). *Water resources planning in the Ma river basin*.
- Pfahl, S., O’Gorman, P. A., & Fischer, E. M. (2017). Understanding the regional pattern of projected future changes in extreme precipitation. *Nature Climate Change*, 7(6), 423–427. <https://doi.org/10.1038/nclimate3287>
- Rosenzweig, C., Elliott, J., Deryng, D., Ruane, A., Müller, C., Arneth, A., Boote, K., Folberth, C., Glotter, M., Khabarov, N., Hermans, K., Piontek, F., Pugh, T., Schmid, E., Stehfest, E., Yang, H., & Jones, J. (2013). Assessing agricultural risks of climate change in the 21st century in a global gridded crop model intercomparison. *Proceedings of the National Academy of Sciences of the United States of America*, 111. <https://doi.org/10.1073/pnas.1222463110>
- Salzmann, N., Frei, C., Vidale, P.-L., & Hoelzle, M. (2007). The application of Regional Climate Model output for the simulation of high-mountain permafrost scenarios. *Global*

- and *Planetary Change*, 56(1), 188–202.
<https://doi.org/https://doi.org/10.1016/j.gloplacha.2006.07.006>
- SCSS. (2007). Stepwise Regression. In *SCSS Statistical Software Manual* (p. 431). https://ncss-wpengine.netdna-ssl.com/wp-content/themes/ncss/pdf/Procedures/NCSS/Stepwise_Regression.pdf
- Seaby, L. P., Refsgaard, J. C., Sonnenborg, T. O., Stisen, S., Christensen, J. H., & Jensen, K. H. (2013). Assessment of robustness and significance of climate change signals for an ensemble of distribution-based scaled climate projections. *Journal of Hydrology*, 486, 479–493. <https://doi.org/https://doi.org/10.1016/j.jhydrol.2013.02.015>
- Seed, E.-W. (2018). *Crop Shifting Model from Rice to Fresh Corn (sweet and waxy corn for human consumption) in Mekong Delta Vietnam*. <https://www.eastwestseed.com/news/crop-shifting-model-from-rice-to-fresh-corn-sweet-and-waxy-corn-for-human-consumption-in-mekong-delta-vietnam>
- Sharma, D., Das Gupta, A., & Babel, M. (2007). Spatial disaggregation of bias-corrected GCM precipitation for improved hydrologic simulation: Ping River Basin, Thailand. *Hydrology and Earth System Sciences*, 11. <https://doi.org/10.5194/hessd-4-35-2007>
- Smith, A. (2015). *Low-cost drip irrigation*.
- Teutschbein, C., & Seibert, J. (2012). Bias correction of regional climate model simulations for hydrological climate-change impact studies: Review and evaluation of different methods. *Journal of Hydrology*, 456–457, 12–29. <https://doi.org/https://doi.org/10.1016/j.jhydrol.2012.05.052>
- Thanh Hoa's Department of Statistic. (2017). *Statistical Yearbook of Thanh Hoa*.
- Thanh Hoa's People Committee. (2013). *Land use map planning of Thanh Hoa province for the period 2011-2015, vision to 2020*. <https://thanhhoa.gov.vn/vi-vn/TaiLieu/QHthanhhoa.jpg>
- The, T. Van, Ha, Q., Thi, B., Loan, P., & Son, H. (2015). *Impact of Climate Change on Rice Production in the Red River and Mekong River Delta of Vietnam*. https://www.naro.affrc.go.jp/archive/niaes/marco/marco2015/text/ws1-44_1_n_h_son.pdf
- Trzaska, S., & Schnarr, E. (2014). *A Review of Downscaling Methods for Climate Change Projections*.
- UNESCO. (2009). *World Water Assessment Programme. 2009. The United Nations World Water Development Report 3: Water in a Changing World*.
- VAST. (2014). *Assessment of capacity to ensure water resources for socio-economic development activities in the Ma river basin in 2020 (Viet Nam territory)*. Vietnam Academy of Science and Technology, Institute of Geography. 10. <http://ig-vast.ac.vn/vi/tin-tuc/danh-gia-kha-nang-dam-bao-nguon-nuoc-cho-cac-hoat-dong-phat-trien-kinh-te---xa-hoi-luu-vuc-song-ma-nam-2020----40-phan-lanh-tho-viet-nam--41--209.html>
- Wilby, R., & Dawson, C. (2007). *Using SDSM Version 3.1 — A decision support tool for the assessment of regional climate change impacts User Manual*.
- Wilby, R., Dawson, C., & Barrow, E. M. (2002). SDSM – A Decision Support Tool for the

Assessment of Regional Climate Change Impacts. *Environmental Modelling & Software*, 17, 145–157. [https://doi.org/10.1016/S1364-8152\(01\)00060-3](https://doi.org/10.1016/S1364-8152(01)00060-3)

Yano, T., Aydin, M., & Haraguchi, T. (2007). Impact of Climate Change on Irrigation Demand and Crop Growth in a Mediterranean Environment of Turkey. *Sensors (Basel, Switzerland)*, 7(10), 2297–2315. <https://doi.org/10.3390/s7102297>

Zeke Hausfather. (2019). *Explainer: The high-emissions ‘RCP8.5’ global warming scenario*. <https://www.carbonbrief.org/explainer-the-high-emissions-rcp8-5-global-warming-scenario>

Zorita, E., & von Storch, H. (1999). The Analog Method as a Simple Statistical Downscaling Technique: Comparison with More Complicated Methods. *Journal of Climate*, 12(8), 2474–2489. [https://doi.org/10.1175/1520-0442\(1999\)012<2474:TAMAAS>2.0.CO;2](https://doi.org/10.1175/1520-0442(1999)012<2474:TAMAAS>2.0.CO;2)

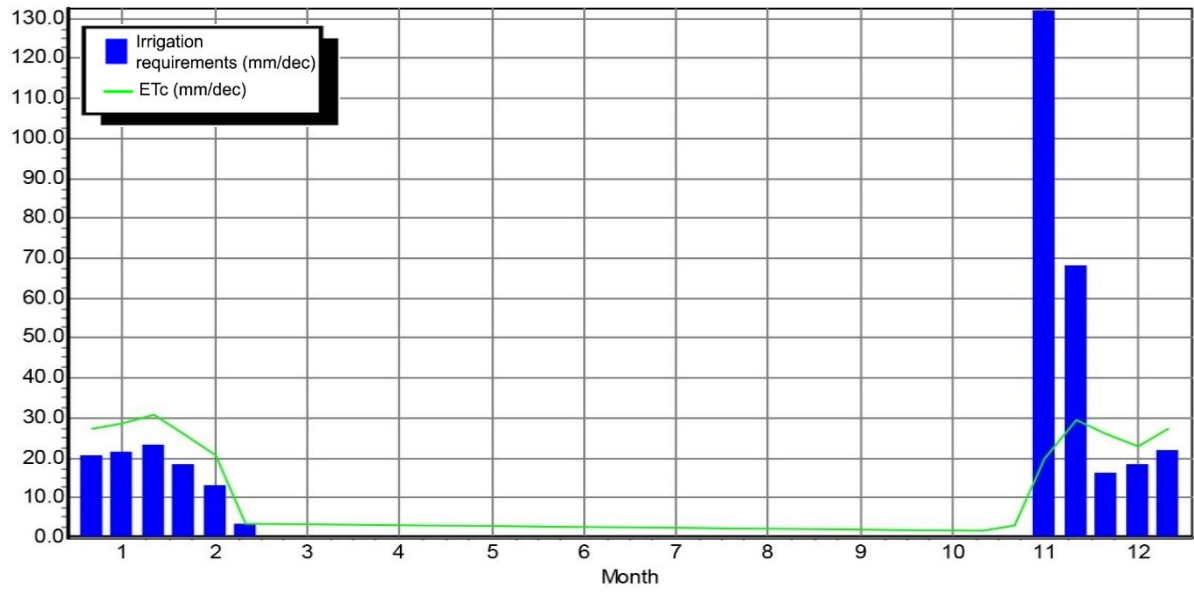


Figure A - 1 Crop water requirement and evapotranspiration of winter rice for 2040-2049

Table A - 2 Crop water requirement for summer rice for 2040-2049

RICE DATA

(File: C:\ProgramData\CROPWAT\data\crops\ThanhHoa\Rice2.CRO)

Crop Name: Rice2		Transplanting date: 05/08		Harvest: 02/11				
Stage	nursery	landprep		growth stage			total	
		total	puddling	initial	develop	mid		late
Length (days)	30	10	5	15	25	30	20	120
Kc dry	0.70		0.30	0.50	-->	1.05	0.70	
Kc wet	1.04		1.08	1.15	-->	1.38	0.95	
Rooting depth (m)				0.10	-->	0.60	0.60	
Puddling depth (m)			0.40					
Nursery area (%)	10							
Critical depletion	0.20			0.20	-->	0.20	0.20	
Yield response f.				1.00		1.09	1.09	1.09
Cropheight (m)						1.00		

CROP WATER REQUIREMENTS

ETo station: ThanhHoa
Rain station: ThanhHoa

Crop: Rice2
Planting date: 05/08

Month	Decade	Stage	Kc coeff	ETc mm/day	ETc mm/dec	Eff rain mm/dec	Irr. Req. mm/dec
Jul	1	Nurs	1.04	0.47	2.3	21.9	0.0
Jul	2	Nurs	1.04	0.45	4.5	43.5	0.0
Jul	3	Nurs/LPr	1.06	2.74	30.2	46.0	131.2
Aug	1	Init	1.12	4.82	48.2	49.0	52.8
Aug	2	Deve	1.15	4.91	49.1	51.3	0.0
Aug	3	Deve	1.17	4.78	52.5	52.5	0.0
Sep	1	Deve	1.20	4.67	46.7	54.3	0.0
Sep	2	Mid	1.21	4.52	45.2	55.9	0.0
Sep	3	Mid	1.22	4.28	42.8	54.0	0.0
Oct	1	Mid	1.22	4.05	40.5	54.1	0.0
Oct	2	Late	1.15	3.62	36.2	53.8	0.0
Oct	3	Late	0.93	2.85	31.4	42.7	0.0
Nov	1	Late	0.79	2.36	4.7	5.8	4.7
					434.3	584.7	188.7

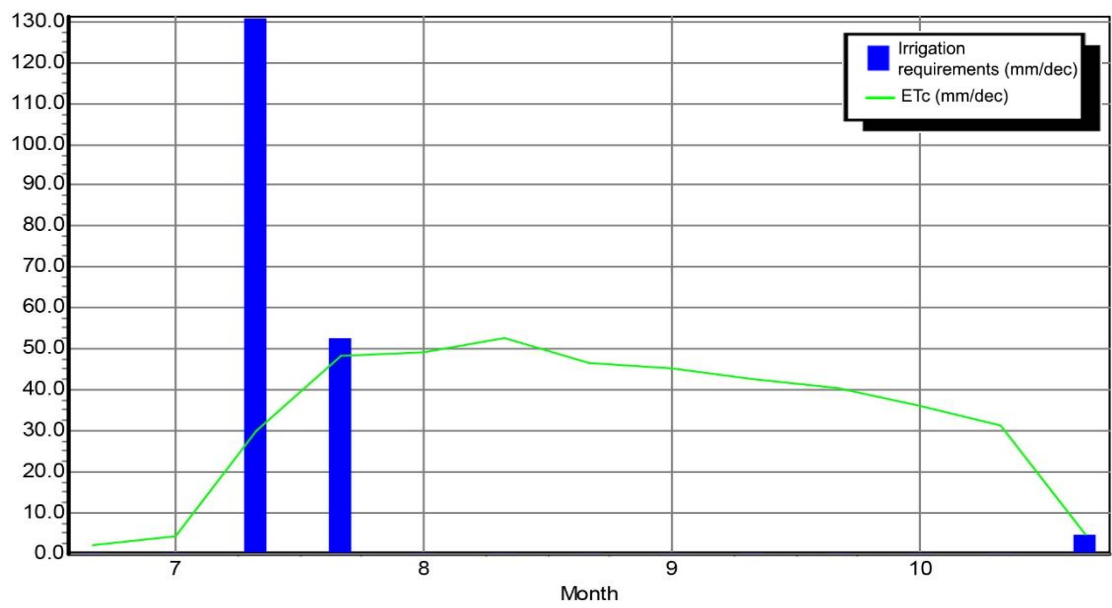


Figure A - 2 Crop water requirement and evapotranspiration of summer rice for 2040-2049

Table A - 3: Crop water requirement of maize for 2040-2049

DRY CROP DATA

(File: C:\ProgramData\CROPWAT\data\crops\ThanhHoa\MAIZE.CRO)

Crop Name: MAIZE (Grain)	Planting date: 15/05		Harvest: 16/09		
Stage	initial	develop	mid	late	total
Length (days)	20	35	40	30	125
Kc Values	0.30	-->	1.20	1.05	
Rooting depth (m)	0.30	-->	1.00	1.00	
Critical depletion	0.55	-->	0.55	0.80	
Yield response f.	0.40	0.40	1.30	0.50	1.25
Cropheight (m)			2.00		

CROP WATER REQUIREMENTS

ETo station: ThanhHoa
Rain station: ThanhHoa

Crop: MAIZE (Grain)
Planting date: 15/05

Month	Decade	Stage	Kc coeff	ETc mm/day	ETc mm/dec	Eff rain mm/dec	Irr. Req. mm/dec
May	2	Init	0.30	1.14	6.9	27.7	0.0
May	3	Init	0.30	1.24	13.6	45.7	0.0
Jun	1	Deve	0.36	1.60	16.0	44.4	0.0
Jun	2	Deve	0.55	2.64	26.4	44.8	0.0
Jun	3	Deve	0.74	3.47	34.7	44.7	0.0
Jul	1	Mid	0.93	4.18	41.8	43.9	0.0
Jul	2	Mid	0.99	4.30	43.0	43.5	0.0
Jul	3	Mid	0.99	4.28	47.0	46.0	1.0
Aug	1	Mid	0.99	4.25	42.5	49.0	0.0
Aug	2	Late	0.99	4.21	42.1	51.3	0.0
Aug	3	Late	0.94	3.86	42.5	52.5	0.0
Sep	1	Late	0.89	3.49	34.9	54.3	0.0
Sep	2	Late	0.85	3.18	19.1	33.5	0.0
					410.5	581.3	1.0

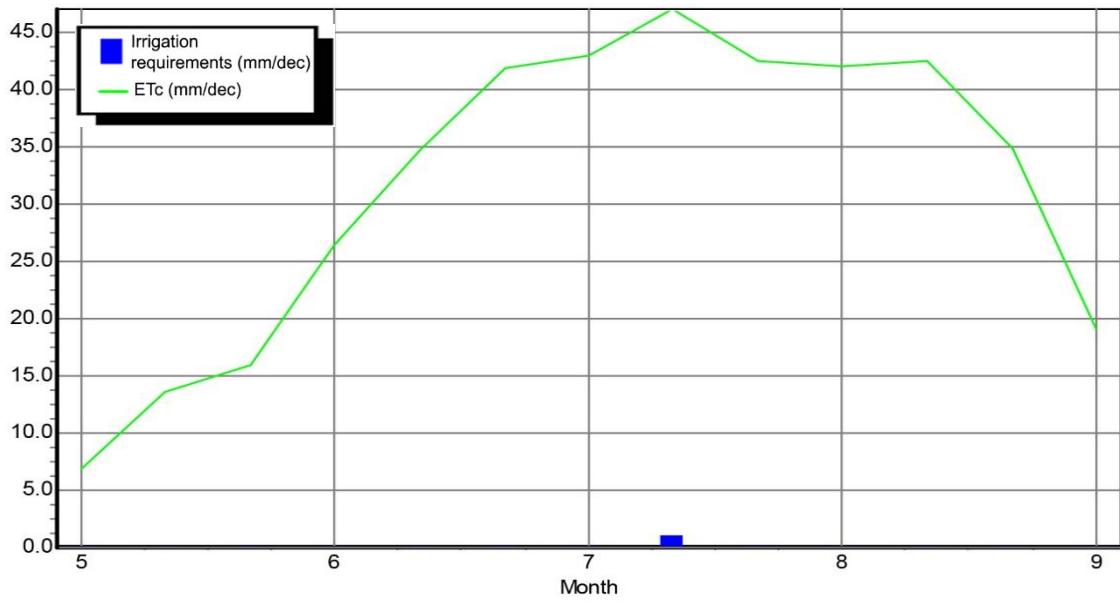


Figure A - 3: Crop water requirement and evapotranspiration of maize for 2040-2049

Table A - 4: Crop water requirement of soybean for 2040-2049

DRY CROP DATA

(File: C:\ProgramData\CROPWAT\data\crops\ThanhHoa\SOYBEAN.CRO)

Crop Name:	Soybean	Planting date:	24/04	Harvest:	17/07
Stage	initial	develop	mid	late	total
Length (days)	15	15	40	15	85
Kc Values	0.40	-->	1.15	0.75	
Rooting depth (m)	0.30	-->	1.00	1.00	
Critical depletion	0.50	-->	0.60	0.90	
Yield response f.	0.40	0.80	1.00	0.40	0.85
Cropheight (m)			0.60		

CROP WATER REQUIREMENTS

ETo station: ThanhHoa Crop: Soybean
 Rain station: ThanhHoa Planting date: 24/04

Month	Decade	Stage	Kc coeff	ETc mm/day	ETc mm/dec	Eff rain mm/dec	Irr. Req. mm/dec
Apr	3	Init	0.40	1.27	8.9	20.1	0.0
May	1	Deve	0.41	1.44	14.4	38.4	0.0
May	2	Deve	0.70	2.69	26.9	46.2	0.0
May	3	Mid	1.00	4.12	45.3	45.7	0.0
Jun	1	Mid	1.01	4.54	45.4	44.4	1.1
Jun	2	Mid	1.01	4.89	48.9	44.8	4.1
Jun	3	Mid	1.01	4.72	47.2	44.7	2.6
Jul	1	Late	0.91	4.09	40.9	43.9	0.0
Jul	2	Late	0.69	2.99	20.9	30.4	0.0
					298.9	358.5	7.8

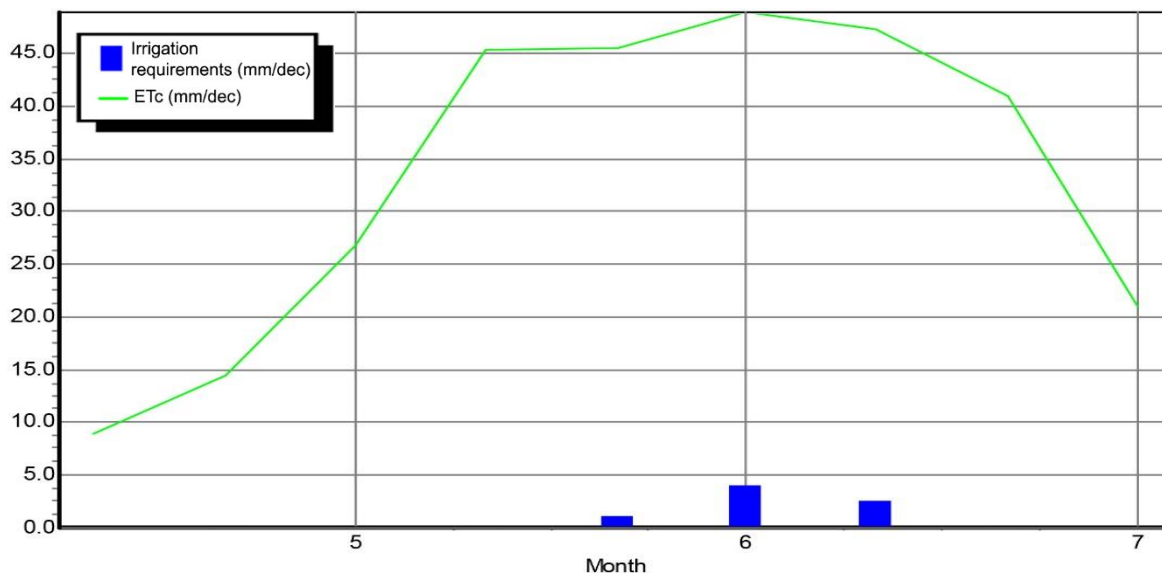


Figure A - 4: Crop water requirement and evapotranspiration of maize for 2040-2049

Table A - 5: Crop water requirement of groundnut for 2040-2049

DRY CROP DATA

(File: C:\ProgramData\CROPWAT\data\crops\ThanhHoa\GRONDNUT.CRO)

Crop Name:	Groudnut	Planting date:	24/04	Harvest:	31/08
Stage	initial	develop	mid	late	total
Length (days)	25	35	45	25	130
Kc Values	0.55	-->	1.15	0.90	
Rooting depth (m)	0.30	-->	0.80	0.80	
Critical depletion	0.45	-->	0.45	0.50	
Yield response f.	0.20	0.80	0.60	0.20	0.70
Cropheight (m)			0.40		

CROP WATER REQUIREMENTS

ETo station: ThanhHoa Crop: Groudnut
 Rain station: ThanhHoa Planting date: 24/04

Month	Decade	Stage	Kc coeff	ETc mm/day	ETc mm/dec	Eff rain mm/dec	Irr. Req. mm/dec
Apr	3	Init	0.55	1.75	12.3	20.1	0.0
May	1	Init	0.55	1.92	19.2	38.4	0.0
May	2	Deve	0.55	2.11	21.1	46.2	0.0
May	3	Deve	0.66	2.71	29.8	45.7	0.0
Jun	1	Deve	0.80	3.60	36.0	44.4	0.0
Jun	2	Deve	0.93	4.53	45.3	44.8	0.5
Jun	3	Mid	1.02	4.78	47.8	44.7	3.1
Jul	1	Mid	1.02	4.58	45.8	43.9	1.9
Jul	2	Mid	1.02	4.45	44.5	43.5	1.0
Jul	3	Mid	1.02	4.42	48.6	46.0	2.6
Aug	1	Late	1.01	4.35	43.5	49.0	0.0
Aug	2	Late	0.92	3.95	39.5	51.3	0.0
Aug	3	Late	0.82	3.34	36.7	52.5	0.0
					470.0	570.4	9.1

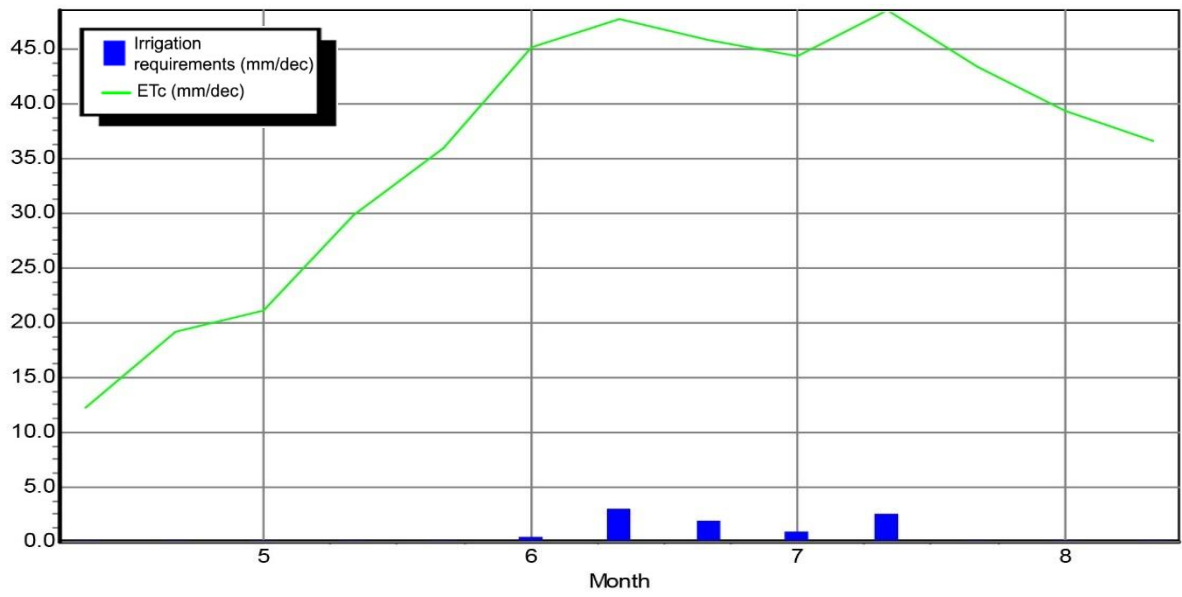


Figure A - 5: Crop water requirements and evapotranspiration of groundnut for 2040-2049

Table A - 6: Crop water requirements of sugarcane for 2040-2049

DRY CROP DATA

(File: C:\ProgramData\CROPWAT\data\crops\ThanhHoa\SUGARCAN.CRO)

Crop Name:	Sugarcane (Ratoon)	Planting date:	10/05	Harvest:	09/05
Stage	initial	develop	mid	late	total
Length (days)	30	60	180	95	365
Kc Values	0.40	-->	1.25	0.95	
Rooting depth (m)	1.50	-->	1.50	1.50	
Critical depletion	0.65	-->	0.65	0.65	
Yield response f.	0.50	0.75	1.20	0.10	1.20
Cropheight (m)			3.00		

CROP WATER REQUIREMENTS

ETo station: ThanhHoa Crop: Sugarcane (Ratoon)
 Rain station: ThanhHoa Planting date: 10/05

Month	Decade	Stage	Kc coeff	ETc mm/day	ETc mm/dec	Eff rain mm/dec	Irr. Req. mm/dec
May	1	Init	0.73	2.57	2.6	3.8	0.0
May	2	Init	0.40	1.52	15.2	46.2	0.0
May	3	Init	0.40	1.65	18.1	45.7	0.0
Jun	1	Deve	0.40	1.81	18.1	44.4	0.0
Jun	2	Deve	0.48	2.31	23.1	44.8	0.0
Jun	3	Deve	0.58	2.72	27.2	44.7	0.0
Jul	1	Deve	0.68	3.07	30.7	43.9	0.0
Jul	2	Deve	0.79	3.43	34.3	43.5	0.0
Jul	3	Deve	0.90	3.88	42.7	46.0	0.0
Aug	1	Mid	1.00	4.30	43.0	49.0	0.0
Aug	2	Mid	1.02	4.36	43.6	51.3	0.0
Aug	3	Mid	1.02	4.18	45.9	52.5	0.0
Sep	1	Mid	1.02	3.99	39.9	54.3	0.0
Sep	2	Mid	1.02	3.80	38.0	55.9	0.0
Sep	3	Mid	1.02	3.60	36.0	54.0	0.0
Oct	1	Mid	1.02	3.40	34.0	54.1	0.0
Oct	2	Mid	1.02	3.20	32.0	53.8	0.0
Oct	3	Mid	1.02	3.12	34.3	42.7	0.0
Nov	1	Mid	1.02	3.04	30.4	28.9	1.5
Nov	2	Mid	1.02	2.95	29.5	18.2	11.3
Nov	3	Mid	1.02	2.67	26.7	14.3	12.4
Dec	1	Mid	1.02	2.32	23.2	9.8	13.4
Dec	2	Mid	1.02	2.00	20.0	4.5	15.6
Dec	3	Mid	1.02	2.13	23.4	5.3	18.1
Jan	1	Mid	1.02	2.29	22.9	6.9	16.0
Jan	2	Mid	1.02	2.38	23.8	7.1	16.8
Jan	3	Mid	1.02	2.34	25.8	7.4	18.4
Feb	1	Late	1.01	2.28	22.8	7.5	15.4
Feb	2	Late	0.98	2.17	21.7	7.7	14.1
Feb	3	Late	0.95	2.10	16.8	8.9	7.8
Mar	1	Late	0.93	2.02	20.2	9.7	10.5
Mar	2	Late	0.89	1.94	19.4	10.5	8.9
Mar	3	Late	0.86	2.07	22.7	14.6	8.2
Apr	1	Late	0.83	2.18	21.8	18.1	3.8
Apr	2	Late	0.80	2.29	22.9	21.3	1.5
Apr	3	Late	0.76	2.44	24.4	28.7	0.0
May	1	Late	0.73	2.57	23.1	34.5	0.0
					1000.5	1094.2	193.7

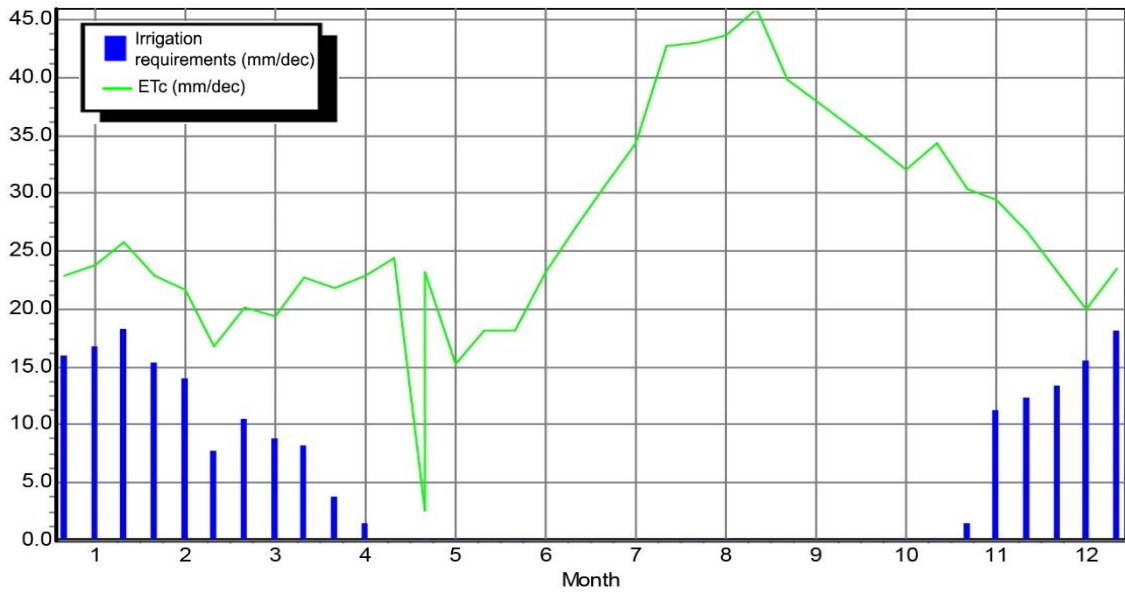


Figure A - 6: Crop water requirement and evapotranspiration of sugarcane for 2040-2049

Table A - 7: Crop water requirement of perennial crops for 2040-2049

DRY CROP DATA

(File: C:\ProgramData\CROPWAT\data\crops\ThanhHoa\PerennialCrops.CRO)

Crop Name:	Perennial crops	Planting date:	05/05	Harvest:	04/05
Stage	initial	develop	mid	late	total
Length (days)	30	60	180	95	365
Kc Values	0.70	-->	0.65	0.70	
Rooting depth (m)	1.50	-->	1.50	1.50	
Critical depletion	0.65	-->	0.65	0.65	
Yield response f.	0.50	0.75	1.20	0.10	1.20
Cropheight (m)			3.00		

CROP WATER REQUIREMENTS

ETo station: ThanhHoa Crop: Perennial crops
 Rain station: ThanhHoa Planting date: 05/05

Month	Decade	Stage	Kc coeff	ETc mm/day	ETc mm/dec	Eff rain mm/dec	Irr. Req. mm/dec
May	1	Init	0.47	1.65	9.9	23.0	0.0
May	2	Init	0.70	2.67	26.7	46.2	0.0
May	3	Init	0.70	2.88	31.7	45.7	0.0
Jun	1	Deve	0.69	3.09	30.9	44.4	0.0
Jun	2	Deve	0.64	3.11	31.1	44.8	0.0
Jun	3	Deve	0.60	2.79	27.9	44.7	0.0
Jul	1	Deve	0.55	2.46	24.6	43.9	0.0
Jul	2	Deve	0.50	2.19	21.9	43.5	0.0
Jul	3	Deve	0.45	1.96	21.6	46.0	0.0
Aug	1	Mid	0.42	1.81	18.1	49.0	0.0
Aug	2	Mid	0.42	1.80	18.0	51.3	0.0
Aug	3	Mid	0.42	1.72	18.9	52.5	0.0
Sep	1	Mid	0.42	1.64	16.4	54.3	0.0
Sep	2	Mid	0.42	1.56	15.6	55.9	0.0
Sep	3	Mid	0.42	1.48	14.8	54.0	0.0
Oct	1	Mid	0.42	1.40	14.0	54.1	0.0
Oct	2	Mid	0.42	1.32	13.2	53.8	0.0
Oct	3	Mid	0.42	1.28	14.1	42.7	0.0
Nov	1	Mid	0.42	1.25	12.5	28.9	0.0
Nov	2	Mid	0.42	1.22	12.2	18.2	0.0
Nov	3	Mid	0.42	1.10	11.0	14.3	0.0
Dec	1	Mid	0.42	0.96	9.6	9.8	0.0
Dec	2	Mid	0.42	0.83	8.3	4.5	3.8
Dec	3	Mid	0.42	0.88	9.7	5.3	4.3
Jan	1	Mid	0.42	0.94	9.4	6.9	2.5
Jan	2	Mid	0.42	0.98	9.8	7.1	2.7
Jan	3	Late	0.43	0.99	10.8	7.4	3.5
Feb	1	Late	0.47	1.06	10.6	7.5	3.2
Feb	2	Late	0.47	1.04	10.4	7.7	2.8
Feb	3	Late	0.47	1.04	8.3	8.9	0.0
Mar	1	Late	0.47	1.03	10.3	9.7	0.6
Mar	2	Late	0.47	1.02	10.2	10.5	0.0
Mar	3	Late	0.47	1.13	12.5	14.6	0.0
Apr	1	Late	0.47	1.24	12.4	18.1	0.0
Apr	2	Late	0.47	1.35	13.5	21.3	0.0
Apr	3	Late	0.47	1.50	15.0	28.7	0.0
May	1	Late	0.47	1.65	6.6	15.3	0.0
					572.5	1094.2	23.4

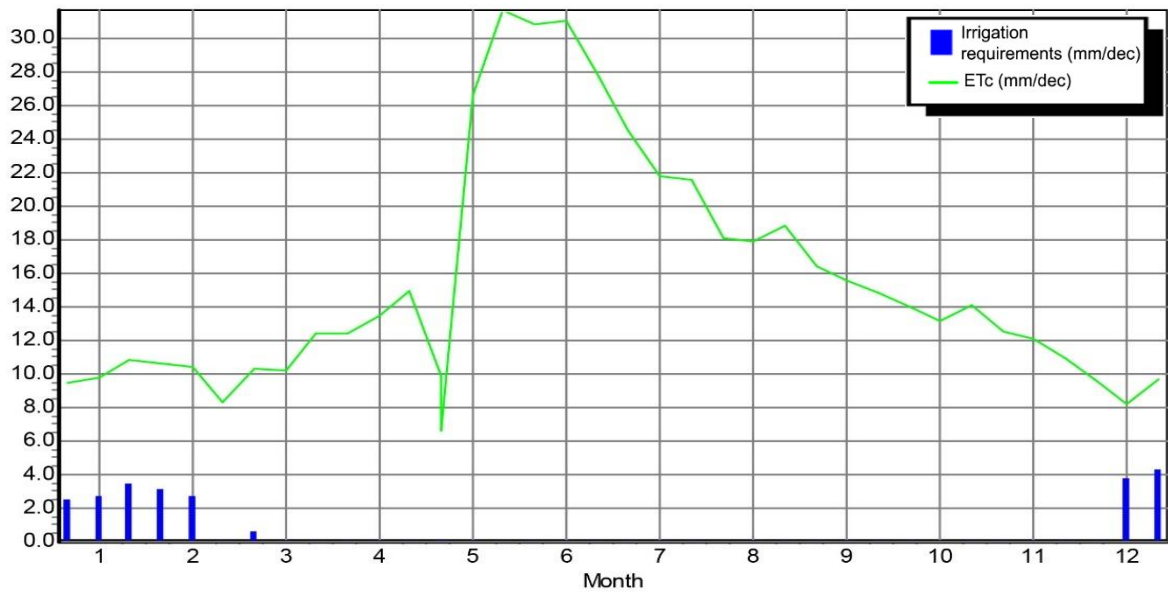


Figure A - 7: Crop water requirement and evapotranspiration of perennial crops for 2040-2049

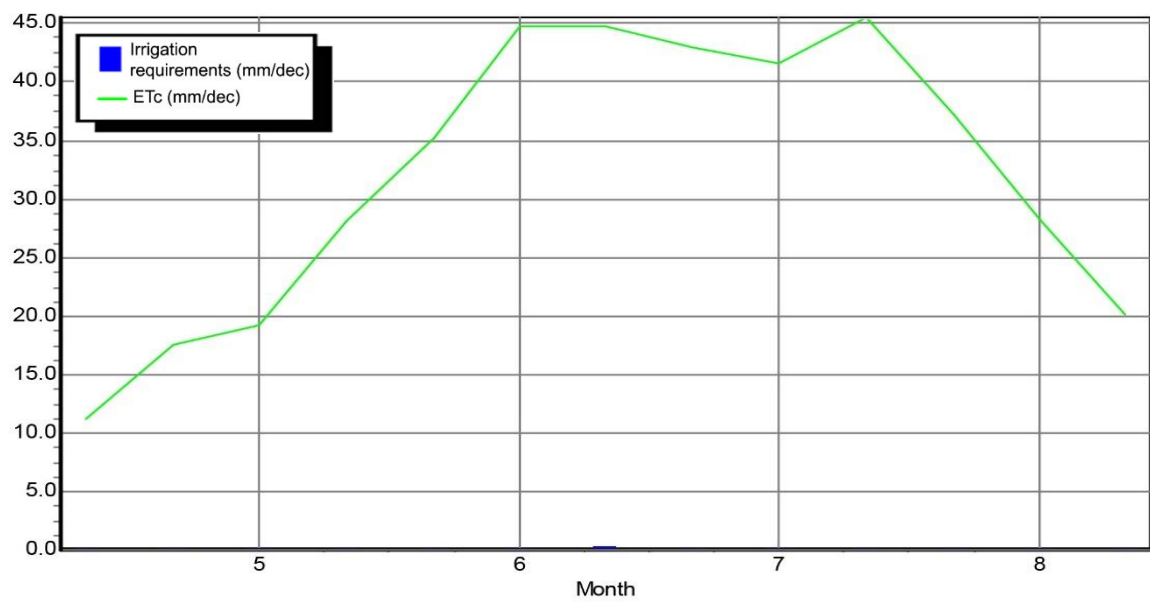


Figure A - 8: Crop water requirement and evapotranspiration of potato for 2040-2049

Appendix B - Crop water requirements for each type of crop during 2090-2099

Table B - 1 Crop water requirement of winter rice for 2090-2099

CROP WATER REQUIREMENTS

ETo station: ThanhHoa
Rain station: ThanhHoa

Crop: Rice1
Planting date: 25/11

Month	Decade	Stage	Kc coeff	ETc mm/day	ETc mm/dec	Eff rain mm/dec	Irr. Req. mm/dec
Oct	3	Nurs	1.04	0.34	2.0	23.7	0.0
Nov	1	Nurs	1.04	0.33	3.3	24.8	0.0
Nov	2	Nurs/LPr	1.06	2.09	20.9	10.9	140.9
Nov	3	Init	1.12	3.09	30.9	8.9	80.5
Dec	1	Deve	1.15	2.77	27.7	7.1	20.7
Dec	2	Deve	1.17	2.45	24.5	3.2	21.3
Dec	3	Deve	1.20	2.70	29.7	4.4	25.4
Jan	1	Mid	1.22	2.99	29.9	6.1	23.8
Jan	2	Mid	1.22	3.15	31.5	6.8	24.7
Jan	3	Mid	1.22	3.08	33.8	7.3	26.5
Feb	1	Late	1.15	2.82	28.2	7.5	20.6
Feb	2	Late	0.93	2.24	22.4	7.9	14.5
Feb	3	Late	0.81	1.90	3.8	2.5	3.8
					288.7	121.0	402.6

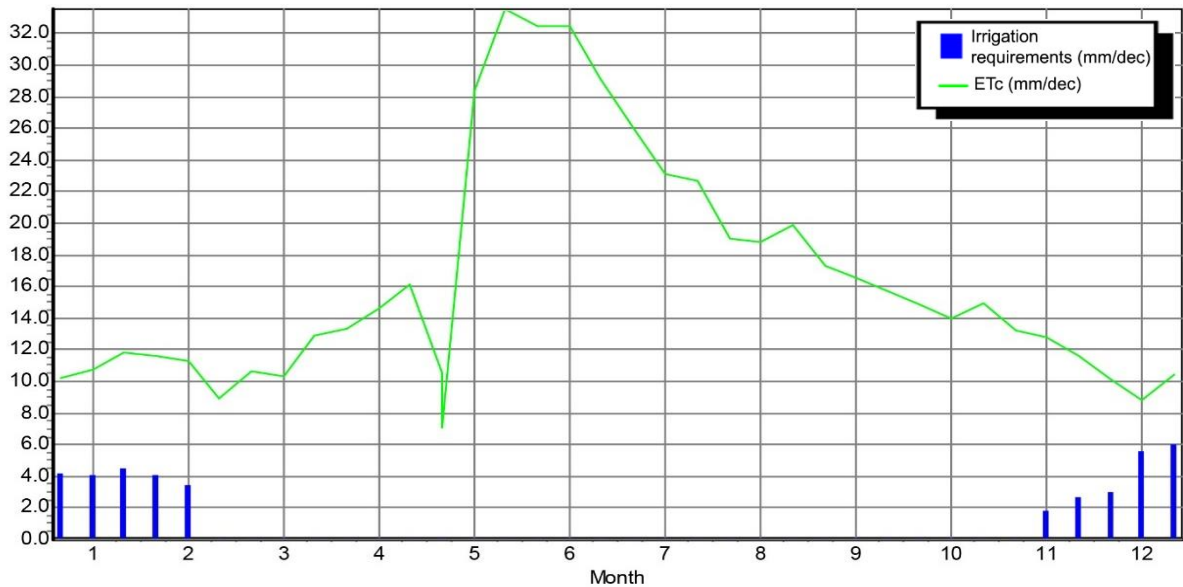


Figure B - 1 Crop water requirement and evapotranspiration of rice for 2090-2099

Table B - 2 Crop water requirement of summer rice for 2090-2099

RICE DATA

(File: C:\ProgramData\CROPWAT\data\crops\ThanhHoa\Rice2.CRO)

Crop Name:	Rice2	Transplanting date:		05/08	Harvest:		02/11	
Stage	nursery	landprep		growth stage			total	
		total	puddling	initial	develop	mid	late	
Length (days)	30	10	5	15	25	30	20	120
Kc dry	0.70		0.30	0.50	-->	1.05	0.70	
Kc wet	1.04		1.08	1.15	-->	1.38	0.95	
Rooting depth (m)				0.10	-->	0.60	0.60	
Puddling depth (m)			0.40					
Nursery area (%)	10							
Critical depletion	0.20			0.20	-->	0.20	0.20	
Yield response f.				1.00	1.09	1.09	1.09	1.09
Cropheight (m)						1.00		

CROP WATER REQUIREMENTS

ETo station: ThanhHoa
Rain station: ThanhHoa

Crop: Rice2
Planting date: 05/08

Month	Decade	Stage	Kc coeff	ETc mm/day	ETc mm/dec	Eff rain mm/dec	Irr. Req. mm/dec
Jul	1	Nurs	1.04	0.49	2.5	23.1	0.0
Jul	2	Nurs	1.04	0.48	4.8	45.4	0.0
Jul	3	Nurs/LPr	1.06	2.90	31.9	47.6	131.2
Aug	1	Init	1.12	5.07	50.7	50.3	54.0
Aug	2	Deve	1.15	5.16	51.6	52.3	0.0
Aug	3	Deve	1.17	5.03	55.3	53.2	2.2
Sep	1	Deve	1.20	4.93	49.3	54.4	0.0
Sep	2	Mid	1.21	4.78	47.8	55.6	0.0
Sep	3	Mid	1.22	4.54	45.4	54.6	0.0
Oct	1	Mid	1.22	4.30	43.0	56.8	0.0
Oct	2	Late	1.15	3.86	38.6	57.7	0.0
Oct	3	Late	0.93	3.03	33.3	43.4	0.0
Nov	1	Late	0.79	2.49	5.0	5.0	5.0
					459.1	599.3	192.3

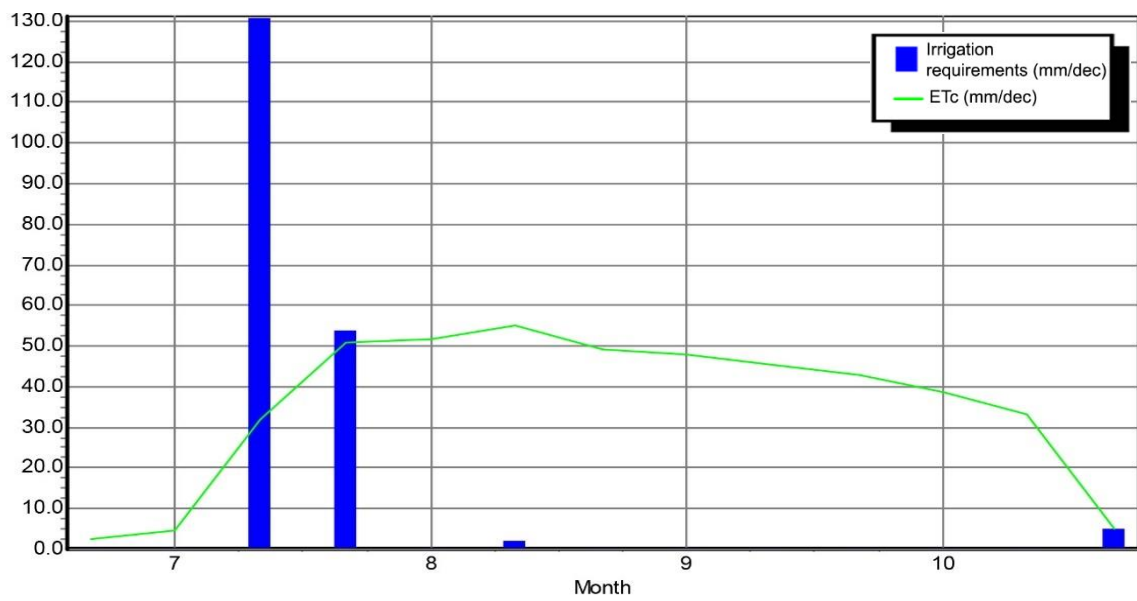


Figure B - 2 Crop water requirement and evapotranspiration of summer rice for 2090-2099

Table B - 3 Crop water requirement of maize for 2090-2099

DRY CROP DATA

(File: C:\ProgramData\CROPWAT\data\crops\ThanhHoa\MAIZE.CRO)

Crop Name: MAIZE (Grain)	Planting date: 15/05	Harvest: 16/09			
Stage	initial	develop	mid	late	total
Length (days)	20	35	40	30	125
Kc Values	0.30	-->	1.20	1.05	
Rooting depth (m)	0.30	-->	1.00	1.00	
Critical depletion	0.55	-->	0.55	0.80	
Yield response f.	0.40	0.40	1.30	0.50	1.25
Cropheight (m)			2.00		

CROP WATER REQUIREMENTS

ETo station: ThanhHoa Crop: MAIZE (Grain)
 Rain station: ThanhHoa Planting date: 15/05

Month	Decade	Stage	Kc coeff	ETc mm/day	ETc mm/dec	Eff rain mm/dec	Irr. Req. mm/dec
May	2	Init	0.30	1.22	7.3	27.0	0.0
May	3	Init	0.30	1.31	14.4	45.9	0.0
Jun	1	Deve	0.36	1.68	16.8	46.6	0.0
Jun	2	Deve	0.55	2.76	27.6	48.3	0.0
Jun	3	Deve	0.74	3.64	36.4	47.7	0.0
Jul	1	Mid	0.93	4.41	44.1	46.1	0.0
Jul	2	Mid	0.99	4.55	45.5	45.4	0.1
Jul	3	Mid	0.99	4.52	49.7	47.6	2.1
Aug	1	Mid	0.99	4.48	44.8	50.3	0.0
Aug	2	Late	0.99	4.42	44.2	52.3	0.0
Aug	3	Late	0.94	4.07	44.7	53.2	0.0
Sep	1	Late	0.89	3.68	36.8	54.4	0.0
Sep	2	Late	0.85	3.36	20.2	33.4	0.0
					432.5	598.1	2.2

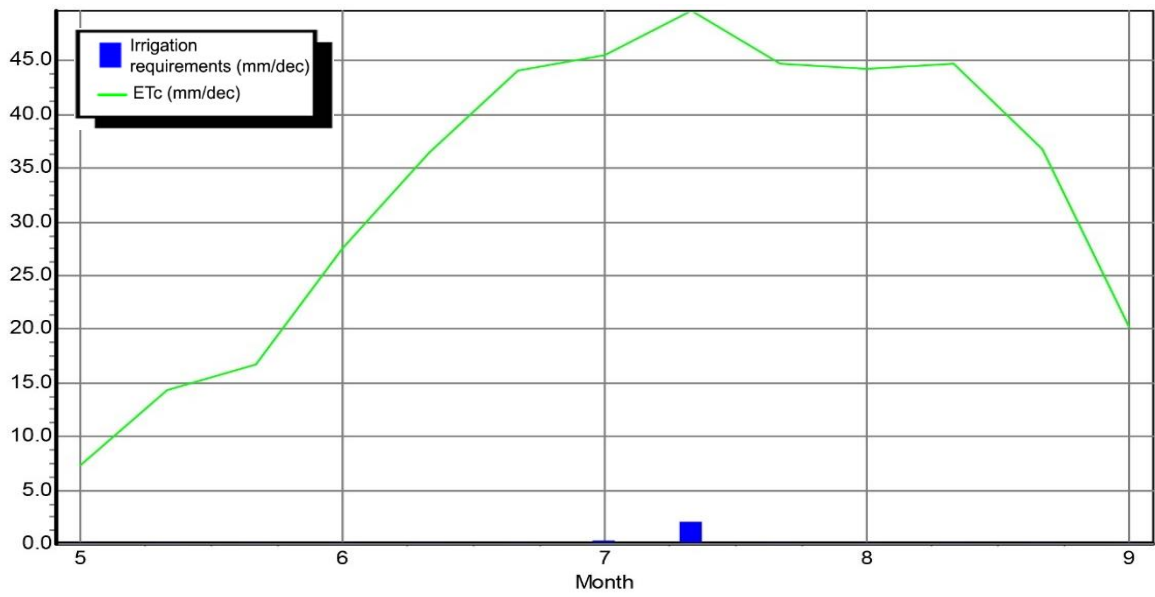


Figure B - 3 Crop water requirement and evapotranspiration of maize for 2090-2099

Table B - 4 Crop water requirement of soybean for 2090-2099

DRY CROP DATA

(File: C:\ProgramData\CROPWAT\data\crops\ThanhHoa\SOYBEAN.CRO)

Crop Name: Soybean			Planting date: 24/04	Harvest: 17/07	
Stage	initial	develop	mid	late	total
Length (days)	15	15	40	15	85
Kc Values	0.40	-->	1.15	0.75	
Rooting depth (m)	0.30	-->	1.00	1.00	
Critical depletion	0.50	-->	0.60	0.90	
Yield response f.	0.40	0.80	1.00	0.40	0.85
Cropheight (m)			0.60		

CROP WATER REQUIREMENTS

ETo station: ThanhHoa Crop: Soybean
 Rain station: ThanhHoa Planting date: 24/04

Month	Decade	Stage	Kc coeff	ETc mm/day	ETc mm/dec	Eff rain mm/dec	Irr. Req. mm/dec
Apr	3	Init	0.40	1.37	9.6	22.0	0.0
May	1	Deve	0.41	1.54	15.4	38.8	0.0
May	2	Deve	0.70	2.86	28.6	45.1	0.0
May	3	Mid	1.00	4.35	47.9	45.9	2.0
Jun	1	Mid	1.01	4.77	47.7	46.6	1.1
Jun	2	Mid	1.01	5.11	51.1	48.3	2.8
Jun	3	Mid	1.01	4.95	49.5	47.7	1.9
Jul	1	Late	0.91	4.31	43.1	46.1	0.0
Jul	2	Late	0.69	3.17	22.2	31.8	0.0
					315.1	372.2	7.7

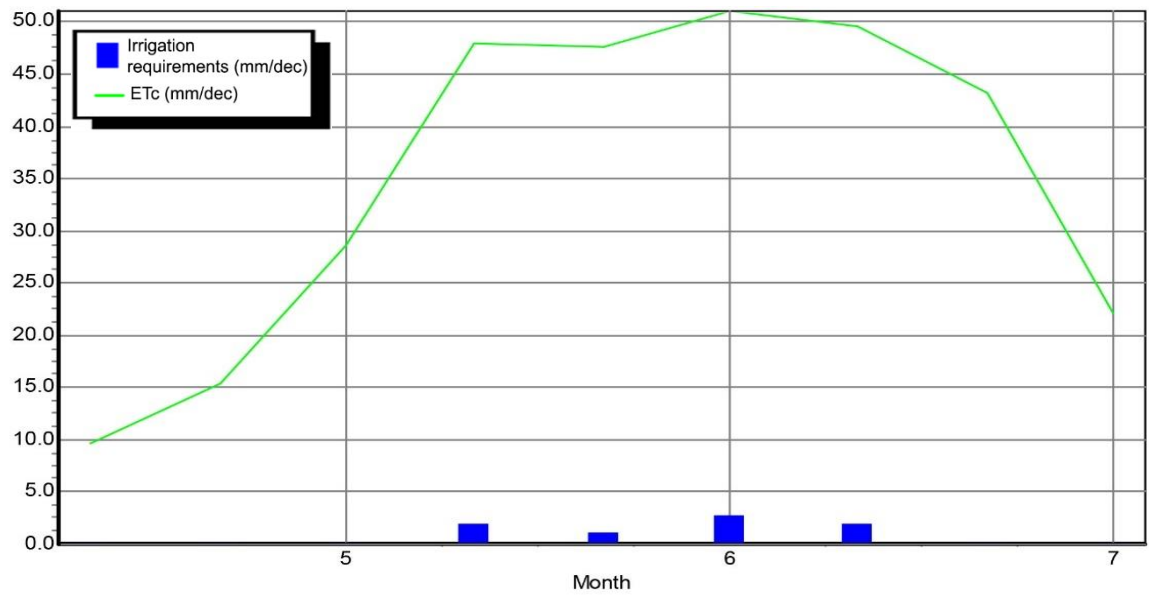


Figure B - 4 Crop water requirement and evapotranspiration of soybean for 2090-2099

Table B - 5 Crop water requirements of groundnut for 2090-2099

DRY CROP DATA

(File: C:\ProgramData\CROPWAT\data\crops\ThanhHoa\GRONDNUT.CRO)

Crop Name: Groudnut			Planting date: 24/04	Harvest: 31/08	
Stage	initial	develop	mid	late	total
Length (days)	25	35	45	25	130
Kc Values	0.55	-->	1.15	0.90	
Rooting depth (m)	0.30	-->	0.80	0.80	
Critical depletion	0.45	-->	0.45	0.50	
Yield response f.	0.20	0.80	0.60	0.20	0.70
Cropheight (m)			0.40		

CROP WATER REQUIREMENTS

ETo station: ThanhHoa Crop: Groudnut
 Rain station: ThanhHoa Planting date: 24/04

Month	Decade	Stage	Kc coeff	ETc mm/day	ETc mm/dec	Eff rain mm/dec	Irr. Req. mm/dec
Apr	3	Init	0.55	1.88	13.2	22.0	0.0
May	1	Init	0.55	2.06	20.6	38.8	0.0
May	2	Deve	0.55	2.25	22.5	45.1	0.0
May	3	Deve	0.66	2.87	31.5	45.9	0.0
Jun	1	Deve	0.80	3.78	37.8	46.6	0.0
Jun	2	Deve	0.93	4.72	47.2	48.3	0.0
Jun	3	Mid	1.02	5.01	50.1	47.7	2.4
Jul	1	Mid	1.02	4.83	48.3	46.1	2.2
Jul	2	Mid	1.02	4.71	47.1	45.4	1.7
Jul	3	Mid	1.02	4.67	51.4	47.6	3.8
Aug	1	Late	1.01	4.58	45.8	50.3	0.0
Aug	2	Late	0.92	4.15	41.5	52.3	0.0
Aug	3	Late	0.82	3.51	38.6	53.2	0.0
					495.5	589.2	10.0

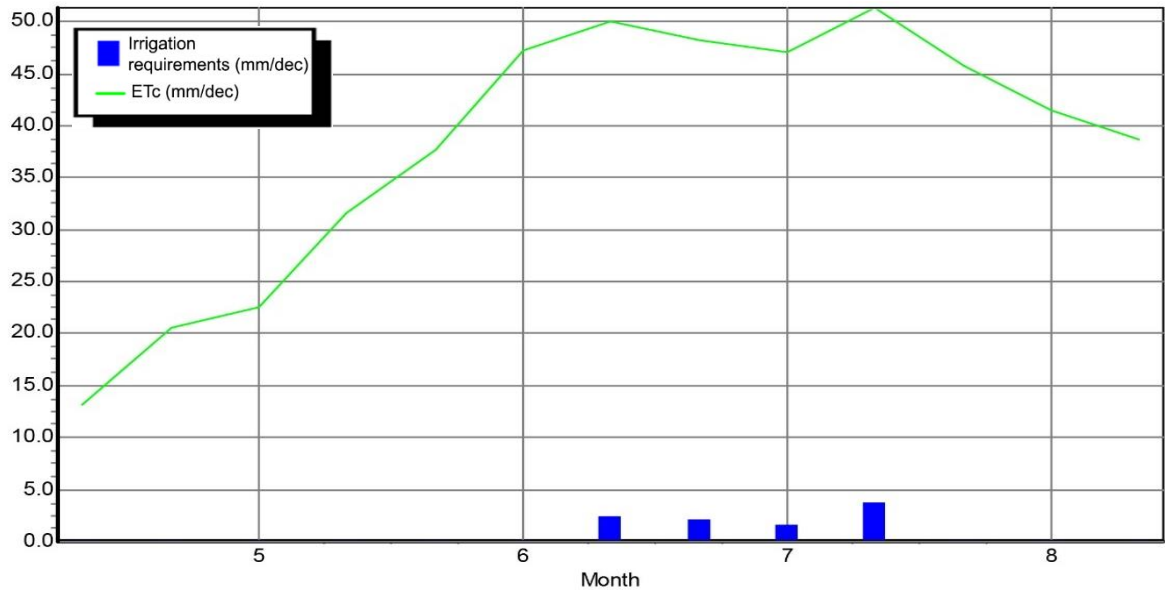


Figure B - 5 Crop water requirements and evapotranspiration of groundnut for 2090-2099

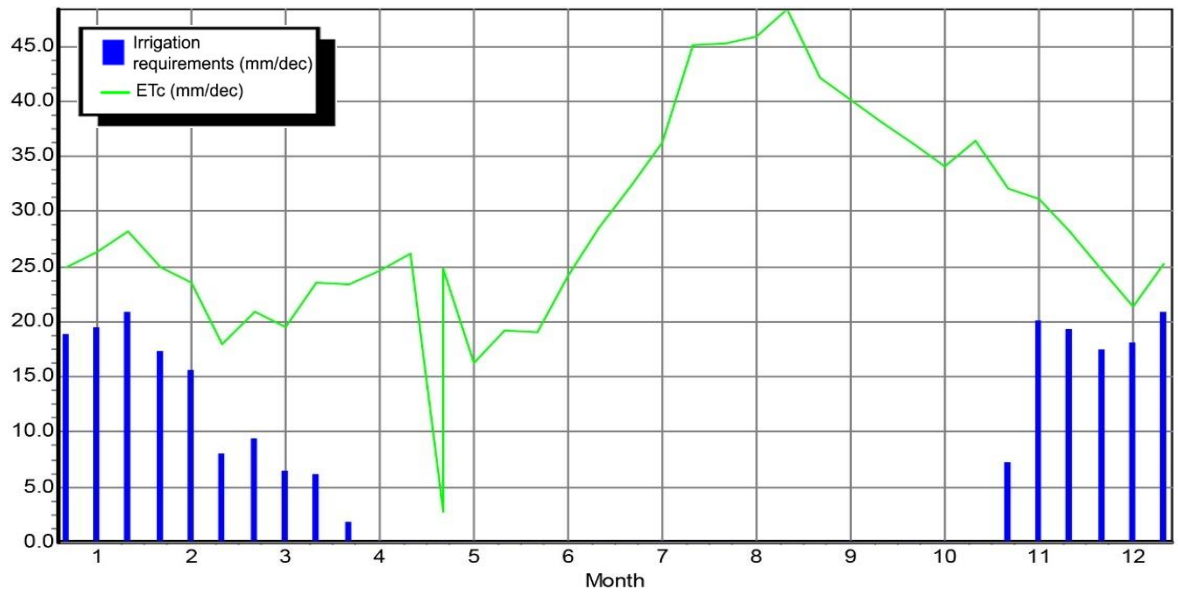


Figure B - 6 Crop water requirement and evapotranspiration of sugarcane for 2090-2099

Table B - 7 Crop water requirement of perennial crops for 2090-2099

DRY CROP DATA

(File: C:\ProgramData\CROPWAT\data\crops\ThanhHoa\PerennialCrops.CRO)

Crop Name:	Perennial crops	Planting date:	05/05	Harvest:	04/05
Stage	initial	develop	mid	late	total
Length (days)	30	60	180	95	365
Kc Values	0.70	-->	0.65	0.70	
Rooting depth (m)	1.50	-->	1.50	1.50	
Critical depletion	0.65	-->	0.65	0.65	
Yield response f.	0.50	0.75	1.20	0.10	1.20
Cropheight (m)			3.00		

CROP WATER REQUIREMENTS

ETo station: ThanhHoa Crop: Perennial crops
 Rain station: ThanhHoa Planting date: 05/05

Month	Decade	Stage	Kc coeff	ETc mm/day	ETc mm/dec	Eff rain mm/dec	Irr. Req. mm/dec
May	1	Init	0.47	1.76	10.6	23.3	0.0
May	2	Init	0.70	2.84	28.4	45.1	0.0
May	3	Init	0.70	3.05	33.5	45.9	0.0
Jun	1	Deve	0.69	3.24	32.4	46.6	0.0
Jun	2	Deve	0.64	3.24	32.4	48.3	0.0
Jun	3	Deve	0.60	2.92	29.2	47.7	0.0
Jul	1	Deve	0.55	2.59	25.9	46.1	0.0
Jul	2	Deve	0.50	2.31	23.1	45.4	0.0
Jul	3	Deve	0.45	2.07	22.8	47.6	0.0
Aug	1	Mid	0.42	1.91	19.1	50.3	0.0
Aug	2	Mid	0.42	1.89	18.9	52.3	0.0
Aug	3	Mid	0.42	1.81	19.9	53.2	0.0
Sep	1	Mid	0.42	1.73	17.3	54.4	0.0
Sep	2	Mid	0.42	1.66	16.6	55.6	0.0
Sep	3	Mid	0.42	1.57	15.7	54.6	0.0
Oct	1	Mid	0.42	1.49	14.9	56.8	0.0
Oct	2	Mid	0.42	1.41	14.1	57.7	0.0
Oct	3	Mid	0.42	1.36	15.0	43.4	0.0
Nov	1	Mid	0.42	1.32	13.2	24.8	0.0
Nov	2	Mid	0.42	1.28	12.8	10.9	1.9
Nov	3	Mid	0.42	1.16	11.6	8.9	2.7
Dec	1	Mid	0.42	1.01	10.1	7.1	3.1
Dec	2	Mid	0.42	0.88	8.8	3.2	5.6
Dec	3	Mid	0.42	0.95	10.4	4.4	6.1
Jan	1	Mid	0.42	1.03	10.3	6.1	4.2
Jan	2	Mid	0.42	1.08	10.8	6.8	4.1
Jan	3	Late	0.43	1.08	11.9	7.3	4.6
Feb	1	Late	0.47	1.16	11.6	7.5	4.1
Feb	2	Late	0.47	1.13	11.3	7.9	3.4
Feb	3	Late	0.47	1.11	8.9	9.9	0.0
Mar	1	Late	0.47	1.06	10.6	11.5	0.0
Mar	2	Late	0.47	1.03	10.3	13.0	0.0
Mar	3	Late	0.47	1.17	12.9	17.4	0.0
Apr	1	Late	0.47	1.33	13.3	21.6	0.0
Apr	2	Late	0.47	1.46	14.6	25.5	0.0
Apr	3	Late	0.47	1.61	16.1	31.4	0.0
May	1	Late	0.47	1.76	7.1	15.5	0.0
					606.8	1115.0	39.7

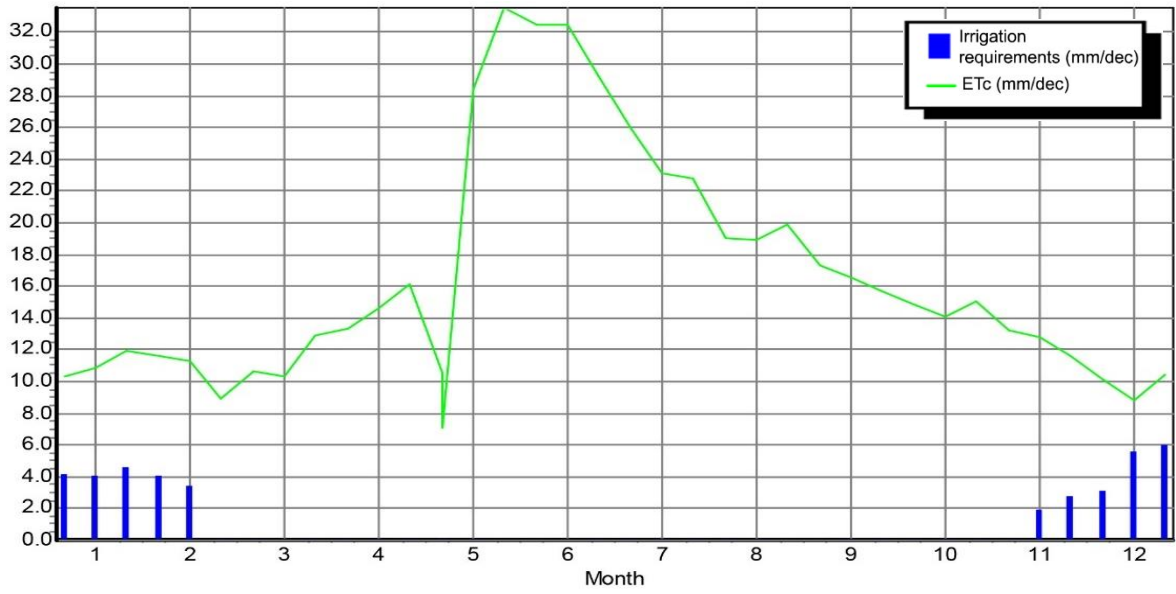


Figure B - 7 Crop water requirement and evapotranspiration of perennial crops for 2090-2099

Table B - 8 Crop water requirement of potato for 2090-2099

DRY CROP DATA

(File: C:\ProgramData\CROPWAT\data\crops\ThanhHoa\POTATO.CRO)

Crop Name: Potato			Planting date: 24/04	Harvest: 31/08	
Stage	initial	develop	mid	late	total
Length (days)	25	30	45	30	130
Kc Values	0.50	-->	1.10	0.50	
Rooting depth (m)	0.30	-->	0.60	0.60	
Critical depletion	0.25	-->	0.30	0.50	
Yield response f.	0.45	0.80	0.80	0.30	1.10
Cropheight (m)			0.60		

CROP WATER REQUIREMENTS

ETo station: ThanhHoa Crop: Potato
 Rain station: ThanhHoa Planting date: 24/04

Month	Decade	Stage	Kc coeff	ETc mm/day	ETc mm/dec	Eff rain mm/dec	Irr. Req. mm/dec
Apr	3	Init	0.50	1.71	12.0	22.0	0.0
May	1	Init	0.50	1.87	18.7	38.8	0.0
May	2	Deve	0.50	2.05	20.5	45.1	0.0
May	3	Deve	0.62	2.71	29.8	45.9	0.0
Jun	1	Deve	0.78	3.69	36.9	46.6	0.0
Jun	2	Mid	0.92	4.68	46.8	48.3	0.0
Jun	3	Mid	0.96	4.69	46.9	47.7	0.0
Jul	1	Mid	0.96	4.52	45.2	46.1	0.0
Jul	2	Mid	0.96	4.41	44.1	45.4	0.0
Jul	3	Mid	0.96	4.37	48.1	47.6	0.5
Aug	1	Late	0.87	3.92	39.2	50.3	0.0
Aug	2	Late	0.66	2.97	29.7	52.3	0.0
Aug	3	Late	0.45	1.93	21.2	53.2	0.0
					439.0	589.2	0.5

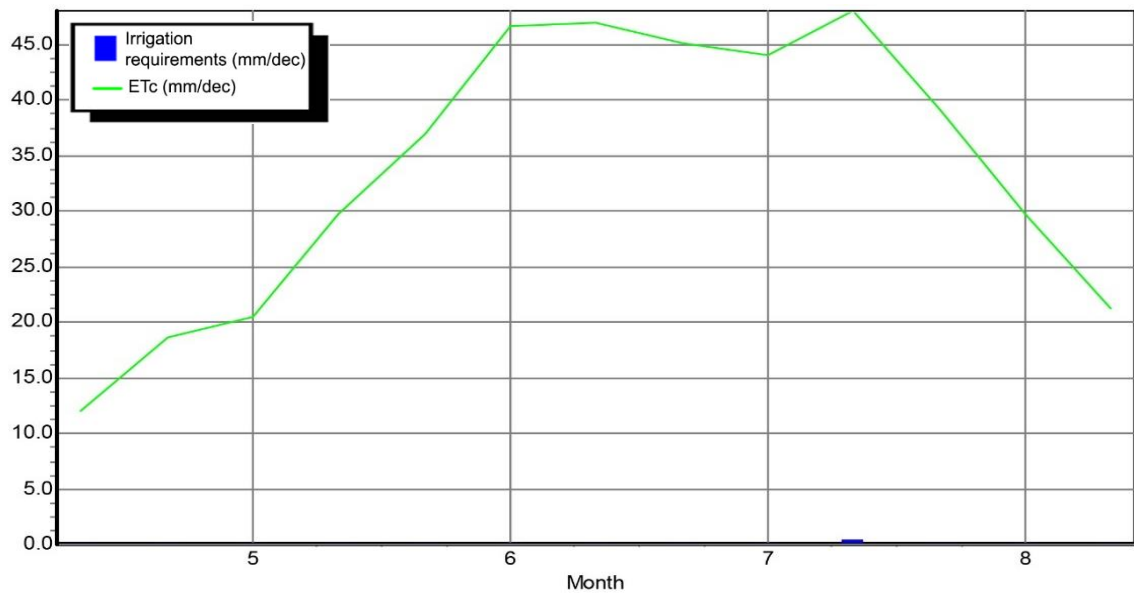


Figure B - 8 Crop water requirement and evapotranspiration of potato for 2090-2099